Géométrie sans frontières
Paris VII. 12-16 mars 2012
Hommage à Daniel Bennequin

Some elements of neurogeometry

Jean Petitot

CREA, Ecole Polytechnique, Paris

Introduction

- What I call neurogeometry concerns the neural implementation of geometric structures of visual perception.
- It concerns perceptive geometry "from within" (in the sense of Gromov) and not 3D Euclidean geometry of the outside world .
- The general problem is to understand how the visual system can be a neural geometric engine.

- Many non trivial mathematical structures have been introduced recently to explain natural early vision.
- Contact, symplectic and sub-Riemannian geometry arise naturally in modeling V1 functional architecture.
- Sub-Riemannian geometry provides the <u>simplest</u> model of the horizontal cortico-cortical connections in V1.

- In relation with wavelet analysis this leads naturally to noncommutative harmonic analysis on Heisenberg type groups.

Limitations

- We focus on V1, but there are of course many top-down feedbacks from other areas to V1.
- Neural implementation varies with species (rat, ferret, tree shrew, cat, macaque, man, etc.). The same functional architecture can be implemented in different ways.

- Stephen van Hooser on “Similarity and diversity” of V1 in mammals (comparative study).
- The gross laminar interconnections and the major functional responses are nearly invariant: 6 layers, LGN projecting mainly on the granular 4th layer.
- Three principal classes of LGN cells: parvocellular (P), magnocellular (M), koniocellular (K).

- But the fine laminar structures are quite different.
- Tree shrew (Tupaya), Cat, Macaque have orientation maps with orientation hypercolumns and a functional "horizontal" architecture connecting neurons of similar orientation.
- Rat and Gray squirrel have not.

- Figure. Orientation simple cells (red) are absent in macaque 4B and tree shrew layer 4.
  - Direction selectivity dominates in the cat but is only common in specific layers of macaque and squirrel.
  - End-stopped VS lengthsumming cells : they decrease VS increase their responses as bars or gratings length increases.

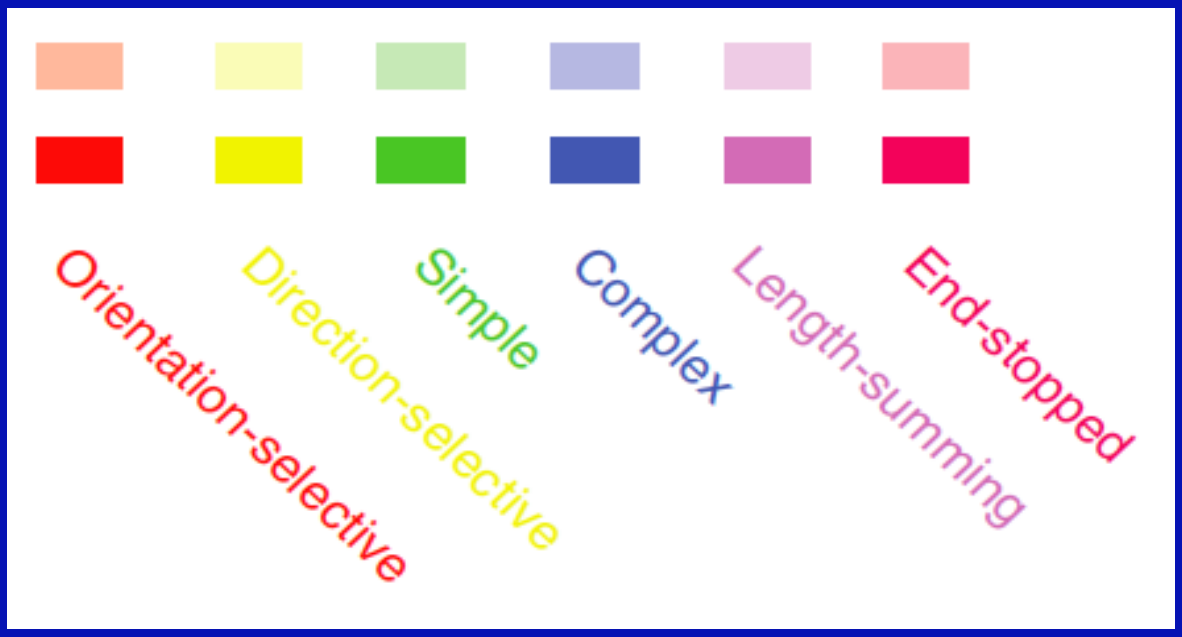
Orientation-selective
Direction-selective
Simple
Complex
Length-summing
End-stopped

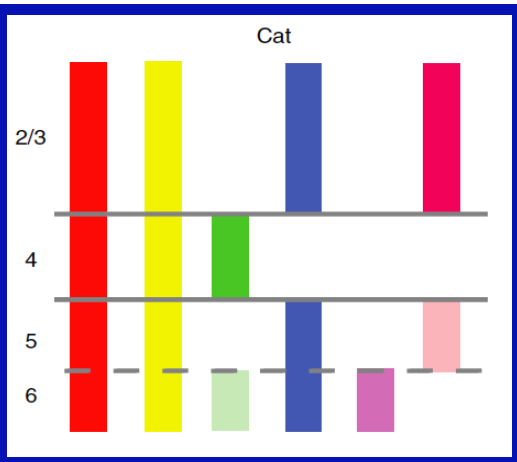
Cat
2/3
4
5
6

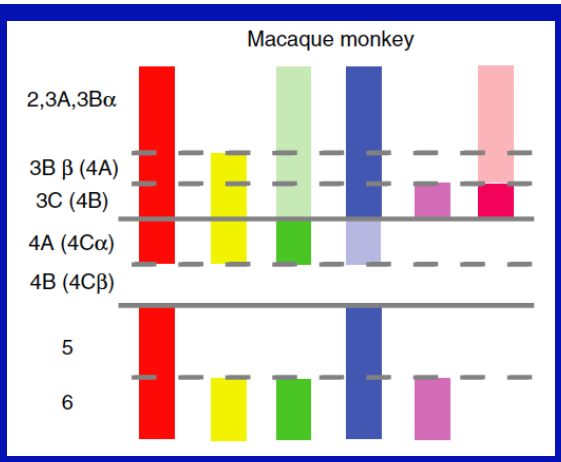
Macaque monkey
2,3A,3Bα
3B β (4A)
3C (4B)
4A (4Cα)
4B (4Cβ)
5
6

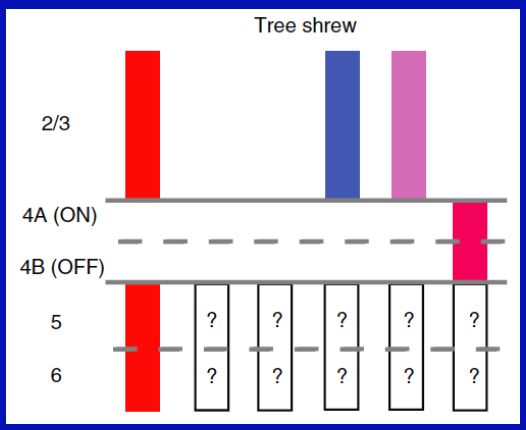
Tree shrew
2/3
4A (ON)
4B (OFF)
5
6
?

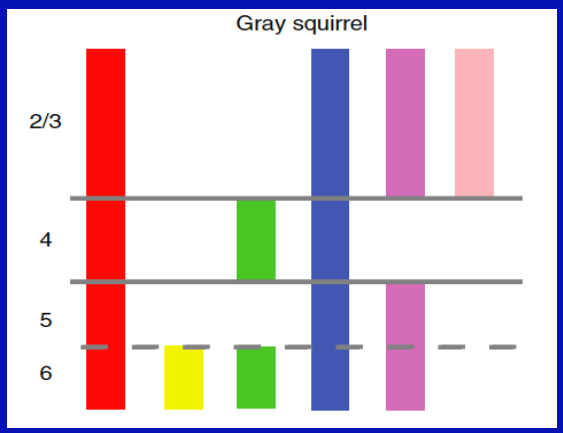
Gray squirrel
2/3
4
5
6

- *Another limitation*. Neural coding is a statistical population coding and, for each elementary computation, a lot of neurons are involved.
- We will not take into account explicitely this redundancy which leads to stochastic models.

The primary visual cortex: area V1

- In mammals (especially higher mammals with frontal eyes), due to the optic chiasm, each visual hemifield projects onto the contralateral hemisphere.
- The fibers from nasal hemiretinae cross the optic chiasm, while the fibers from temporal hemiretinae remain on the ipsilateral side.

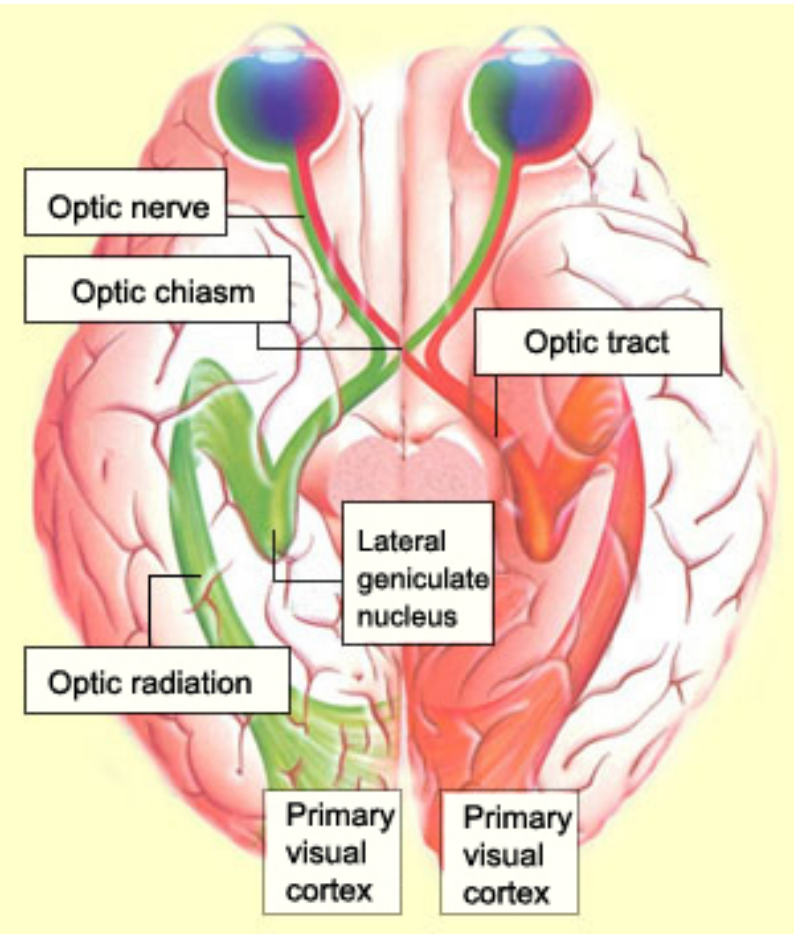
Optic nerve
Optic chiasm
Optic tract
Lateral geniculate nucleus
Optic radiation
Primary visual cortex
Primary visual cortex

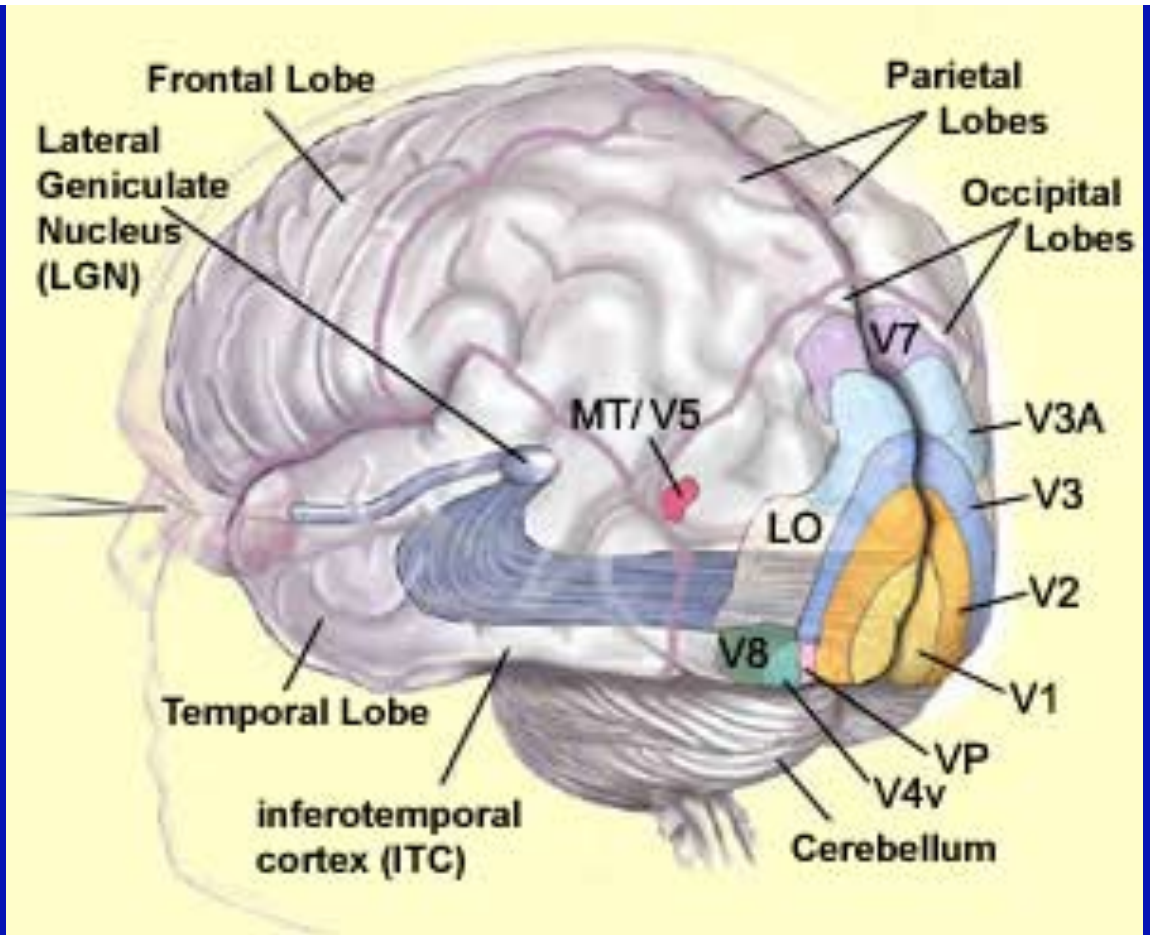
Frontal Lobe
Lateral Geniculate Nucleus (LGN)
Parietal Lobes
Occipital Lobes
V7
MT/V5
V3A
V3
LO
V2
V8
V1
Temporal Lobe
VP
V4v
inferotemporal cortex (ITC)
Cerebellum

- In the linear approximation, neurons of V1 operate as filters on the optic signal coming from the retina.
- Their *receptive fields* (the bundle of photoreceptors they are connected with via the retino-geniculo-cortical pathways) have *receptive profiles* (i.e. transfert function) with a characteristic shape.

- We look only at the simplest and most classical definition of the RFs by spiking responses (minimal discharge field).
- We don't take into account the <u>global contextual subthreshold</u> activity of neurons.
- We look at the simplest models.

- For "simple" cells, RFs are highly anisotropic and elongated along a preferential orientation.
- Level curves of the receptive profiles can be recorded :

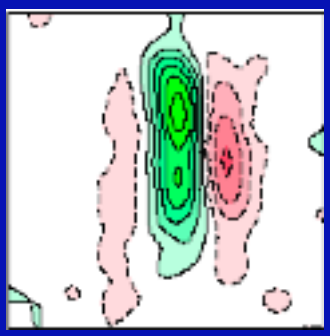

- The receptive profiles can be modeled either
  - by second order derivatives of Gaussians,
  - or by Gabor wavelets

$$\exp(i2x)\exp\left(-\left(x^2+y^2\right)\right)$$

(real part).

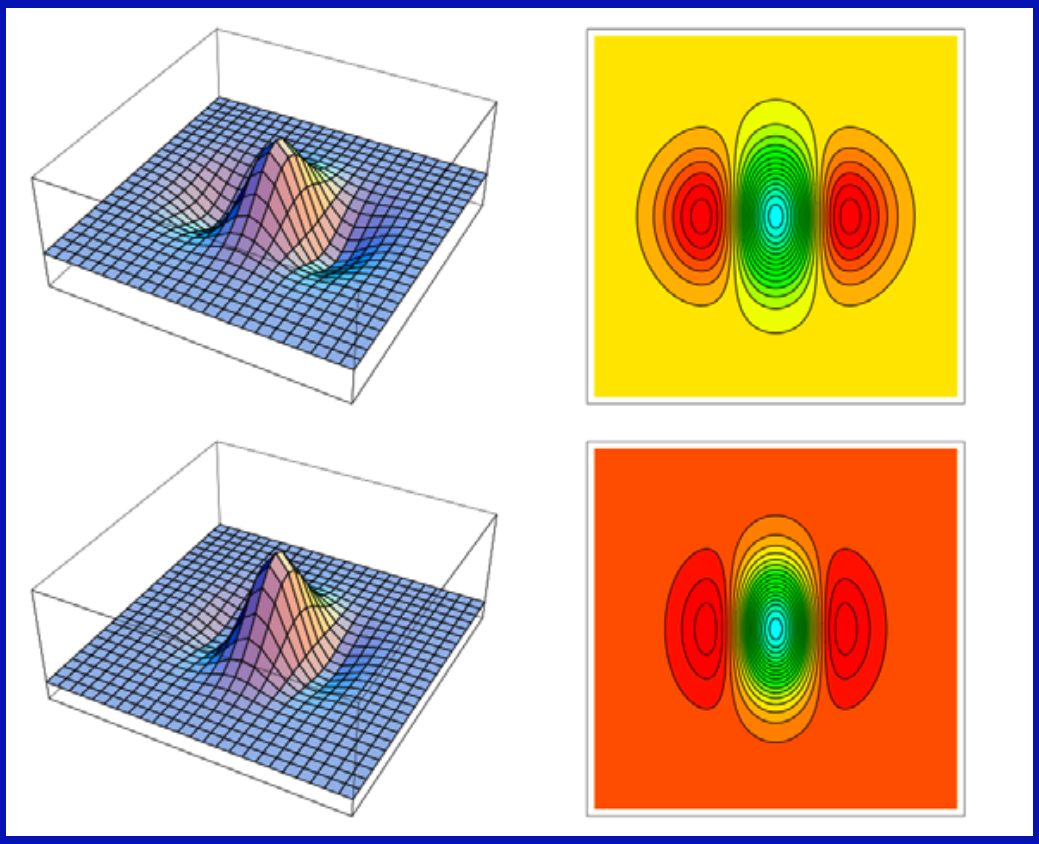

- The RPs operate by <u>convolution</u> on the visual signal.
- Let $I(x, y)$ be the visual signal (x, y are visual coordinates on the retina).

  Let $\varphi(x\text{-}x_0, y\text{-}y_0)$ be the RP of a neuron N whose RF is defined on a domain D of the retina centered on (x_0, y_0).

- N acts on the signal I as a filter :

$$I_\varphi(x_0, y_0) = \int_D I(x', y')\varphi(x' - x_0, y' - y_0)dx'dy'$$

- A field of such neurons act by convolution on the signal. It is a wavelet analysis.

$$I_\varphi(x, y) = \int_D I(x', y')\varphi(x' - x, y' - y)dx'dy' = (I * \varphi)(x, y)$$

- True RF are far more complex. They are adapted to the processing of natural images (and not bars and gratings).
- Joseph Atick, J-P Nadal, have shown that RPs can result from "efficiency of information representation".
- An efficient coding must reduce redundancy and maximize the mutual information between visual input and neural response.

- The statistic of natural images is very particular because there exist strong correlations between nearby RF.
- Yves Frégnac (UNIC) : 4 statistics. Drifting gratings, dense noise, natural images with eye movements, gratings with EM.
- The variability of spikes decreases with complexity and their temporal precision increases.

- In the linear approximation (convolution $T(I) = I_* \varphi$ with a RP $\varphi(x)$), the first thing is to decorrelate the autocorrelation of the signal $R(z)$ defined by $R(x-y) = \langle I(x).\, I(y) \rangle$.
- <u>Field's law</u> (scale invariance of R) : the power spectrum is

$$\widehat{R}(\omega) = \frac{1}{|\omega|^2}$$

If $\omega = \lambda/\alpha$

$$R(\alpha x) = \int \frac{e^{i\omega\alpha x}}{|\omega|^2} d\omega = \int \frac{\alpha^2 e^{i\lambda x}}{|\lambda|^2} \frac{d\lambda}{\alpha} = \alpha R(x)$$

- Decorrelation = whitening

$$\langle T(I)(x) \,.\, T(I)(y) \rangle = \delta(x - y)$$

$$\left|\widehat{T(I)}(\omega)\right|^2 = 1$$

- Covariance matrix, with $\varphi'(x) = \varphi(-x)$

$$T(R) = \varphi * R * \varphi'$$

- To get δ, we need

$$\widehat{T(R)}(\omega) = \widehat{\varphi}(\omega)\widehat{R}(\omega)\overline{\widehat{\varphi}}(\omega) = 1$$

$$|\widehat{\varphi}(\omega)|^2 = \frac{1}{\widehat{R}(\omega)} \qquad \widehat{R}(\omega) = \frac{1}{|\omega|^2} \qquad |\widehat{\varphi}(\omega)| = |\omega|$$

- This method is not adapted to noise and enhance it at high frequencies where it is already dominant.
- We need a smoothing, hence

$$|\widehat{\varphi}(\omega)|^2 = \frac{\widehat{R}(\omega) + N^2}{\widehat{R}(\omega)^2}$$

- Decorrelation + smoothing leads to Laplacian RPs.

Hypercolumns and pinwheels

- Drastic simplification : simple cells of V1 detect a preferential orientation.
- They measure, at a certain scale, pairs (a, p) of a spatial (retinal) position a and of a local orientation p at a.
- Pairs (a, p) are called in geometry "contact elements".

- For a given position $a = (x_0, y_0)$ in R, the simple neurons with variable orientations θ constitute an *anatomically definable micromodule* called an "hypercolumn".
- The hypercolumns associate retinotopically to each position a of the retina R a full exemplar P_a of the space P of orientations p at a.
- Hubel and Wiesel won the Nobel Prize for this discovery.

- So, this part of the functional architecture implements the fibration $\pi : R \times P \rightarrow R$ with base R, fiber P, and total space $V = R \times P$.
- V is an abstract 3D structure. But it is implemented in a 2D neural layer (dimensional collapse).
- It is the pinwheel structure.

Pinwheels

- Hypercolumns are geometrically organized in 2D-pinwheels.
- The cortical layer is reticulated by a lattice of singular points which are the centers of the pinwheels.
- Locally, around these singular points all the orientations are represented by the rays of a “wheel” and the local wheels are glued together into a global structure.

- The method (Bonhöffer & Grinvald, ~ 1990) of *in vivo optical imaging* based on activity-dependent intrinsic signals allows to acquire images of the activity of the superficial cortical layers.
- Gratings with high contrast are presented many times (20-80) with e.g. a width of 6.25° for the dark strips and of 1.25° for the light ones, a velocity of 22.5°/s, different (8) orientations.

- A window is opened in the skull above V1 and the cortex is illuminated with orange light.
- The concentration of deoxy-hemoglobine increases when neurons are activated. The absorption spectrum of deoxy-hemoglobin is maximal for wave lengths about 600 nm.
- The change is only about 0.2% and the recorded images must therefore be analyzed very carefully.

- One does the summation of the images of V1 's activity for the different gratings and constructs differential maps (differences between orthogonal gratings).
- The low frequency noise is eliminated.
- The maps are normalized (by dividing the deviation relative to the mean value at each pixel by the global mean deviation).

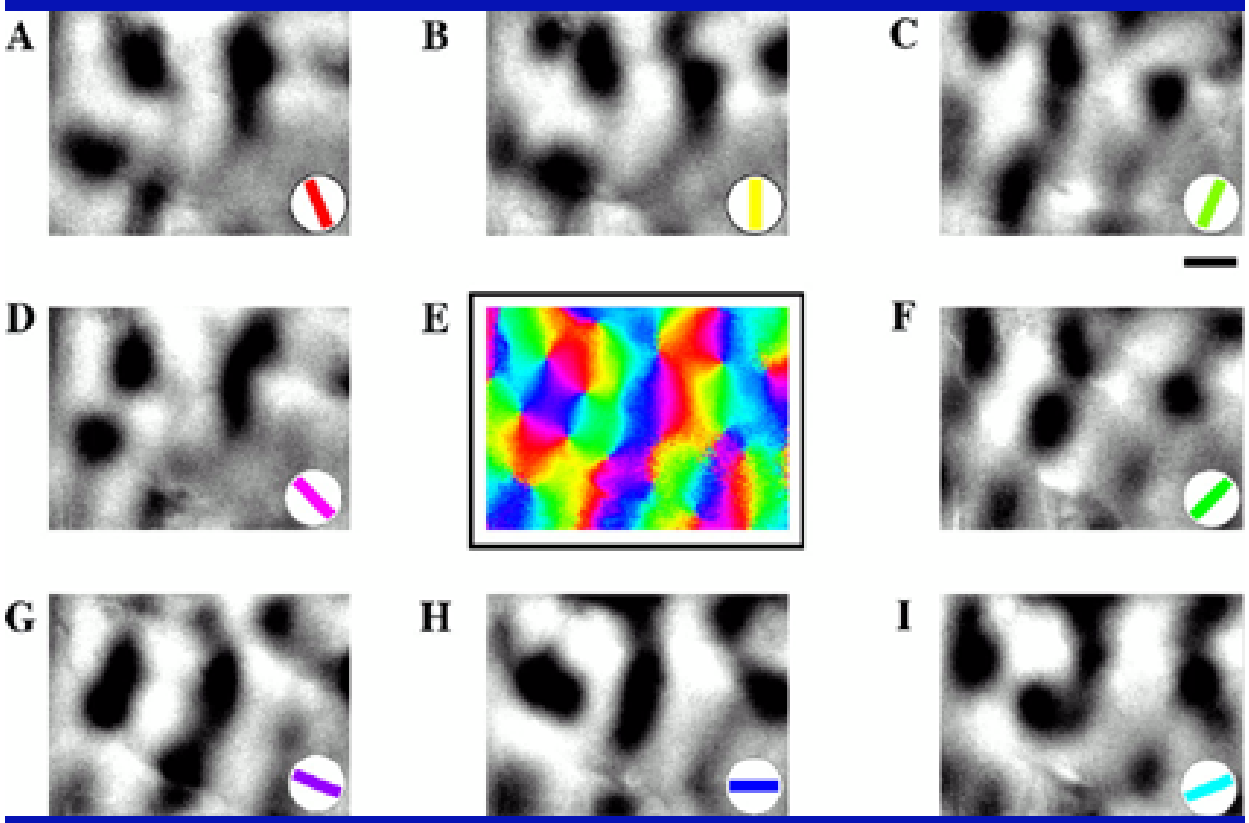

- At a certain resolution and with a population coding, a “point” corresponds to a small assembly of neurons with approximatively the same receptive field and the same preferred orientation.
- It codes a contact element (a, p).

- The following picture shows
- (a) the sub-population (stripe) of V1 neurons activated by a long line stimulus located at a precise (vertical) position (scale bar = 1mm).
- (b) the embedding of the stripe in the population of V1 neurons responding to the same vertical orientation but at different positions.

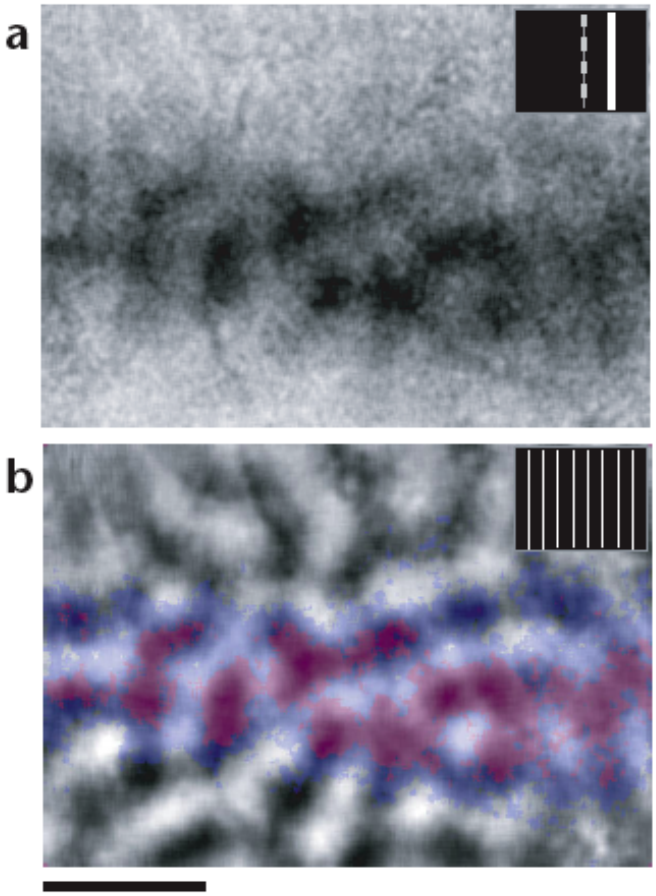

- In the following picture (W. Bosking) the orientations are coded by colors and iso-orientation lines are therefore coded by monocolor lines.

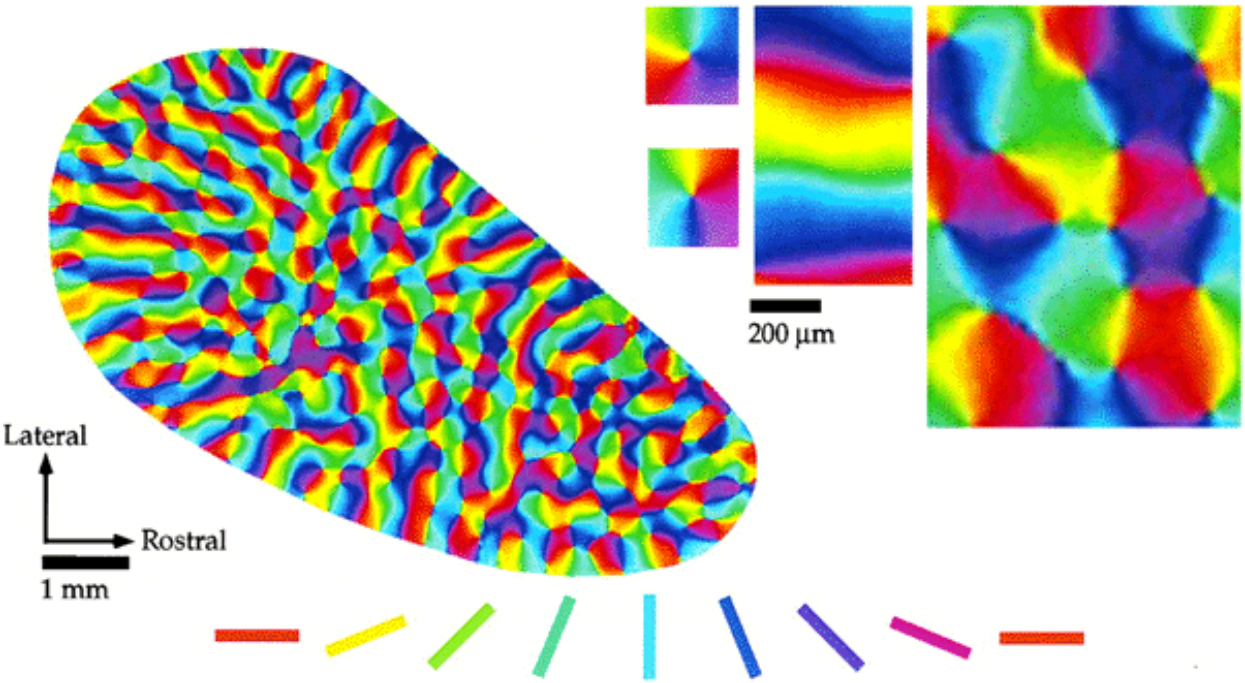

- There are 3 classes of points :
  - regular points where the orientation field is locally trivial;
  - <u>singular points</u> at the center of the pinwheels;
  - saddle-points localized near the centers of the cells of the network.
- Two adjacent singular points are of <u>opposed chirality</u> (CW and CCW).
- It is like a <u>field</u> in *W* generated by topological charges with “field lines” connecting charges of opposite sign.

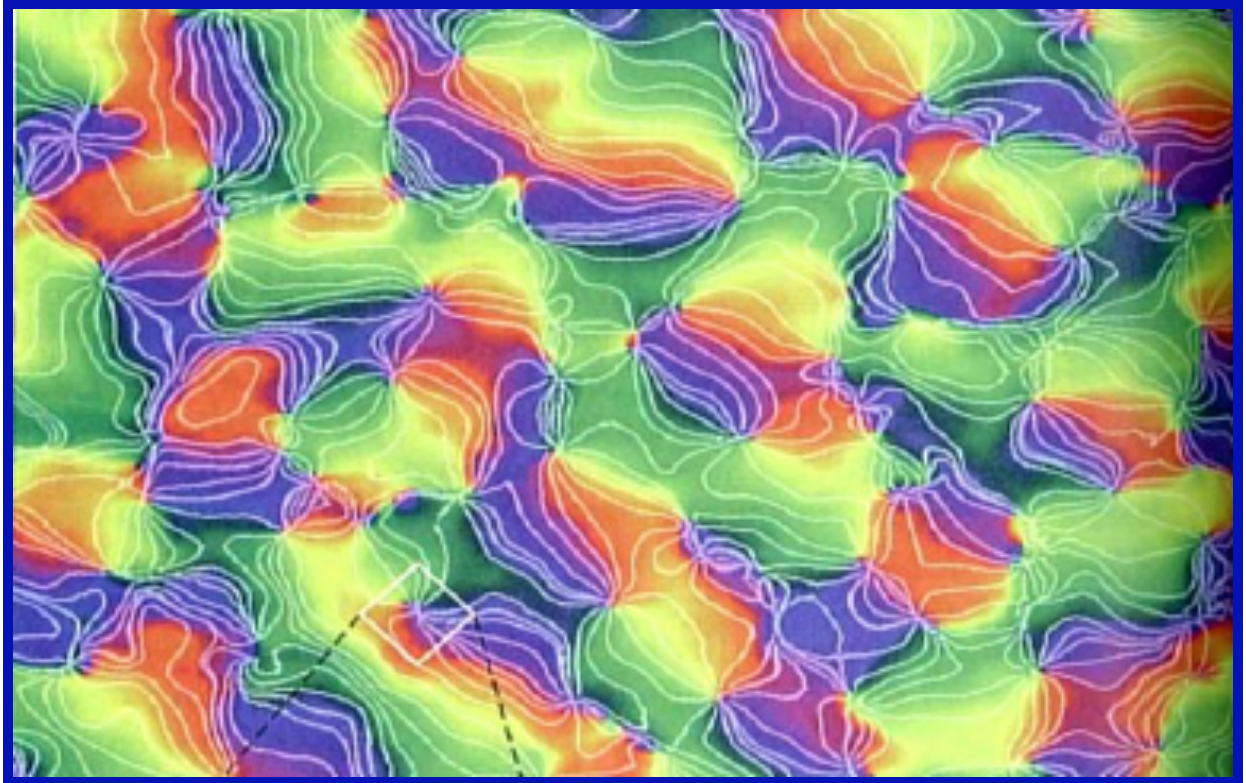

- Another example (primate: prosimian Bush Baby)

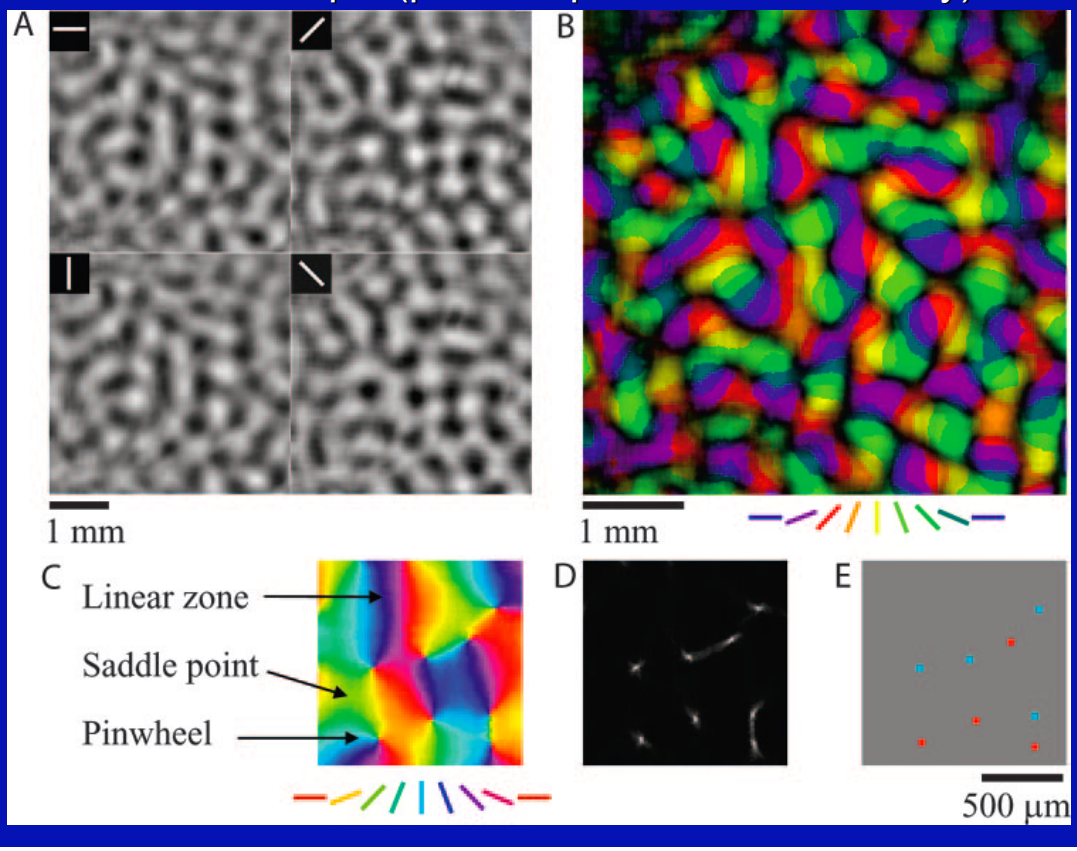

The orientation map

- In polar coordinates one considers the fibration

$$\pi_1 \, : \, \mathbb{R}^2 \times \mathbb{S}^1 \, \rightarrow \, \mathbb{R}^2$$

- On $\mathbb{R}^2 - \{O\}$ the angle

$$\theta(a) \, \in \, [0, 2\pi]$$

defines a section

$$\vartheta_1 : a \rightarrow \vartheta_1(a) = \left(a, e^{i\theta(a)}\right)$$

- The fibration

$$\pi \ : \ \mathbb{R}^2 \times \mathbb{P}^1 \ \rightarrow \ \mathbb{R}^2$$

is the quotient mod π of the fibration

$$\pi_1 \ : \ \mathbb{R}^2 \times \mathbb{S}^1 \ \rightarrow \ \mathbb{R}^2$$

- The orientation map corresponds to the section

$$\psi : a \rightarrow \psi(a) = \left(a, e^{i\theta(a)/2}\right)$$

$$\pi : \left(\mathbb{R}^2 - \{O\}\right) \times \mathbb{P}^1 \rightarrow \mathbb{R}^2 - \{O\}$$

- In the following picture due to Shmuel (cat's area 17), the orientations are coded by colors but are also represented by white segments.

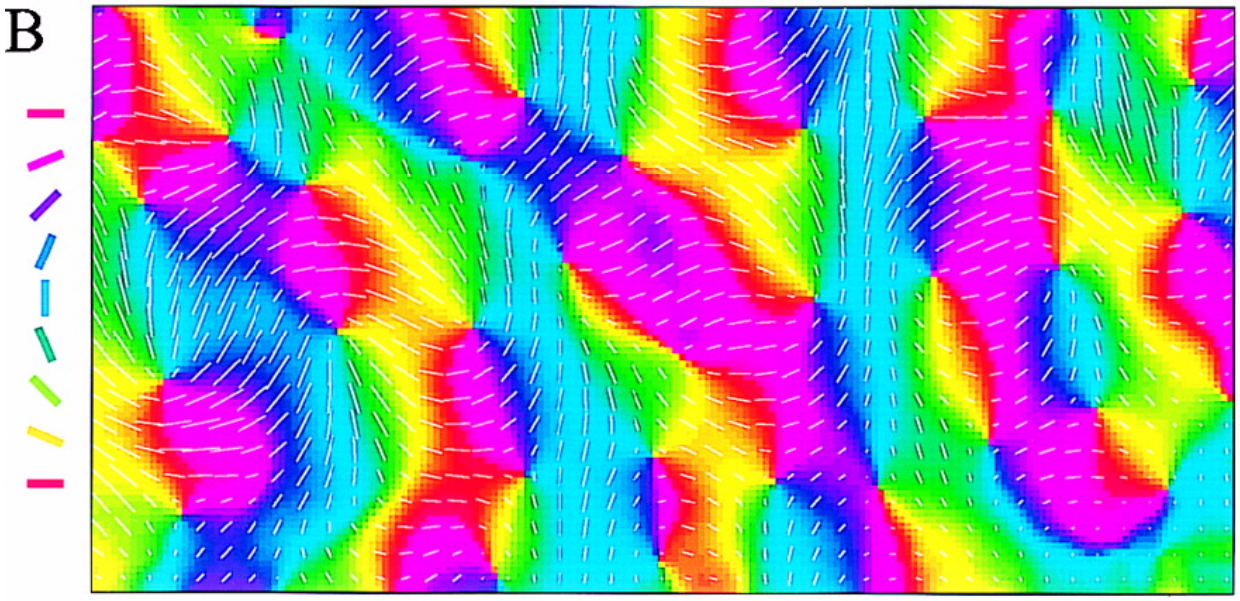

- We observe very well the two types of generic singularities of 1D foliations in the plane.

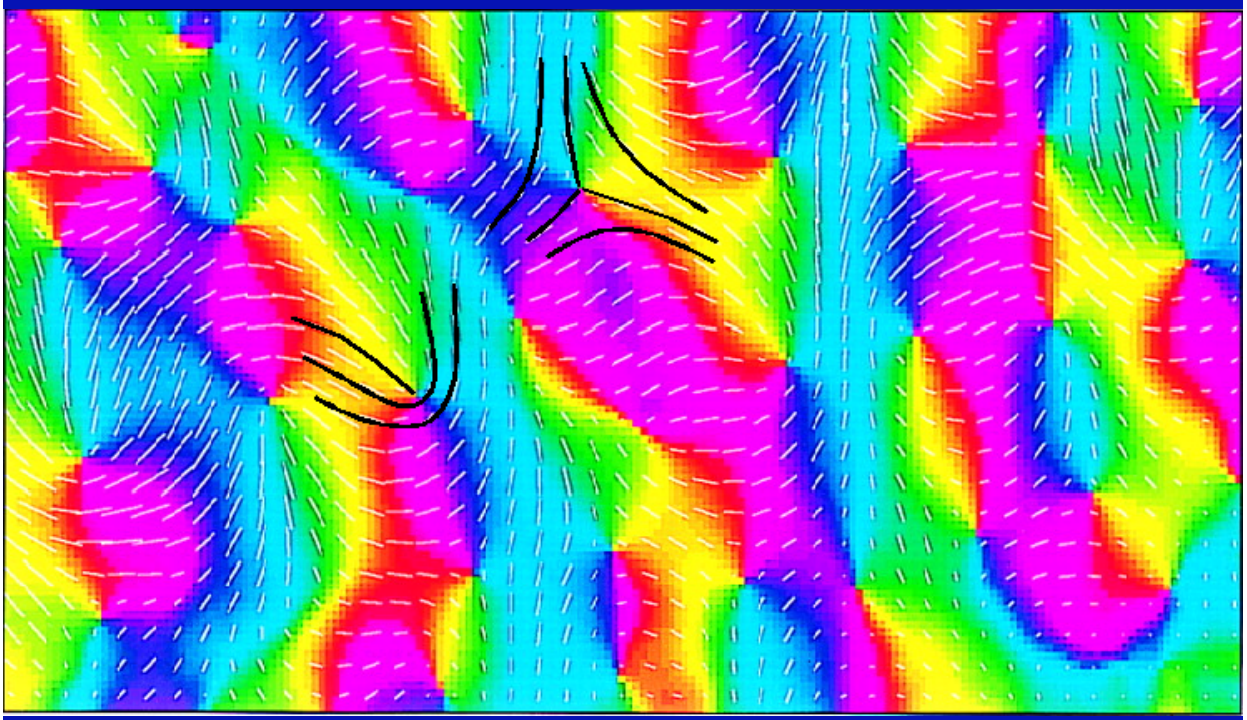

- They arise from the fact that, in general, the direction θ in V1 of a ray of a pinwheel is not the orientation p_θ associated to it in the visual field.
- When the ray spins around the singular point with an angle φ, the associated orientation rotates with an angle $\varphi/2$. Two diametrally opposed rays correspond to orthogonal orientations.
- There are two cases.

- If the orientation p_θ associated with the ray of angle θ is $p_\theta = \alpha + \theta/2$ (with $p_0 = \alpha$), the two orientations will be the same for

$$p_\theta = \alpha + \theta/2 = \theta$$

that is for $\theta = 2\alpha$.

- As α is defined modulo π, there is only one solution : end point.

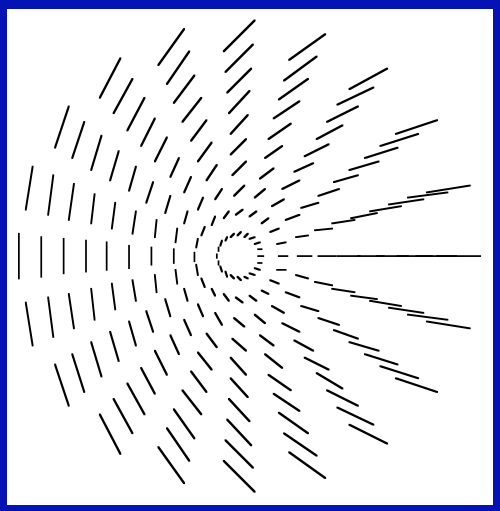

- If the orientation p_θ associated with the ray of angle θ is $p_\theta = \alpha - \theta/2$, the two orientations will be the same for

$$p_\theta = \alpha - \theta/2 = \theta$$

that is for $\theta = 2\alpha/3$.

- As α is defined modulo π, there are three solutions : triple point.

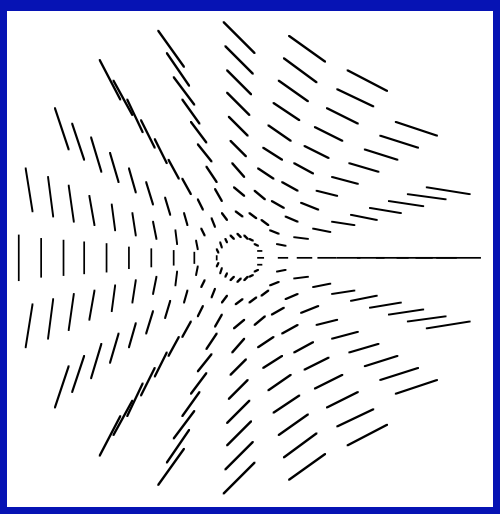

Wolf-Geisel model

- Fred Wolf and Theo Geisel modeled the pinwheel network using a complex field

$$z(a) \quad \left(a = \rho e^{i\theta}, z = re^{i\varphi}\right)$$

where the spatial phase $\varphi\,(a)$ codes the preferred orientation and the module $r\,(a)$ codes the orientation selectivity.

- Singularities are *zeroes* of this field.

- They study the evolution of pinwheels under learning dynamics.
- Starting with $z_0(a) \approx 0$ one applies Hebb's law according to which stimuli strengthen the connections they activate.
- Hence a PDE of evolution (ξ = noise)

$$\frac{\partial z(a,t)}{\partial t} = F\left(z\left(a,t\right)\right) + \xi$$

- Evolution of pinwheels.

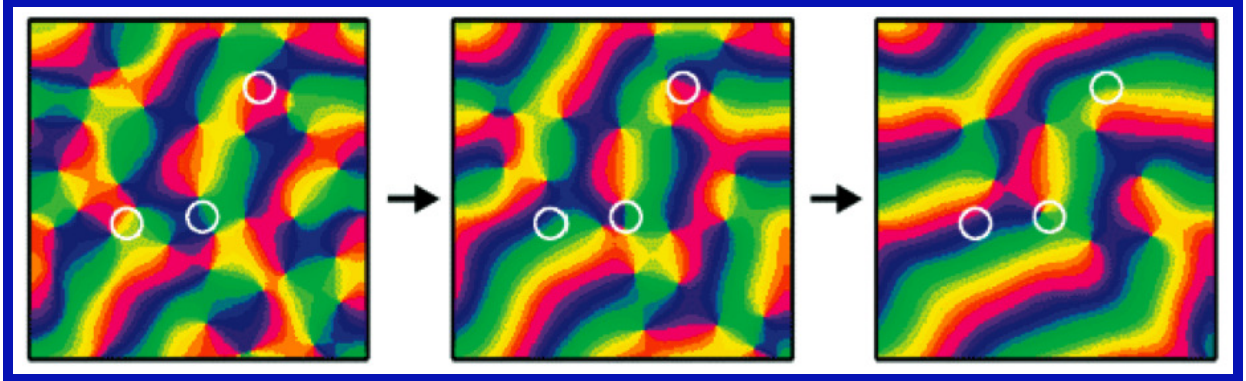

- Let us suppose that the maximal selectivity = 1. The functional architecture is a section of the fibration

$$\pi : \mathbb{C} \times \mathbb{D} \to \mathbb{C} \ \left(a = \rho e^{i\theta}, z = r e^{i\varphi}\right)$$

- Let us take e.g.

$$\varphi = \theta, \, r = \tfrac{1}{2}\rho$$

- Above a small circle C_ρ around $a = 0$ we have the torus

$$C_\rho \times \Sigma_{\rho/2} \to C_\rho$$

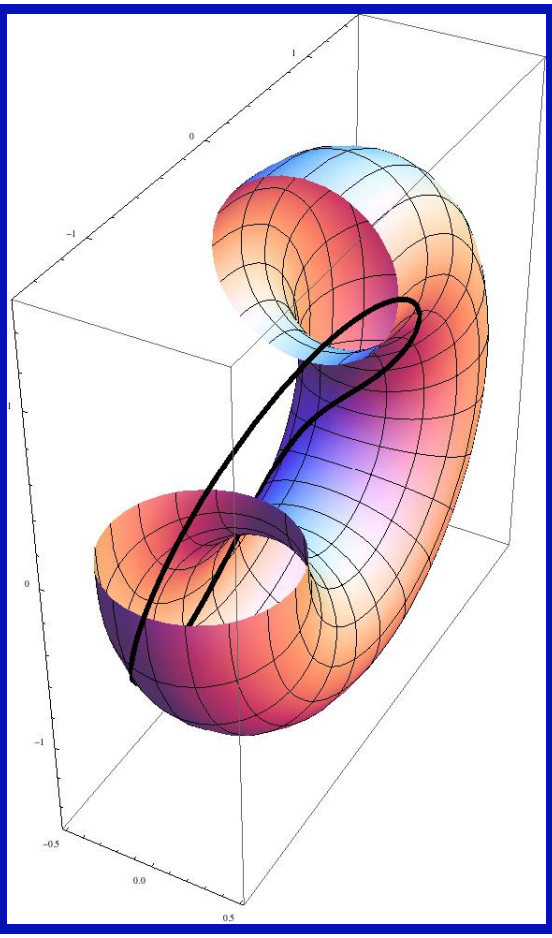

- The lift of C_ρ is the curve Γ_ρ

$$\left(\frac{1}{2}\rho\sin(\theta), \rho\left(1-\frac{1}{2}\cos(\theta)\right)\cos(\theta), \rho\left(1-\frac{1}{2}\cos(\theta)\right)\sin(\theta)\right)$$

- As orientation selectivity vanishes at 0, when $\rho \to 0$ we have also $\Gamma_\rho \to 0$
- The projection is locally a diffeomorphism.

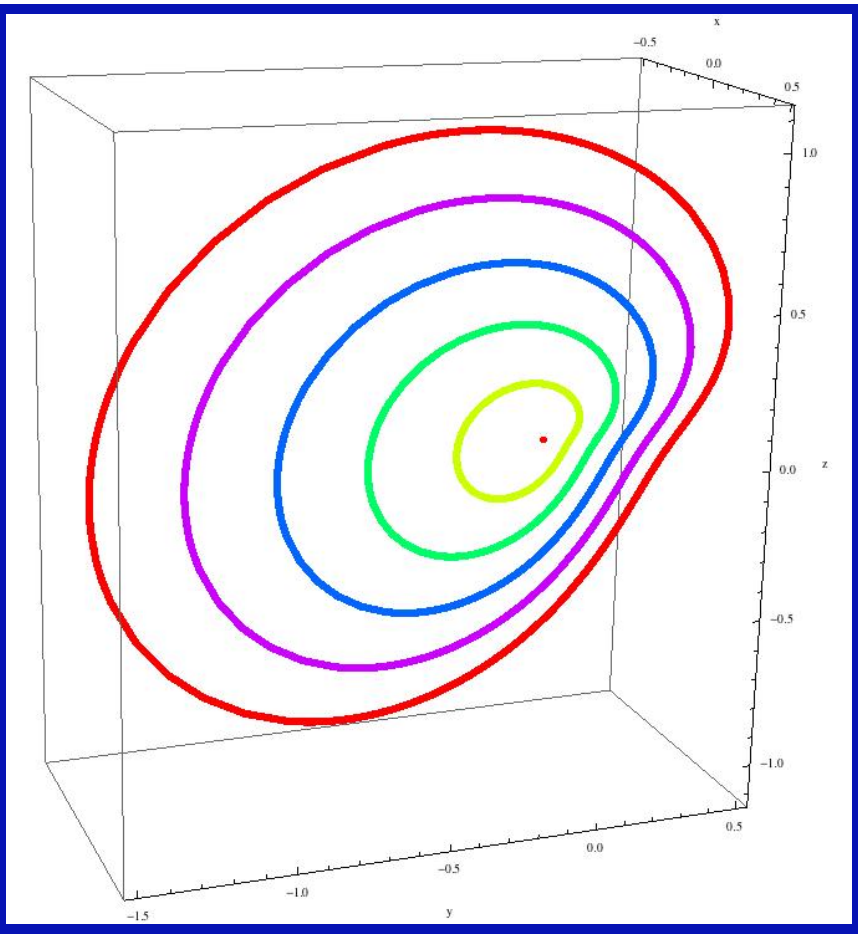

- But many experiments show that orientation selectivity *does not vanish* at singular points.

Structure near pinwheel centers

- P. E. Maldonado *et al.* have analyzed the fine-grained structure of orientation maps at the singularities. They found that

  « orientation columns contain sharply tuned neurons of different orientation preference lying in close proximity ».

- James Schummers has shown that
  - « neurons near pinwheel centers have subthreshold responses to all stimulus orientations but spike responses to only a narrow range of orientations ».

- Far from a pinwheel, cells « show a strong membrane depolarization response only for a limited range of stimulus orientation, and this selectivity is reflected in their spike responses ».
- At a pinwheel center, on the contrary, only the spike response is selective. There is a strong depolarization of the membrane for all orientations.

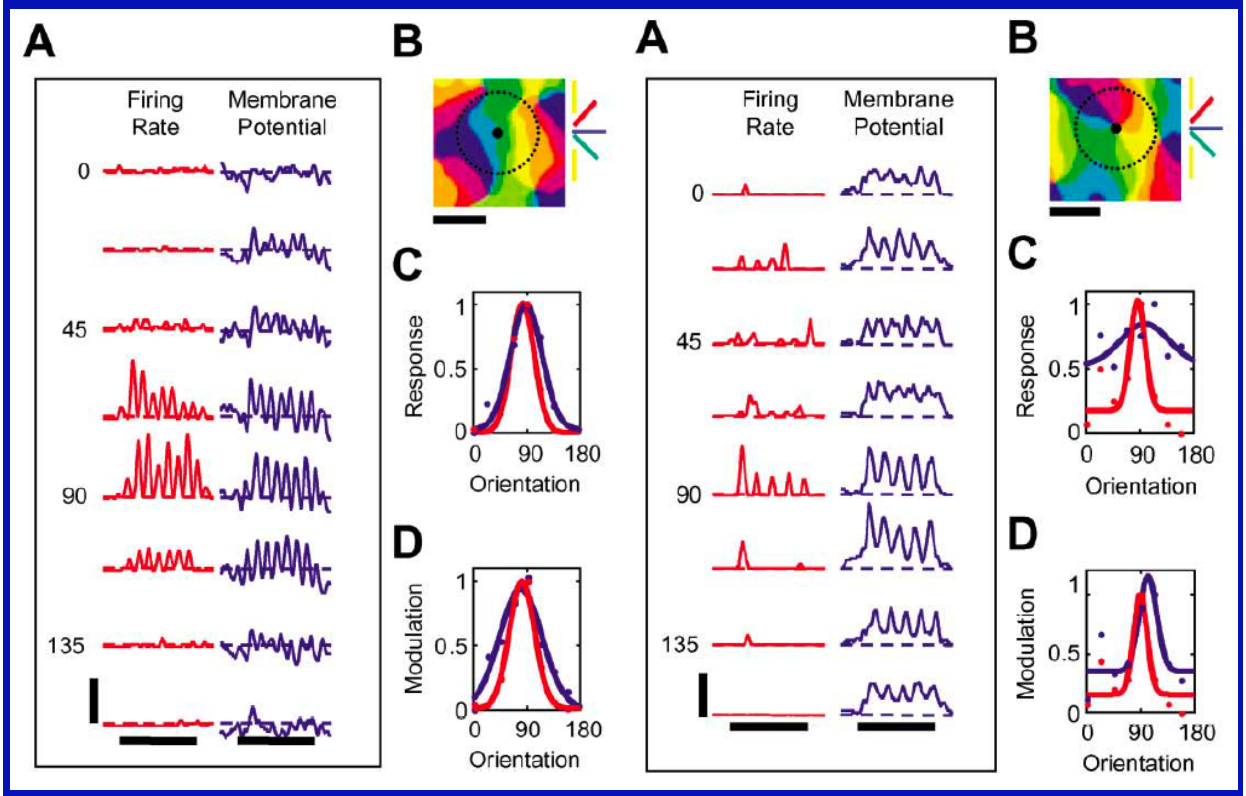

Micro structure

- The spatial (50μ) and depth resolutions of optical imaging is not sufficient.
- Two-photon calcium imaging *in vivo* (confocal biphotonic microscopy) provides functional maps at single-cell resolution.

- Kenichi Ohki, Sooyoung Chung, Prakash Kara, Mark Hübener, Tobias Bonhoeffer and R. Clay Reid:

  Highly ordered arrangement of single neurons in orientation pinwheels, Nature, 442, 925-928 (24 August 2006) .

- (In cat) pinwheels are higly ordered at the micro level and « thus pinwheels centres truly represent singularities in the cortical map ».
- Injection of calcium indicator dye (Oregon Green BAPTA-1 acetoxylmethyl esther) which labels few thousands of neurons in a 300-600μ region.
- Two-photon calcium imaging measures simultaneously calcium signals evoked by visual stimuli on hundreds of such neurons at different depths (from 130 to 290μ by 20μ steps).

- One finds pinwheels with the <u>same</u> orientation wheel.
- « This demonstrates the columnar structure of the orientation map at a very fine spatial scale ».

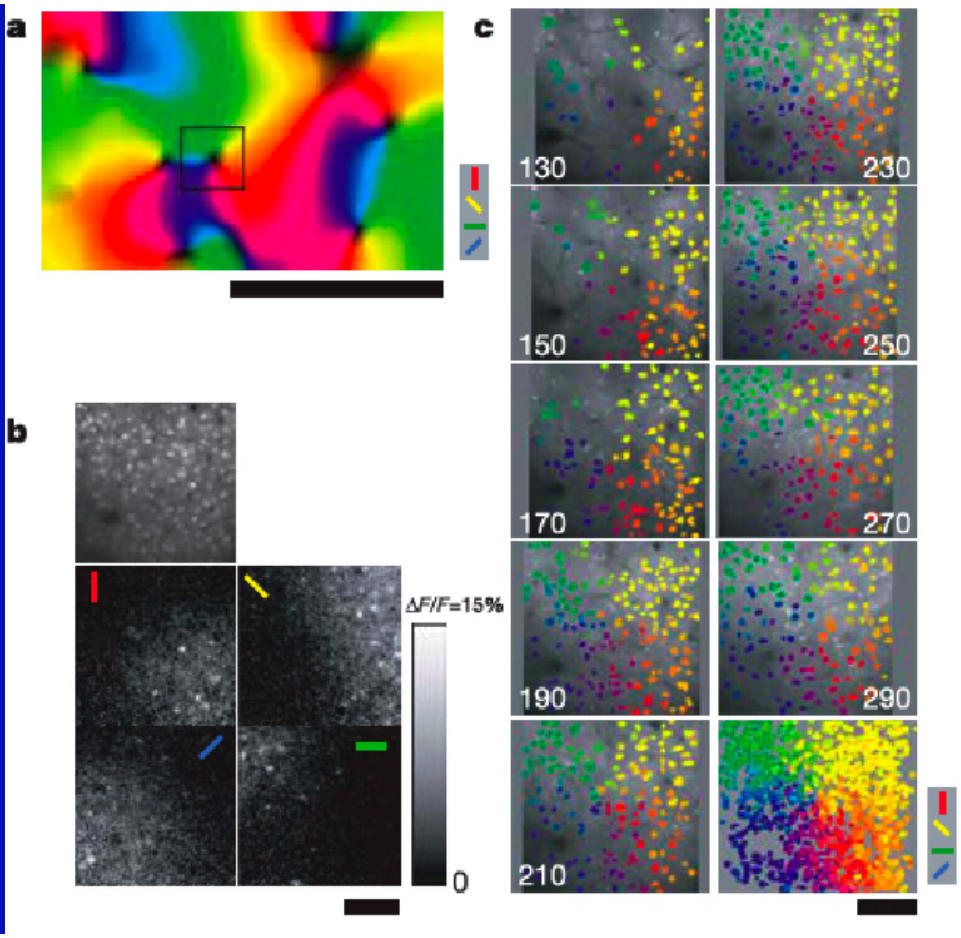

- A simple model would be r = cst = 1.
- The lift of C_ρ would then be the curve Γ_ρ

$$\left(\frac{1}{2}\rho\sin(\theta), \left(1-\frac{1}{2}\rho\cos(\theta)\right)\cos(\theta), \left(1-\frac{1}{2}\rho\cos(\theta)\right)\sin(\theta)\right)$$

- When $\rho \to 0$ we have

$$\Gamma_\rho \to (0, \cos(\theta), \sin(\theta))$$

- The projection is no longer a local diffeomorphism. Exceptional fiber.

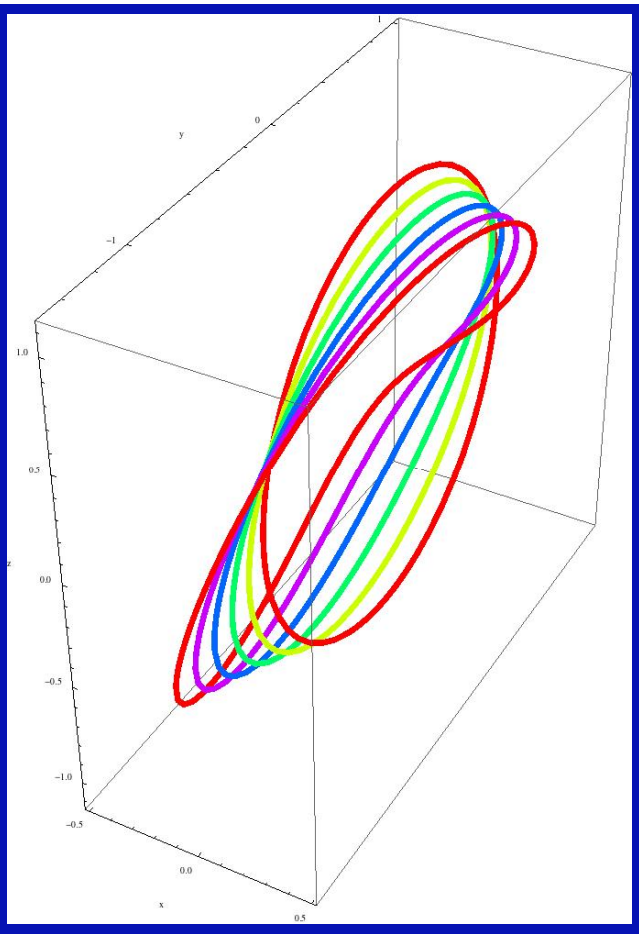

Blow-up models

- All orientations must be present with a good selectivity at the singularities.
- In fact it is a 3D abstract space

$$V = \mathbb{R}^2 \times \mathbb{P}^1$$

which is implemented into 2D neural layers.

- How ?

- An idea could be to use the concept of *blow-up*.
- The blow-up of a point $O = (0, 0)$ in the plane associates to every point

$$a = (x, y) \neq (0, 0)$$

the line Oa.

- One gets the map

$$\begin{array}{rcl} \delta : \mathbb{R}^2 - \{O\} & \longrightarrow & \mathbb{P}^1 \\ a = (x, y) & \longmapsto & \delta(a) = p = \frac{y}{x} \end{array}$$

- The graph of δ is a helicoidal ruled surface H in

$$V = \mathbb{R}^2 \times \mathbb{P}^1$$

which is isomorphic to $\mathbb{R}^2 - \{O\}$

through the projection π .

- Its closure is a helicoid with an exceptional fiber

$$\pi^{-1}(O) = \Delta \simeq \mathbb{P}^1$$

- As the inverse image of O by π is

$$\Delta = \mathbb{P}^1$$

the blow-up is in some sense of intermediary dimension between 2D and 3D. It is an unfolding of a 2D orientation wheel along a third dimension.

- In a second step, one can *localize* the blow-up model of a pinwheel and restrict it to a small neighborhood U of O.
- One can then take the germ, that is the limit w.r.t the filter of neighborhoods.
- In the germ, $p = \frac{dy}{dx}$ is in the kernel of the 1-form

$$\omega = dy - pdx$$

- On can then “compactify” the fiber (à la Kaluza-Klein) and pull it down in the base space.
- One gets that way a model for a single pinwheel.

- In this perspective a pinwheel is like a “fat point” in Deligne's sense.
- In a letter (1986) concerning singularities of analytic functions, P. Deligne introduced the idea of substituting to a point $a = 0$, a small disk D with boundary $\partial D = \Delta$ and consider the space

$$\widetilde{\mathbb{C}} = \mathbb{C}^* \cup D$$

with the topology of the real blowing-up on

$$\mathbb{C}^* \cup \Delta$$

- In a third step, one can blow-up *in parallel* several points a_i and glue the local pinwheels (a_i, Δ_i) using a field endowing the a_i with topological charges (chirality).
- One gets that way a model of a network of pinwheels.

Towards continuous models

- In a fourth step, one can go in a different direction and consider lattices of singular points a_i with a mesh $\to 0$.
- The idea is that one could recover the fibration

$$V = \mathbb{R}^2 \times \mathbb{P}^1$$

and its contact structure by blowing-up in parallel all the points of the plane.

- It is possible to use non standard analysis (Robinson-Luxemburg).
- In his last paper (edited on 1992 by Jean-Pierre Ramis) Jean Martinet proposed to interpret "fat points" using non standard analysis : take for D an infinitesimal disk with only one standard point (the center).

- One restricts the infinitesimal model to the monads

$$\mu(a) = \{(x + dx, y + dy)\}$$

of the standard points a of the plane.

- When one blows-up a in the monad, one gets an exceptional fiber Δ^* whose standard points correspond to standard orientations.
- We work now in the fibration $V = \mathbb{R}^2 \times \mathbb{P}^1$

Functional architecture

- We work now in the fibration $V = \mathbb{R}^2 \times \mathbb{P}^1$
- The "local" "vertical" retino-geniculo-cortical connections inside the pinwheels (hypercolumns) are not sufficient for perception.
- A <u>functional architecture</u> (FA) is necessary.
- With the FA, for neurons: to be activated = to do geometry.

- To implement a global coherence of contours, the visual system must be able to compare two retinotopically neighboring hyper-columns P_a et P_b over two neighboring points a and b.

- This is a process of parallel transport implemented by the lateral ("horizontal") cortico-cortical connections.
- Cortico-cortical connections connect neurons coding contact elements (a, p) and (b, q) such that p is approximately parallel to q and p and q are approximately the orientation of the line ab.
- (a, p) and (b, q) are almost *coaxial (i.e. aligned)*.

- The next slide shows how a marker (biocytin) injected locally in a zone of specific orientation (green-blue in the upper-left corner) diffuses via horizontal cortico-cortical connections.
- The key fact is that the long range diffusion is highly anisotropic and restricted to zones of the same orientation (the same color) as the initial one.
- Moreover, the clustering along the diagonal means *coaxiality*.

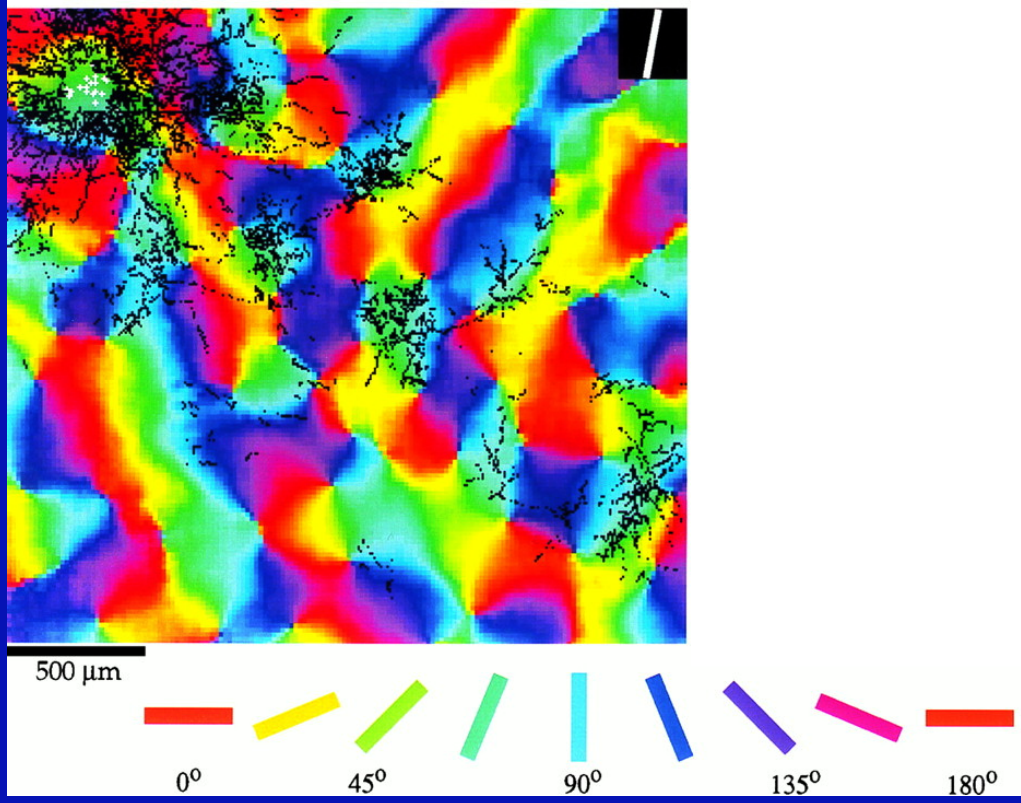

- W. Bosking :
  - « The system of long-range horizontal connections can be summarized as preferentially linking neurons with co-oriented, co-axially aligned receptive fields ».
- So, the well known Gestalt law of “good continuation” is neurally implemented.
- In fact, a certain amount of <u>curvature</u> is allowed in alignements.

- These experimental results mean essentially that the <u>contact structure</u> of the fiber bundle

$$\pi : V = R \times P \rightarrow R$$

is neurally implemented with

- dimensional collapse,
- discretization,
- population coding.

The contact structure of V1

- The simplest model of the functional architecture of V1 is the space of 1-jets of curves C in R.
- If C is a regular curve in R (a contour), it can be lifted to V. The lifting Γ is the map (1-jet)

$$j : C \rightarrow \quad V = R \times P$$

  wich associates to every point a of C the pair (a, p_a) where p_a is the tangent of C at a.
- Γ is the Legendrian lift of C.

- Conversely, if $\Gamma = (a, p) = (x, y(x), p(x))$ is a curve in V, the projection $a = (x, y(x))$ of Γ is a curve C in R. But Γ is the lifting of C iff $p(x) = y'(x)$.
- This is an integrability condition. It says that to be a coherent curve in V, Γ must be an integral curve of the contact structure of the fibration π.

- The condition is that at every point (a, p) of Γ the tangent vector t is in the kernel of the differential 1-form

$$\omega = dy - pdx$$

This kernel is the *contact plane* of V at (a, p).

- <u>The underlying neural functional micro connectivity is expressed geometrically by a differential form</u>.

- The vertical component p' of the tangent vector is the <u>curvature</u> :

$$p = y' \Rightarrow p' = y''$$

- The 2D contact distribution is <u>not integrable</u>. It has no integral surfaces but only integral curves.
- Indeed, $\omega \wedge d\omega = \text{volume form}$ while Frobenius integrability condition is $\omega \wedge d\omega = 0$.

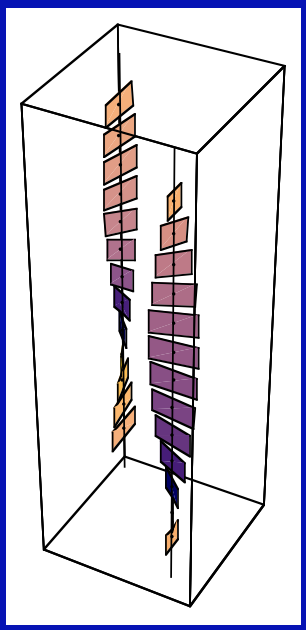

- V1 is like a Lie-Cartan neural machine : a 2D neural implementation of (at least) a contact structure.
- Hence the idea of translating visual problems into problems of contact geometry.
- Even if the mathematical tools are rather elementary, <u>the fact that they are neurally implemented is highly non trivial</u>.

- For instance developement and learning can be translated into a problem of deformation of an initial functional architecture into a contact structure.

Fonctionality of jet spaces

- The functional interest of jet spaces is that they can be implemented by “point processors” (Koenderink) such as neurons.
- But then a functional architecture is needed.
- Functional architectures between point processors can compute features of differential geometry.

- The key idea is
  - (1) to add new independent variables describing local features such as orientation.
  - (2) to introduce an integrability constraint to integrate them into global structures.
- Neuro-physiologically, this means to add feature detectors and to couple them via a functional architecture in order to ensure binding.

Integrability condition and Association field

- The integrability condition corresponds to the psychophysical experiments on the <u>association field</u> (David Field, Anthony Hayes and Robert Hess).
- They explain experiments on good continuation : pop out of a global curve against a background of randomly distributed distractors

- Let (a_i, p_i) be a set of segments embedded in a background of randomly distributed distractors. The segments generate a perceptively salient curve (pop-out) iff the p_i are tangent to the curve C optimally interpolating between the a_i.

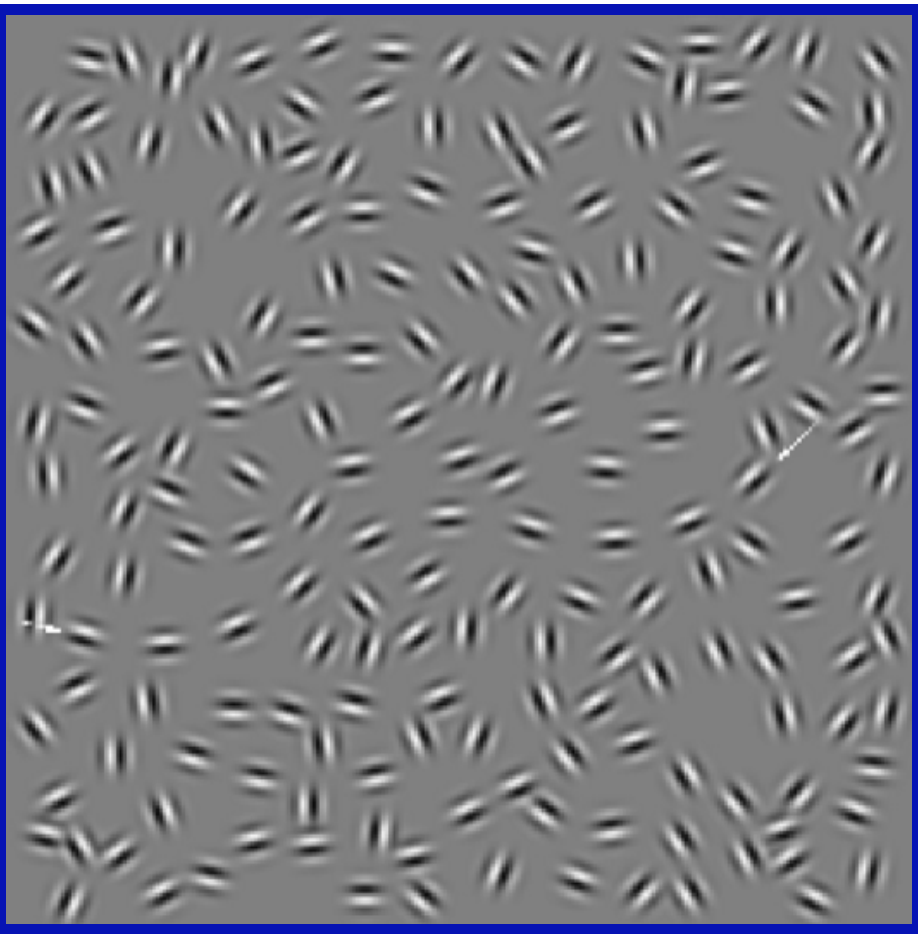

- This is a discretized version of the integrability condition.
- The integrability induces a binding of the local elements. The activities of the neurons detecting them are synchronized and the synchronization produces the pop out.

- One must have the following type of horizontal connectivity :

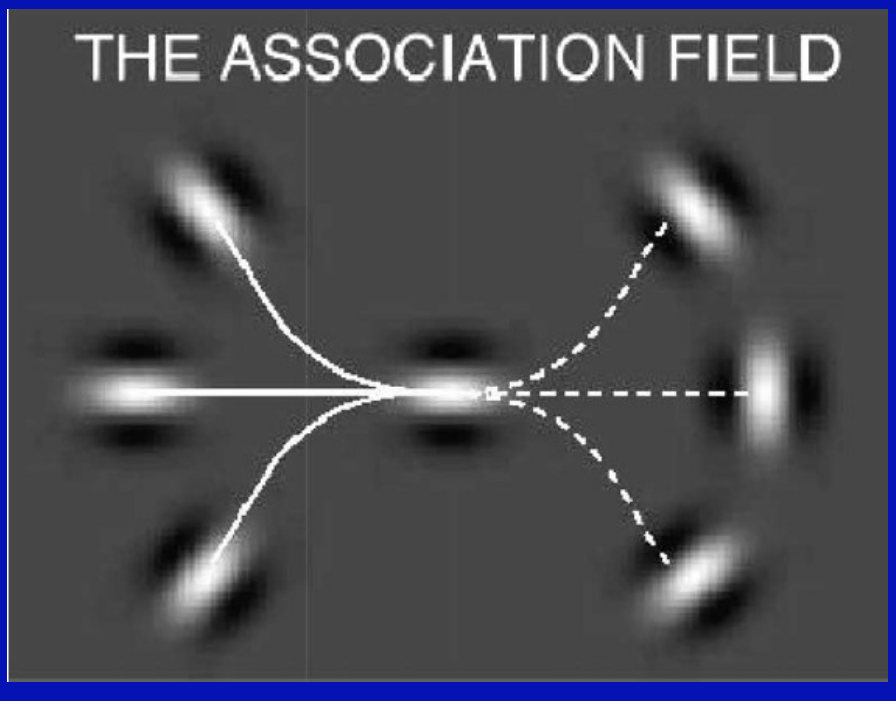

- But this is exactly the integrability condition : the association field (left) correspond to the simplest integral curves of the contact distribution (right).

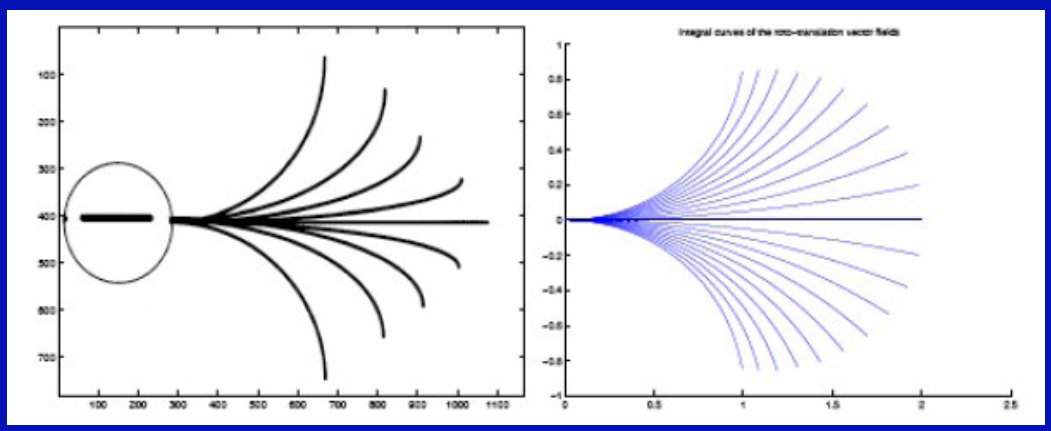

Other “engrafted” variables

- Orientation is not the only engrafted variable.

- Variation of phase (De Angelis 1999) : in a single column « spatial phase is the single parameter that accounts for most of the difference between receptive fields of nearby neurons ».
- The figure compares the complete RFs (*X*, *Y* = space, *T* = time = delay correlation) of two nearby cells in a column. Visuotopy, orientations, spatial frequencies are the same, but not the phases.

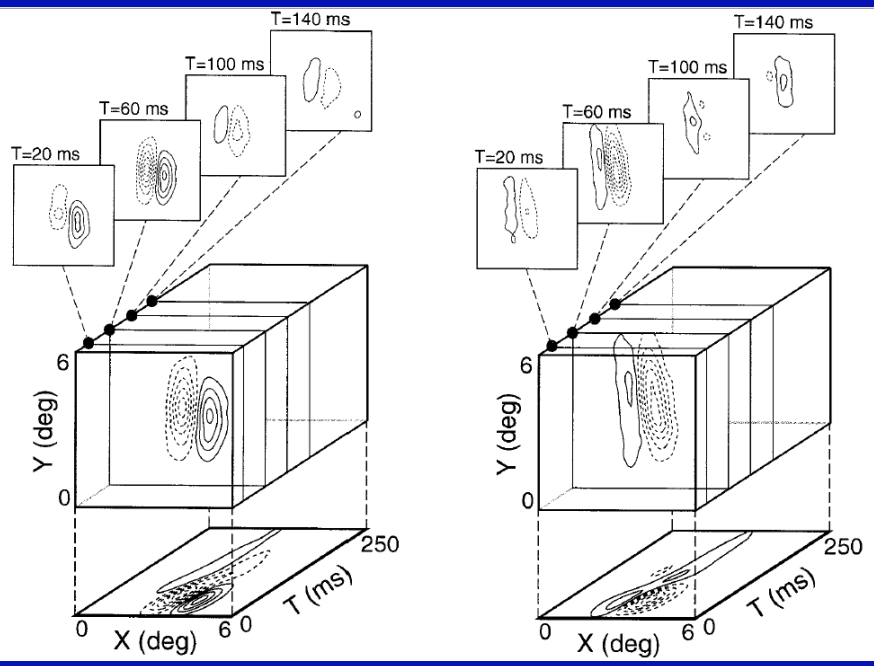

Spatial frequency

- Pinwheels (A) and spatial frequencies (B. red = low SF, purple = high SF) (Issa *et al.*)

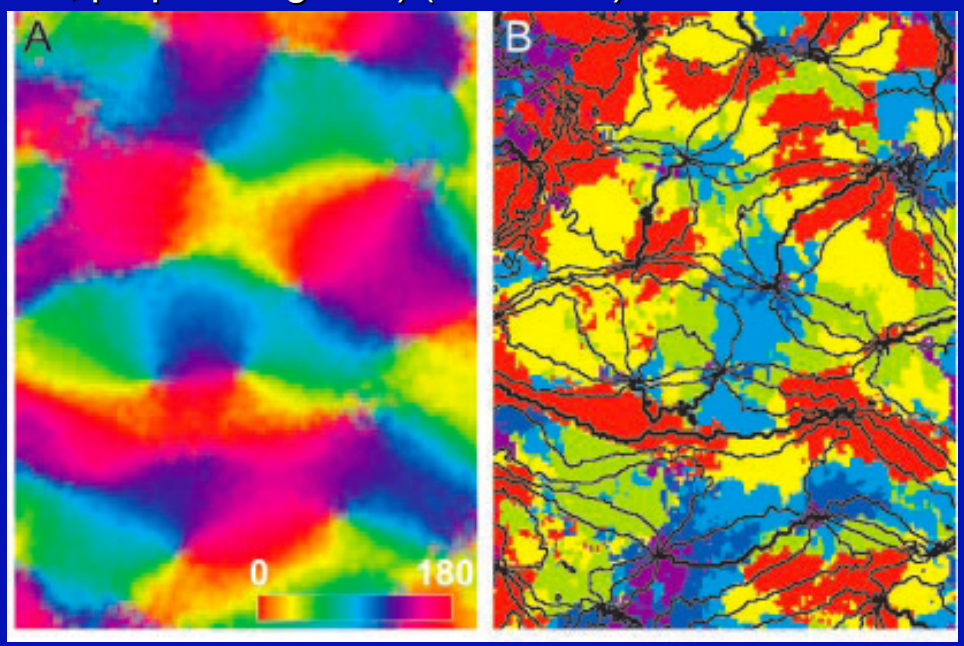

- Pinwheels and ocular dominance (G. Goodhill).
- The independance of the two features is expressed by strong transversality conditions.

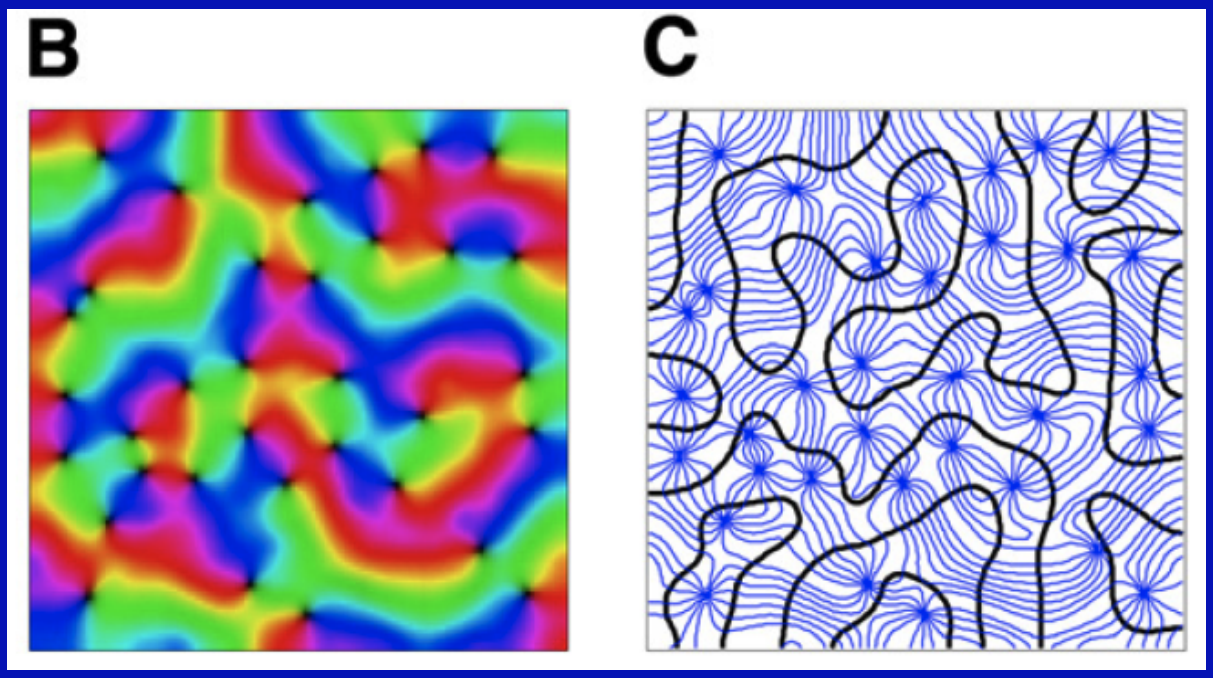

- Pinwheels, ocular dominance, blobs (Blasdel, Oster).

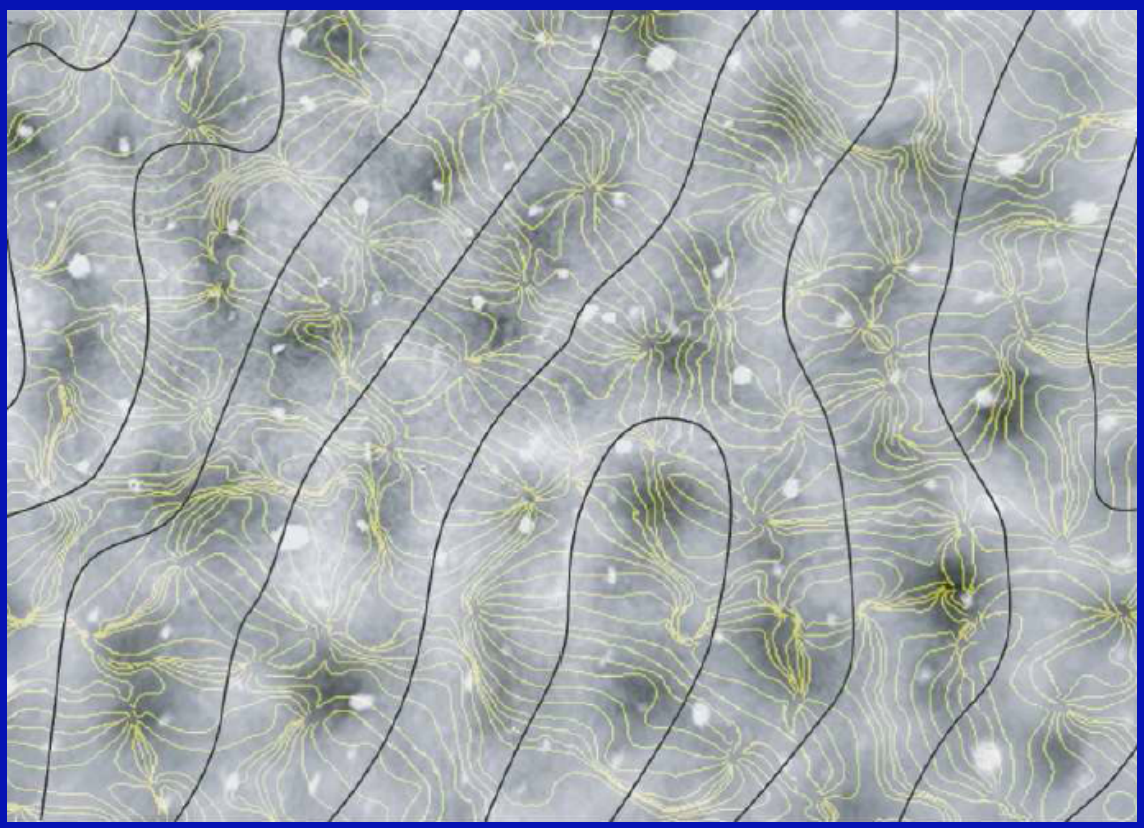

Gluing processes

- We mention also the gluing process performed by callosal connexions between the two hemispheric parts of V1.
- The corpus callosum is the largest bundle of neural fibers in mammals. For man, it contains 200 millions axons (to compare with the 1.5 million axons of the optic nerve).

- The function of the Corpus Callosum is fundamental since it glues the two V1 areas along a transition zone (TZ) mapping the region near the vertical visual meridian (VM).
- The TZ is located near the boundary V1 / V2 (areas 17/18 in the cat).

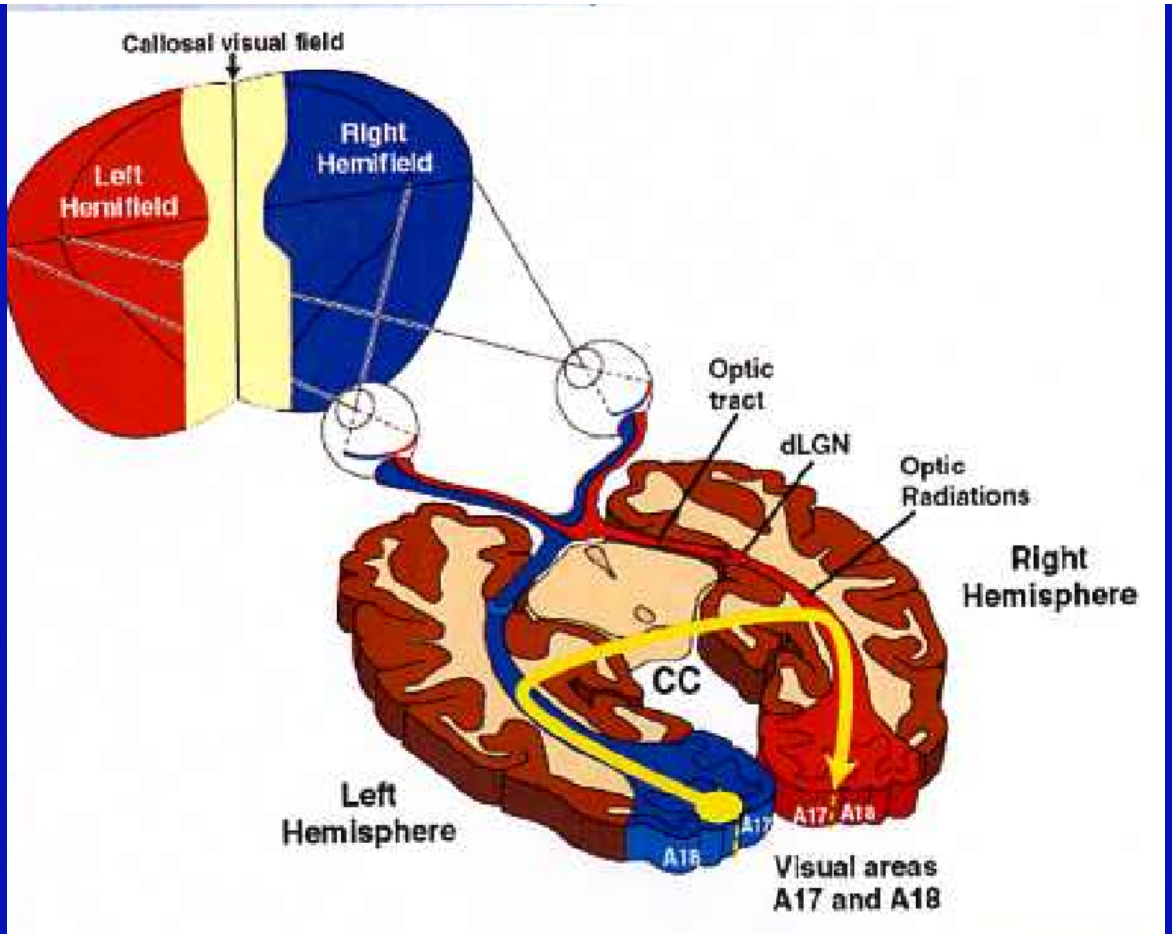

- The gluing map is quite fascinating. In the following figure, cortical loci A,B,C,D,E in one hemisphere are callosally connected to the loci identically labeled in the other hemisphere.
- The loci inside TZ are connected to loci outside TZ and conversely.

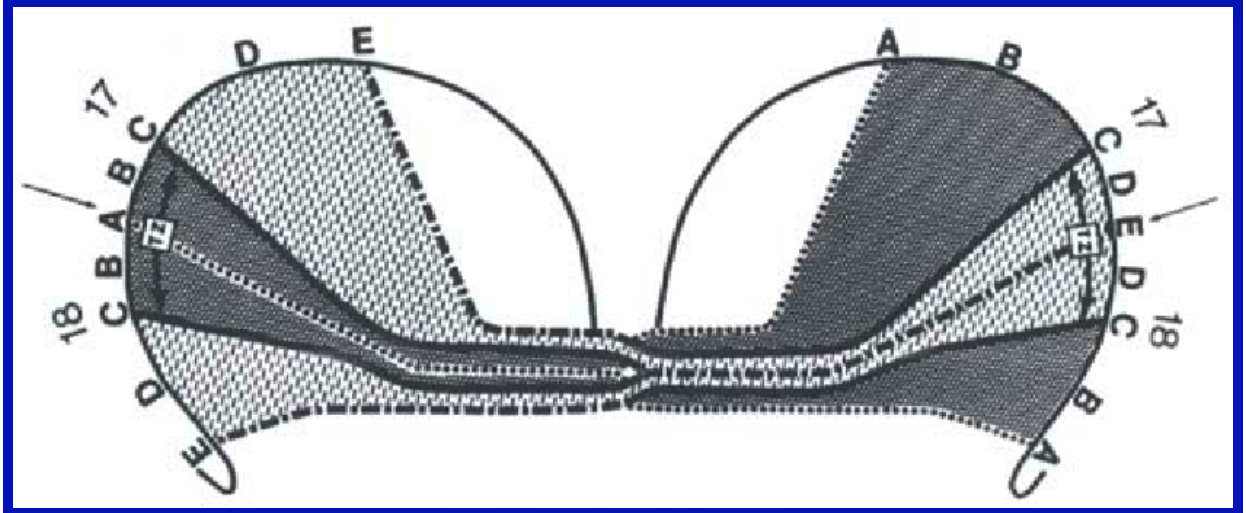
D
E
A
B
17
C
B
A
C
18
C
D
E
D
C
18
B
A
E

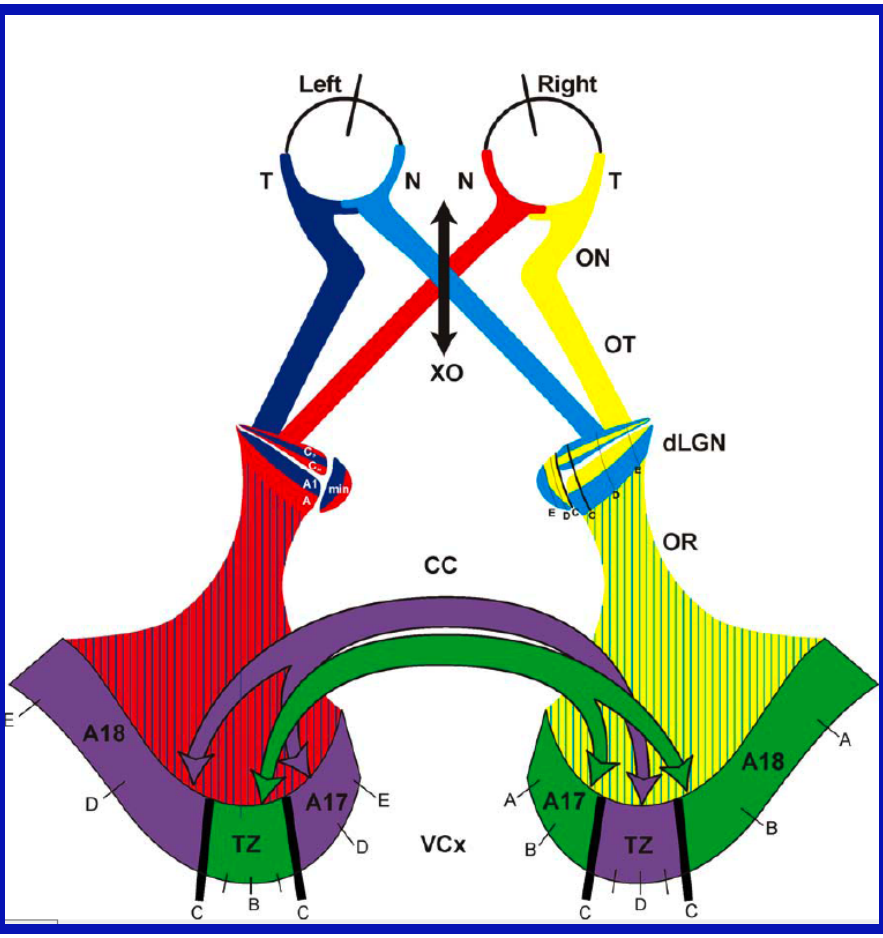
Left
Right
T
N
N
T
ON
OT
XO
dLGN
OR
CC
A18
A17
TZ
VCx
A18
A17
TZ

- For the tree shrew (tupaya), if one injects rhodamine in a small region of $V1_L$ of vertical preference (red circle in a black region) and fluorescein in another of horizontal preference (green circle in a nearby white region), the callosal projections on $V1_R$ show no orientation specificity.

W. Bosking et al., *The Journal of Neuroscience*, 2000, 20(6), 2346-2359

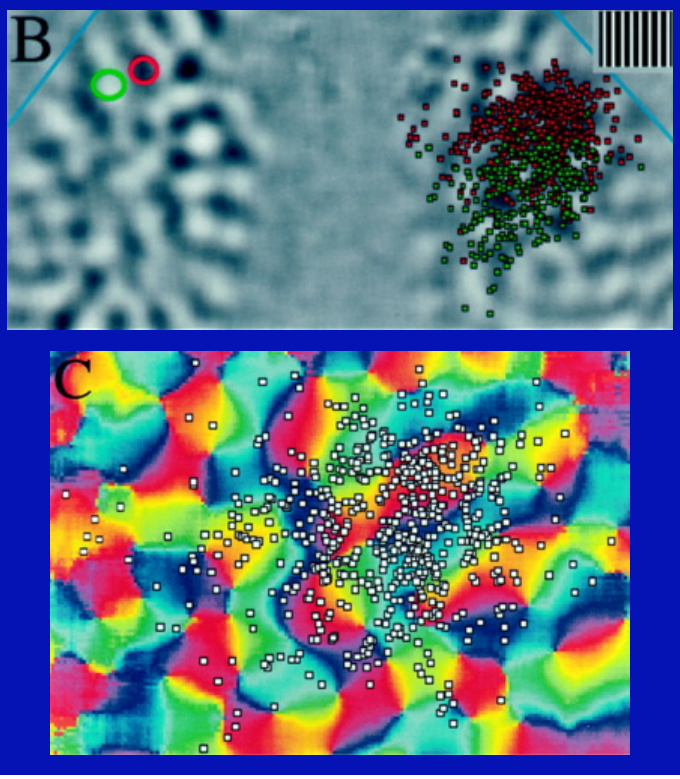

- But Chantal Milleret and Nathalie Rochefort (Collège de France, Paris) have shown that it is completely different for the cat : callosal connections preserve orientation selectivity.
- “Layout of transcallosal activity in cat visual cortex revealed by optical imaging”, *Neuroimage*, 2007, 36(3): 804-21.
- Rochefort’s thesis : “Functional specificity of callosal connections in the cat visual cortex”.

- The method is that of split-chiasm preparation. If you section the optic chiasm, you cut the crossed fibers coming from the nasal hemiretinae. Only the ipsilateral pathes (coming from the temporal retinae) remain.
- If only the right eye is activated, then the activity of the left V1 comes entirely from the callosal connections.

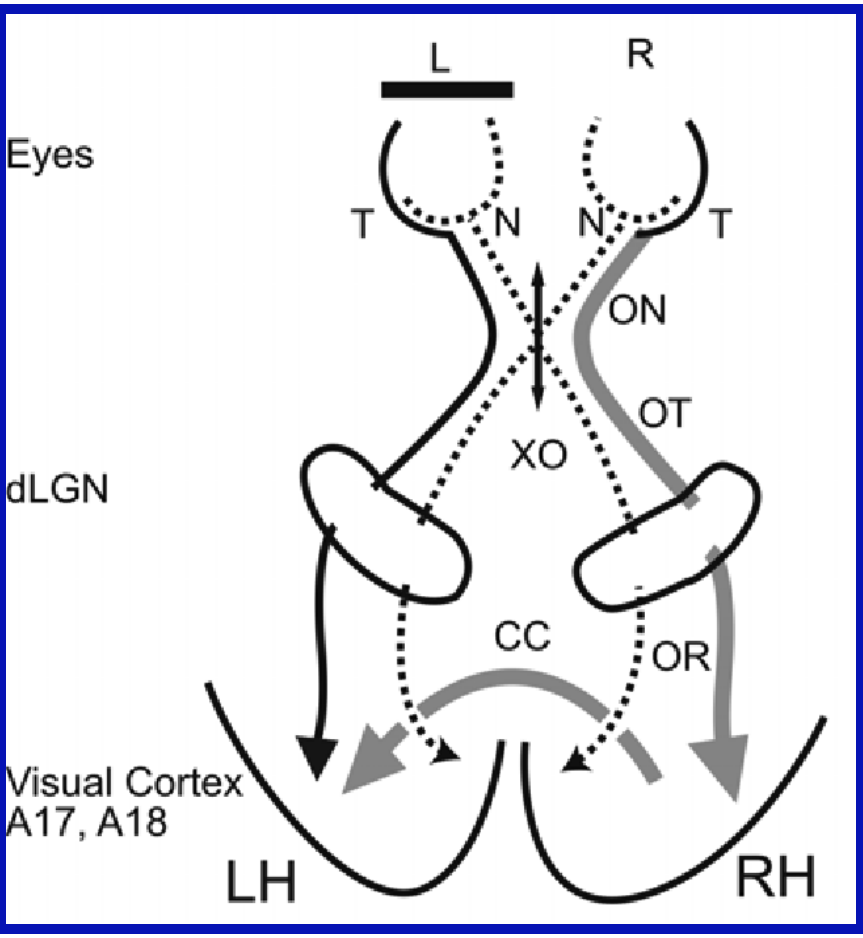

- In the beautiful following figure, the injection site is in the left hemisphere and the distribution of the synaptic boutons of one callosal axon (axon 7 of cat 9) is marked in the right hemisphere.
- The concerned pinwheel zones are isochromatic, which proves that orientation is preserved by callosal connections.

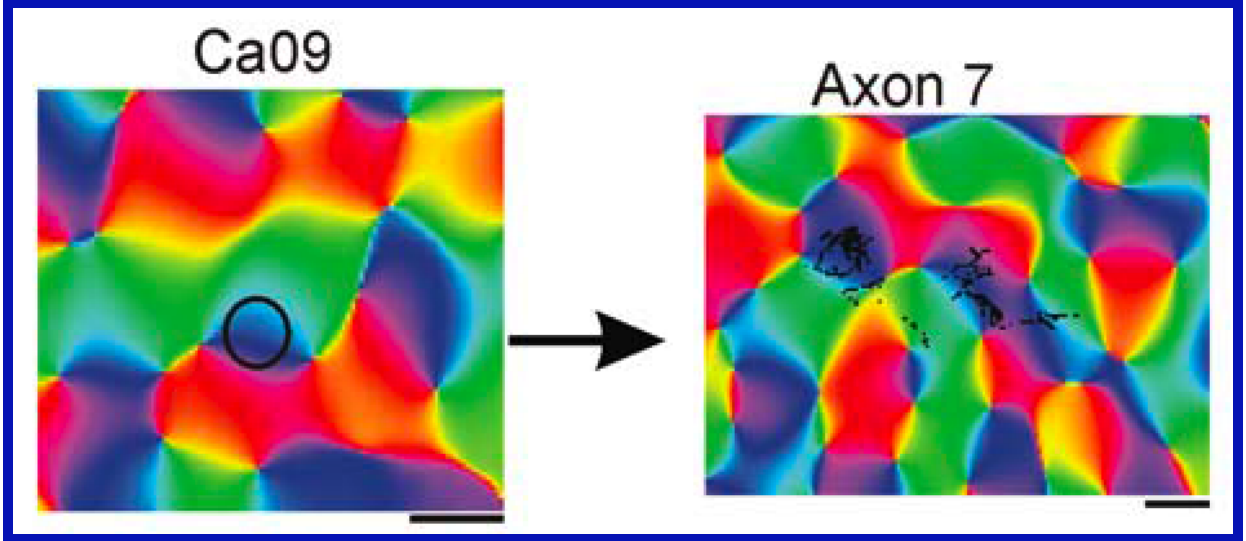

Towards neurogeometry

- The apparently trivial condition

$$\omega = dy - pdx = 0$$

  contains in fact a rich geometry.

- It results from the action of a group.

Contact structure and Heisenberg group

- The contact structure on V is a left-invariant distribution of planes for a group structure which is the <u>polarized</u> Heisenberg group :

$$(x, y, p).(x', y', p') = (x + x', y + y' + px', p + p')$$

- If $t = (\xi, \eta, \pi)$ are the tangent vectors of $\mathfrak{V} = T_0 V$, the Lie algebra of V has the Lie bracket

$$[t, t'] = [(\xi, \eta, \pi), (\xi', \eta', \pi')] = (0, \xi'\pi - \xi\pi', 0)$$

- $(0, 0, 0)$ is the neutral element.
- If $v = (x, y, p)$, v^{-1} (or $-v$ in additive notation) is $(-x, -y + px, -p)$.

- The Lie algebra $\mathfrak{V} = T_0 V$ is spanned by
  $X_1 = \partial_x + p\partial_y = (1, p, 0)$,
  $X_2 = \partial_p = (0, 0, 1)$,
  and
  $[X_1, X_2] = -X_3 = -\partial_y = (0, -1, 0)$
  (other brackets $= 0$).

- The contact plane are spanned by X_1 and X_2, and the contact distribution is therefore <u>bracket generating</u> (Hörmander condition).

- A consequence is <u>Chow theorem</u> : two points of V can always be joined by an integral curve.

- In matrix terms, $v = (x, y, p)$ and $t = (\xi, \eta, \pi)$ can be written

$$\begin{pmatrix} 1 & p & y \\ 0 & 1 & x \\ 0 & 0 & 1 \end{pmatrix} \qquad \begin{pmatrix} 0 & \pi & \eta \\ 0 & 0 & \xi \\ 0 & 0 & 0 \end{pmatrix}$$

- So the inner automorphisms are :

$$\begin{array}{llll} A_v : & v' & \mapsto & v.v'.v^{-1} \\ & (x', y', p') & \mapsto & (x', y' + px' - p'x, p') \end{array}$$

- The tangent map of A_v at 0 is :

$$Ad_v = \begin{pmatrix} 1 & 0 & 0 \\ p & 1 & -x \\ 0 & 0 & 1 \end{pmatrix}$$

$$Ad_v(t) = (\xi, p\xi + \eta - x\pi, \pi)$$

- This yields the <u>adjoint representation</u> of the Lie group V on its Lie algebra $\mathfrak{V} = T_0V$.

- For the <u>coadjoint representation</u>, take the basis $\{dx, dy, dp\}$ for the 1-forms of $\mathfrak{V}^*$:

$$\gamma = \mu dx + \lambda dy + \nu dp \in \mathfrak{V}^*$$

- We get, using $\langle Ad_v^*(\gamma), t\rangle = \langle \gamma, Ad_{-v}(t)\rangle$

(verify – *v*)

$$Ad_v^*(\gamma) = \mu' dx + \lambda' dy + \nu' dp$$

$$\begin{cases} \mu' = \mu - \lambda p \\ \lambda' = \lambda \\ \nu' = \nu + \lambda x \end{cases}$$

- <u>Orbits</u> :
  - If $\lambda \neq 0$, planes $\lambda = \mathrm{cst}$.
  - If $\lambda = 0$, every point of the $(\mu, 0, \nu)$ plane is a degenerate orbit.

Unitary irreducible representations

- The unitary irreducible representations (unirreps) of this group are given by the Stone - von Neumann theorem.

- The unirreps of V are either trivial ones of dimension 1 multiplying $z \in \mathbb{C}$ by

$$\pi_{\mu,\nu}(x, y, p) = e^{i(\mu x + \nu p)}$$

or infinite dimensional ones operating in the Hilbert space $L^2(\mathbb{R})$

$$\pi_\lambda(x, y, p)\, u(s) = e^{i\lambda(y + xs)} u(s + p), \text{ with } \lambda \neq 0$$

- Kirillov : they correspond to the orbits of the coadjoint representation of V.
- Planes $\lambda = \mathrm{cst}$ for $\lambda \neq 0$ correspond to

$$\pi_\lambda(x, y, p)\, u(s) = e^{i\lambda(y+xs)} u(s+p), \text{ with } \lambda \neq 0$$

- Points of the $(\mu, 0, \nu)$ plane for $\lambda = 0$ correspond to

$$\pi_{\mu,\nu}(x, y, p) = e^{i(\mu x + \nu p)}$$

The neurogeometrical problem of illusory contours

- A typical example of the problems of neuro-geometry is given by well known Gestalt phenomena such as Kanizsa illusory contours.
- The visual system (V1 with some feedback from V2) constructs very long range and crisp virtual contours.
- They are in fact boundaries of virtual *surfaces* but we will restrict to the 1D problem.

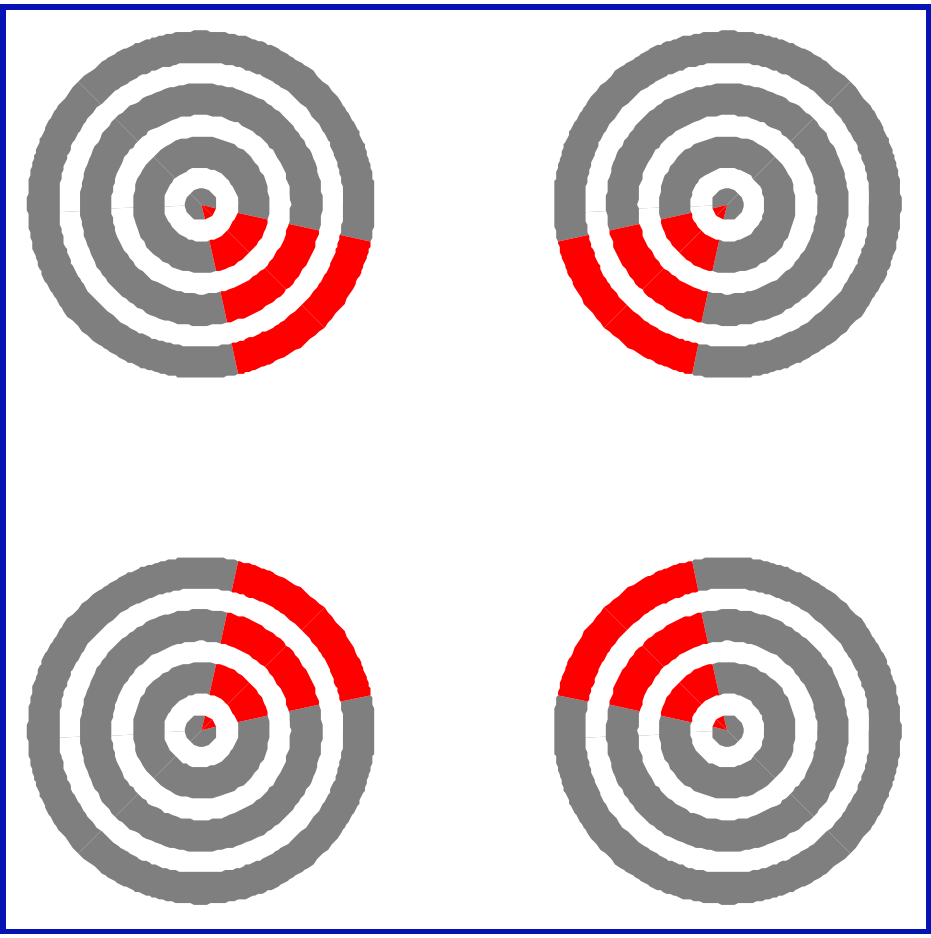

Sub-Riemannian geometry

- In this neuro-geometrical framework, we can easily interpret the variational process giving rise to illusory contours.
- The idea is to use a <u>geodesic</u> model in the sub-Riemannian geometry associated to the contact structure.
- This generalizes the “elastica” model proposed by David Mumford.

- If $\mathcal{K}$ is the contact structure on V and if one considers only curves Γ in V which are integral curves of $\mathcal{K}$, then metrics $g_{\mathcal{K}}$ defined only on the planes of the distribution $\mathcal{K}$ are called <u>sub-Riemannian</u> metrics.

- In a Kanizsa figure, two pacmen of respective centers a and b with a specific aperture angle define two elements (a, p) and (b, q) of V.
- An illusory contour interpolating between (a, p) and (b, q) is
  - 1. a curve C from a to b in R with tangent p at a and tangent q at b ;
  - 2. a curve minimizing an “energy” (variational problem), that is a geodesic for some sub-Riemannian metric.

- It is natural to take on the contact planes the metric making orthonormal their generators :

$$X_1 = \partial_x + p\partial_y , \quad X_2 = \partial_p .$$

- It is the Euclidean metric for X_2 whose Euclidean norm is 1, but not for X_1 whose Euclidean norm is $(1 + p^2)^{1/2}$ and not 1.

- We compute the <u>sub-Riemannian sphere</u> S and the <u>wave front</u> W (geodesics of SR length 1) (it is a variant of Beals, Gaveau, Greiner computations).

- <u>Sphere</u> $S(v, r) = \{ w : d(v, w) = r$ (geodesics of length r that are global minimizers)$\}$.
- <u>Wave front</u> $W(v, r) = \{ w : \exists$ a geodesic $\gamma : v \to w$ of length r (not necessarily a global minimizer)$\}$.
- <u>Cut locus</u> of $v = \{ w : w$ end point of a geodesic $\gamma : v \to w$ which is no longer globally minimizing $\}$.
- <u>Conjugate locus</u> of v = <u>caustic</u> = Σ_v = { singular locus of the exponential $\mathscr{E}_v$ }.

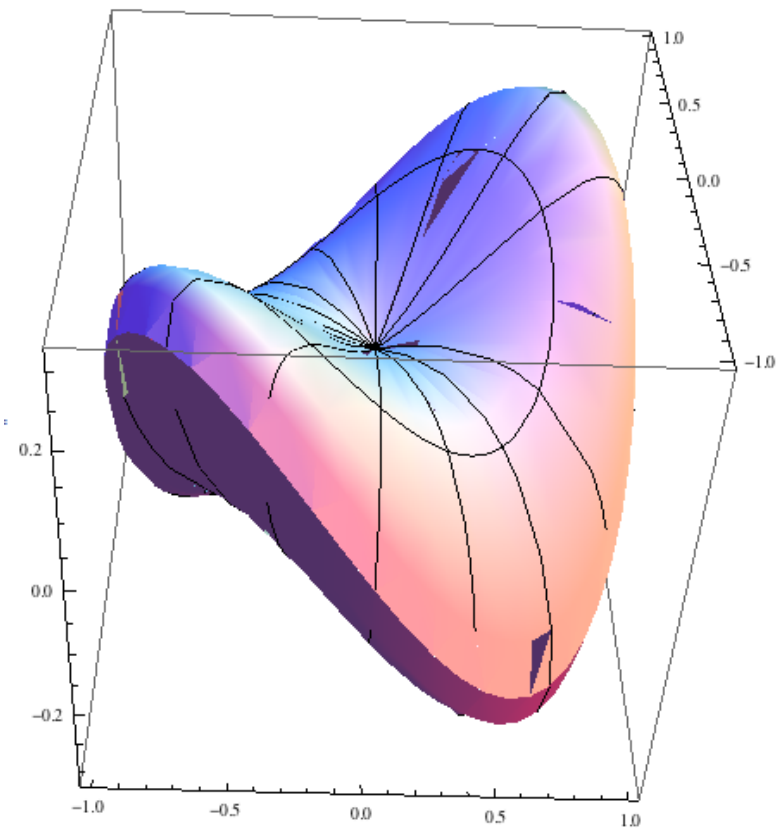

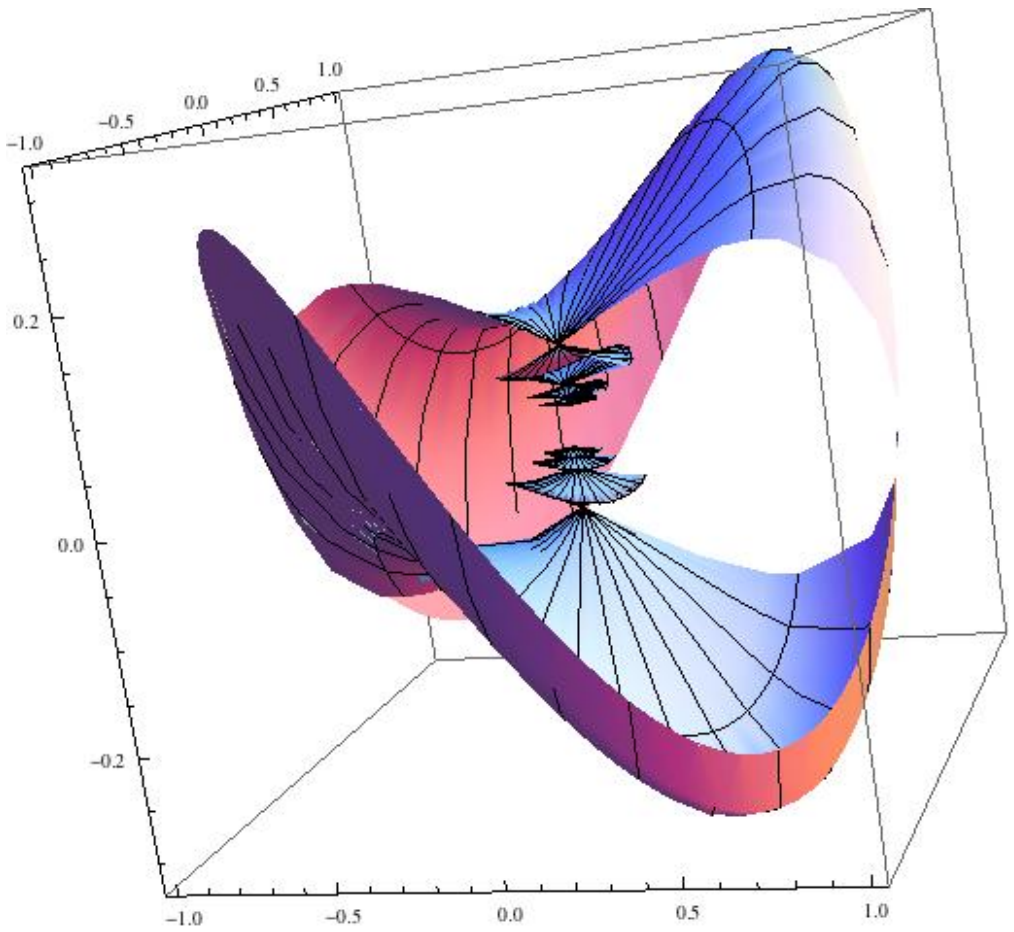

- Geodesics are projections on V of <u>Hamiltonian</u> trajectories of an Hamiltonian H defined on the cotangent bundle of V.
- It is a consequence of Pontryagin maximum principle.

- H corresponds to the kinetic energy (ξ, η, π are the conjugate momenta of x, y, p).

$$H(x, y, p, \xi, \eta, \pi) = \frac{1}{2}\left[(\xi + p\eta)^2 + \pi^2\right]$$

- Hamilton equations are

$$\begin{cases} \dot{x}(s) = \frac{\partial H}{\partial \xi} = \xi + p\eta \\ \dot{y}(s) = \frac{\partial H}{\partial \eta} = p(\xi + p\eta) = p\dot{x}(s) \text{ i.e. } p = \frac{\dot{y}}{\dot{x}} = \frac{dy}{dx} \\ \dot{p}(s) = \frac{\partial H}{\partial \pi} = \pi \\ \dot{\xi}(s) = -\frac{\partial H}{\partial x} = 0 \\ \dot{\eta}(s) = -\frac{\partial H}{\partial y} = 0 \\ \dot{\pi}(s) = -\frac{\partial H}{\partial p} = -\eta(\xi + p\eta) = -\eta\dot{x}(s) \end{cases}$$

- The momenta ξ and η are constant since H is independent of x and y.

- The integration of the (x, p) part is the easiest (τ is the end time and x_1, y_1, p_1 the end point of the geodesic starting at 0).
- Let $z = (x, p)$ and write :

$$\chi = (\xi, \pi),\ \varsigma = (\xi + p\eta, \pi) = \chi + \eta\Lambda(z) = (\dot{x}, \dot{p}),$$

$$\begin{aligned} \Lambda &= \begin{pmatrix} 0 & 1 \\ 0 & 0 \end{pmatrix}, \Lambda^T = \begin{pmatrix} 0 & 0 \\ 1 & 0 \end{pmatrix} \\ -\Lambda^T + \Lambda &= J = \begin{pmatrix} 0 & 1 \\ -1 & 0 \end{pmatrix} \\ J^2 &= -\mathbf{1} \end{aligned}$$

- The Hamilton equations write

$$\begin{cases} \dot{z}(s) = \frac{\partial H}{\partial \boldsymbol{\chi}} = \boldsymbol{\varsigma}(s) \\ \dot{y}(s) = \frac{\partial H}{\partial \boldsymbol{\eta}} = p(\xi + p\eta) = \langle \boldsymbol{\varsigma}, \boldsymbol{\Lambda}(z) \rangle \\ \dot{\boldsymbol{\chi}}(s) = -\frac{\partial H}{\partial z} = (0, -\eta(\xi + p\eta)) = -\eta \boldsymbol{\Lambda}^T(\varsigma) \\ \dot{\eta}(s) = 0, \eta = \text{cst} = \eta_0 \end{cases}$$

- So

$$\begin{aligned} \dot{\boldsymbol{\varsigma}}(s) &= \dot{\boldsymbol{\chi}}(s) + \eta\Lambda\dot{z}(s)\ (\text{car } \eta = \text{cste}) \\ &= -\eta\boldsymbol{\Lambda}^T(\varsigma) + \eta\Lambda\boldsymbol{\varsigma}(s) = \eta J\boldsymbol{\varsigma}(s) \\ (\ddot{x}, \ddot{p}) &= \eta J(\dot{x}, \dot{p}) \end{aligned}$$

- This yields

$$\varsigma(s) = e^{-s\eta J}\varsigma(0)$$

$$\begin{cases} x(s) = \frac{\sin\left(\frac{s}{2}\eta_0\right)}{\sin\left(\frac{\tau}{2}\eta_0\right)}\left(\cos\left(\frac{(\tau-s)}{2}\eta_0\right)x_1 - \sin\left(\frac{(\tau-s)}{2}\eta_0\right)p_1\right) \\ p(s) = \frac{\sin\left(\frac{s}{2}\eta_0\right)}{\sin\left(\frac{\tau}{2}\eta_0\right)}\left(\sin\left(\frac{(\tau-s)}{2}\eta_0\right)x_1 + \cos\left(\frac{(\tau-s)}{2}\eta_0\right)p_1\right) \end{cases}$$

- The integration of y is more complex. We get :

$$\begin{aligned} y(s) - y_0 \quad = \quad & \frac{1}{8(\cos(\eta_0\tau)-1)}[-2\eta_0 s\left(x_1^2+p_1^2\right) - 4x_1p_1\cos(\eta_0(s-\tau)) + \\ & 2\left(x_1^2-p_1^2\right)\sin(\eta_0(s-\tau)) + \\ & 2x_1p_1\cos(\eta_0(2s-\tau)) - \left(x_1^2-p_1^2\right)\sin(\eta_0(2s-\tau)) + \\ & 2x_1p_1\cos(\eta_0\tau) + \left(x_1^2-p_1^2\right)\sin(\eta_0\tau) + \\ & 2\left(x_1^2+p_1^2\right)\sin(\eta_0 s)] \end{aligned}$$

- The key point is that we have, with $z = (x, p)$ and the new variable $\varphi = \frac{\eta_0 \tau}{2}$,

  the relation

$$4\left(y_1 - y_0 - \frac{1}{2}x_1 p_1\right) = \mu(\varphi)\,\|z_1\|^2$$

  with the function :

$$\mu(\varphi) = \frac{\varphi}{\sin^2(\varphi)} - \cot(\varphi)$$

- So geodesics with the <u>same</u> end points correspond to the solutions of the equation

$$\mu(\varphi) = \text{cst}$$

- For instance, for $x_1 = 2$, $p_1 = 4$, $y_1 = 104$, we find $\mu(\varphi) = 20$, which has 11 solutions.

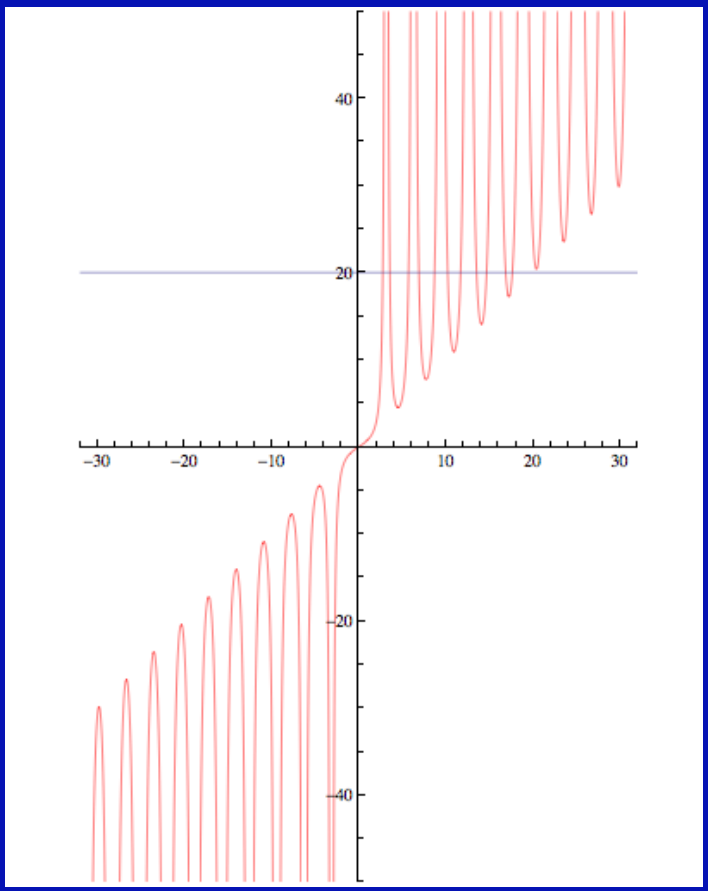
40
20
−20
−40
−30
−20
−10
10
20
30

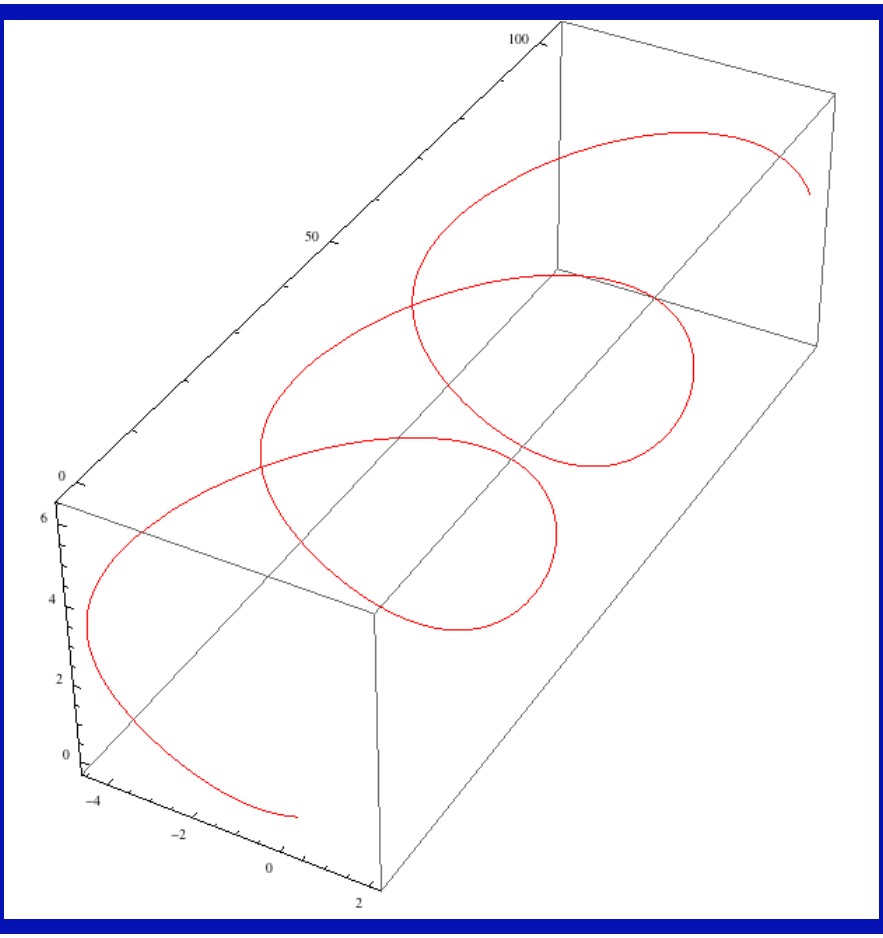
100
50
0
6
4
2
0
−4
−2
0
2

- Projections of geodesics on the $z = (x, p)$ plane are circles

$$x^2 + p^2 - x\left(x_1 + p_1 \cot\left(\frac{\eta_0 \tau}{2}\right)\right) - p\left(p_1 - x_1 \cot\left(\frac{\eta_0 \tau}{2}\right)\right) = 0$$

with center

$$x_c = \frac{1}{2}\left(x_1 + p_1 \cot\left(\frac{\eta_0 \tau}{2}\right)\right), y_c = \frac{1}{2}\left(p_1 - x_1 \cot\left(\frac{\eta_0 \tau}{2}\right)\right)$$

- To compute the sub-Riemannian sphere and wave front we must compute the sub-Riemannian length L of geodesics.

$$L = \int_0^\tau \ell ds \qquad \ell^2 = (\xi + p\eta)^2 + \pi^2$$

- $\ell^2 = 2H = 2H_0$ since $H = \mathrm{cst}$ on trajectories.
- But

$$H_0 = \frac{\eta_0^2}{8} \frac{1}{\sin^2\left(\frac{\eta_0 \tau}{2}\right)} |z_1|^2 \qquad \text{If} \quad \frac{\eta_0 \tau}{2} = \varphi$$

$$L = \sqrt{2}\left(\frac{\eta_0 \tau}{2}\right) \frac{1}{\left|\sin\left(\frac{\eta_0 \tau}{2}\right)\right|} |z_1| = \sqrt{2} \frac{\varphi}{|\sin(\varphi)|} |z_1|$$

- We find the fundamental equation (for $L = \sqrt{2}$)

$$|z_1| = \frac{|\sin(\varphi)|}{\varphi}$$

- And therefore, with

$$z_1 = (|z_1|\cos(\theta), |z_1|\sin(\theta)),$$

$$x_1 = \frac{|\sin(\varphi)|}{\varphi} \cos(\theta)$$

$$p_1 = \frac{|\sin(\varphi)|}{\varphi} \sin(\theta)$$

$$y_1 = \frac{\varphi + 2\sin^2(\varphi)\cos(\theta)\sin(\theta) - \cos(\varphi)\sin(\varphi)}{4\varphi^2}$$

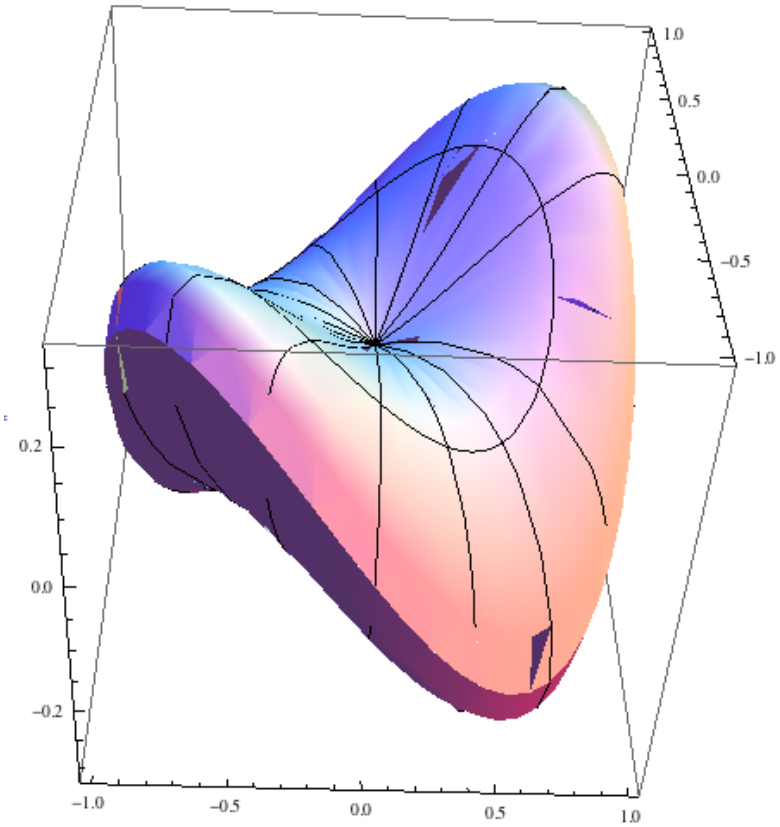
1.0
0.5
0.0
−0.5
−1.0
0.2
0.0
−0.2
−1.0
−0.5
0.0
0.5
1.0

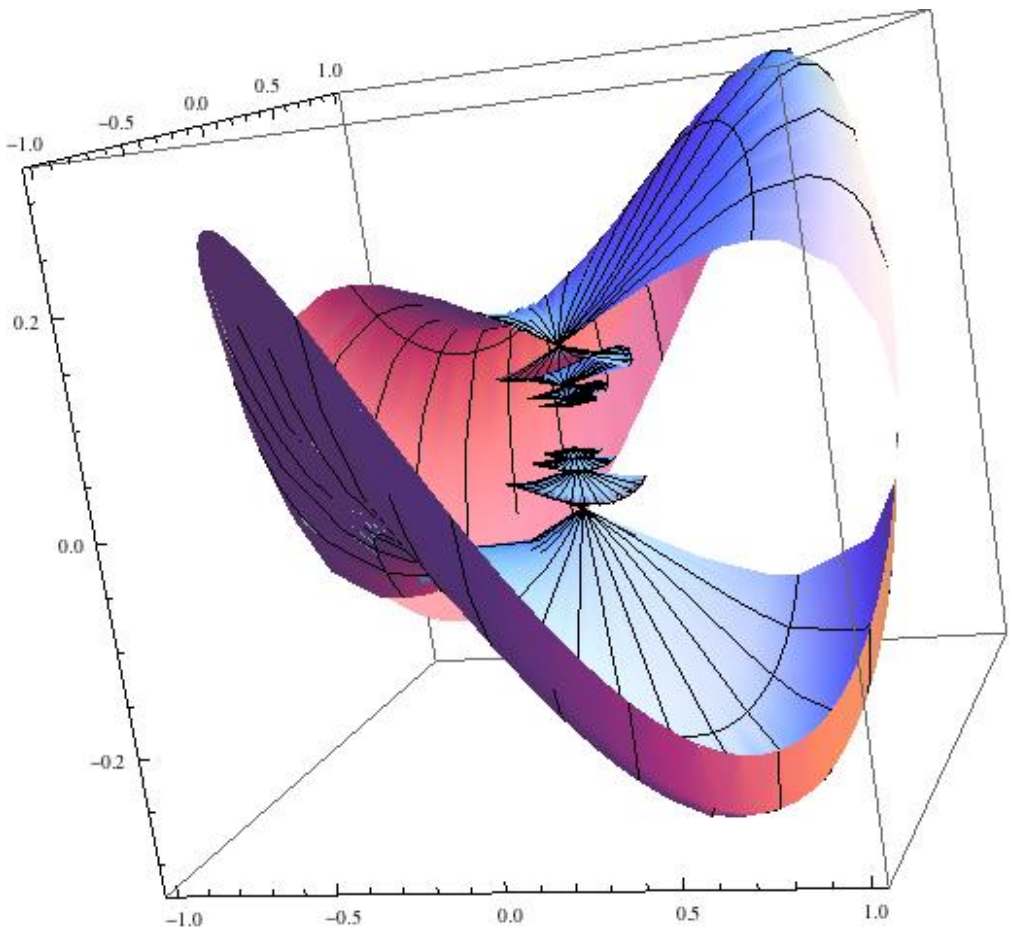
−1.0
−0.5
0.0
0.5
1.0
0.2
0.0
−0.2
−1.0
−0.5
0.0
0.5
1.0

Contact structure and Euclidean group

- With Alessandro Sarti and Giovanna Citti, we emphasized the fact that it is more natural to work with the fibration $\pi : V = \mathbb{R}^2 \times \mathbb{S}^1 \to \mathbb{R}^2$ endowed with the contact form

$$\omega = -\sin(\theta)dx + \cos(\theta)dy$$

which is $\cos(\theta)(dy - pdx)$

- No privileged x-axis.

- The contact planes are spanned by

$$X_1 = \cos(\theta)\,\partial_x + \sin(\theta)\,\partial_y$$
$$X_2 = \partial_\theta$$

with Lie bracket

$$[X_1, X_2] = \sin(\theta)\,\partial_x - \cos(\theta)\,\partial_y = -X_3$$

- (Tangent vectors are interpreted as oriented derivatives.)

- This is a non-holonomic basis.

- V becomes the Euclidean group, which is the semidirect product G =

$$E(2) = SO(2) \ltimes \mathbb{R}^2$$

$$\begin{pmatrix} x_1 \\ y_1 \\ \theta_1 \end{pmatrix} \cdot \begin{pmatrix} x_2 \\ y_2 \\ \theta_2 \end{pmatrix} = \begin{pmatrix} x_1 + x_2 \cos(\theta_1) - y_2 \sin(\theta_1) \\ y_1 + x_2 \sin(\theta_1) + y_2 \cos(\theta_1) \\ \theta_1 + \theta_2 \end{pmatrix}$$

- This group is <u>not</u> nilpotent and its tangent cone is the polarized Heisenberg group.

- By left invariance, the basis at 0

$$\{\partial_x, \partial_y, \partial_\theta\}_0$$

left translates into the non-holonomic basis

$$\{\cos(\theta)\,\partial_x + \sin(\theta)\,\partial_y = X_1, -\sin(\theta)\,\partial_x + \cos(\theta)\,\partial_y = X_3, \partial_\theta = X_2\}_q$$

and the covector at 0

$$\omega_0 = dy$$

left translates into the contact form ω .

Curvature and Engel structure

- Some experiments (Steve Zucker) seems to indicate that there exist in the primary visual cortex curvature detectors.
- If we want to model this possibility, we must use 2-jets spaces and add a new independent variable K, which will be interpreted as the curvature of curves C in the (x, y) base plane R.

In the 3D space

$$V = \mathbb{R}^2 \times \mathbb{S}^1$$

we have the contact structure defined by the 1-form K

$$\omega = -\sin(\theta)dx + \cos(\theta)\, dy$$

The (non holonomic) basis for the contact planes is

$$X_1 = \cos(\theta)\, \partial_x + \sin(\theta)\partial_y$$
$$X_2 = \partial_\theta$$

The Lie bracket is

$$[X_1, X_2] = X_3 = -\sin(\theta)\partial_x + \cos(\theta)\, \partial_y$$

We want to add *curvature* K and work in the 4D space

$$W = \mathbb{R}^2 \times \mathbb{S}^1 \times \mathbb{R}$$

Now, we have a Pfaff system constituted of *two* 1-forms: ω and

$$\tau = d\theta - K ds$$

If we parametrize the curves in the base space (x, y) using the arc length s, the curvature is

$$K = \frac{d\theta}{ds}$$

To express the second 1-form τ, we write

$$dx = \cos(\theta)\, ds$$
$$dy = \sin(\theta) ds$$
$$ds = \cos(\theta)\, dx + \sin(\theta) dy = \left(\cos(\theta)^2 + \sin(\theta)^2\right) ds$$

and therefore

$$\tau = d\theta - K ds$$
$$\tau = d\theta - K\left(\cos(\theta)\, dx + \sin(\theta) dy\right)$$

The kernel of τ is generated by the 3 tangent vectors

$$\begin{aligned} X_1^K &= \cos(\theta)\,\partial_x + \sin(\theta)\partial_y + K\partial_\theta = X_1 + KX_2 \\ X_3 &= -\sin(\theta)\partial_x + \cos(\theta)\,\partial_y \\ X_4^K &= \partial_K \end{aligned}$$

while the kernel of ω extended to W is generated by X_1, X_2 and X_4^K.

In the 4D space W, the tangent vector $X_1 + KX_2$ is helicoidally unfolded along the K-axis.
The distribution of planes is now Span $\{X_1^K, X_4^K\}$.
It generates the whole Lie algebra since

$$\begin{aligned} \left[X_1^K, X_4^K\right] &= -X_2 = -\partial_\theta \\ \left[\left[X_1^K, X_4^K\right], X_1^K\right] &= X_3 = -\sin(\theta)\partial_x + \cos(\theta)\,\partial_y \end{aligned}$$

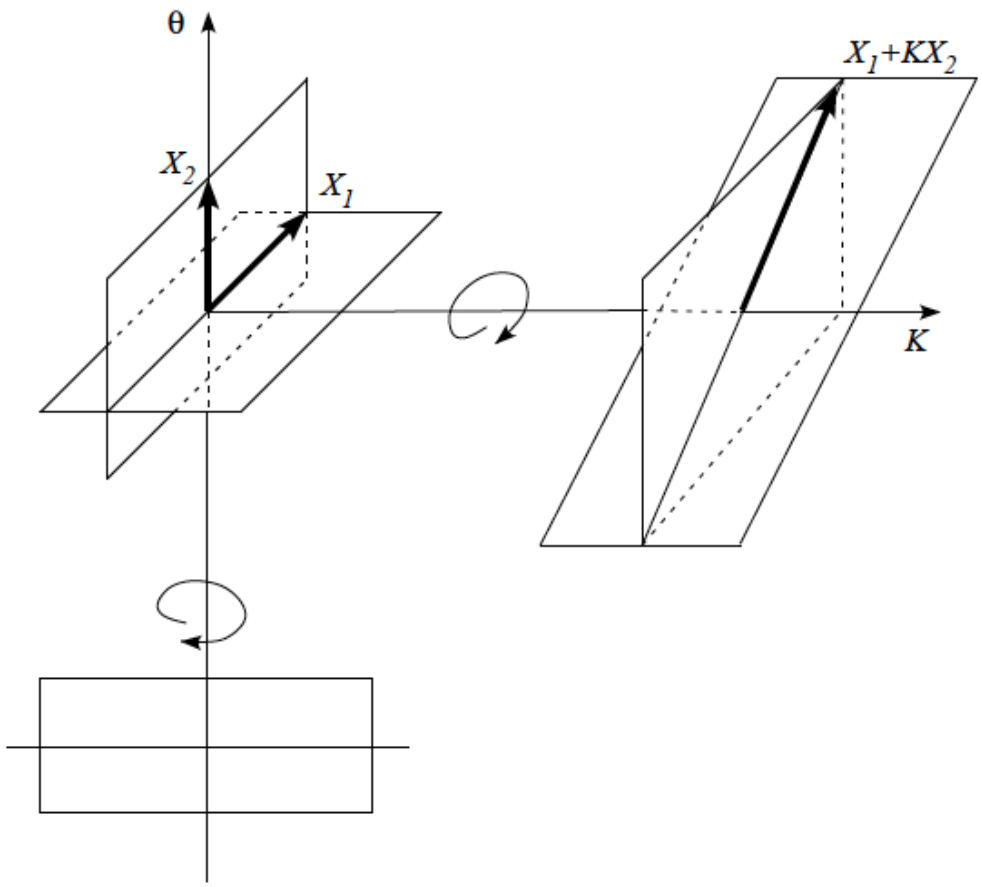

Sub-Riemannian geometry of the Euclidean group E(2)

- For the non nilpotent Euclidean group, Andrei Agrachev and his group at the SISSA (Yuri Sachkov, Ugo Boscain, Igor Moiseev) solved the problem of SR geodesics and Sachkov compared it with Mumford's elastica model.

- One works with the fibration $V = \mathbb{R}^2 \times \mathbb{S}^1$ where the Legendrian lifts are solutions of the control system :

$$\begin{cases} \dot{x} = u_1 \cos(\theta) \\ \dot{y} = u_1 \sin(\theta) \\ \dot{\theta} = u_2 \end{cases}$$

- Let

$$p = (p_x, p_y, p_\theta) \in T_q^* V$$

be the momenta covectors.

- The Hamiltonian on T^*V for geodesics is

$$H(p,q) = \frac{1}{2}\left(u_1^2 + u_2^2\right) = \frac{1}{2}\left(\left(p_x \cos(\theta) + p_y \sin(\theta)\right)^2 + p_\theta^2\right)$$

and corresponds to the X_1 , X_2 basis .

- For θ small $= p$ and momenta ξ, η, π, we find again the polarized Heisenberg case :

$$H(x, y, p, \xi, \eta, \pi) = \frac{1}{2}\left[(\xi + p\eta)^2 + \pi^2\right]$$

- Hamilton equations are therefore :

$$\begin{cases} \dot{x} = \frac{\partial H}{\partial p_x} = p_x \cos^2(\theta) + p_y \cos(\theta)\sin(\theta) \\ \dot{y} = \frac{\partial H}{\partial p_y} = p_y \sin^2(\theta) + p_x \cos(\theta)\sin(\theta) \\ \dot{\theta} = \frac{\partial H}{\partial p_\theta} = p_\theta \end{cases}$$

$$\begin{cases} \dot{p}_x = -\frac{\partial H}{\partial x} = 0 \\ \dot{p}_y = -\frac{\partial H}{\partial y} = 0 \\ \dot{p}_\theta = -\frac{\partial H}{\partial \theta} = (p_x \cos(\theta) + p_y \sin(\theta))(-p_x \sin(\theta) + p_y \cos(\theta)) \end{cases}$$

- The system can be explicitely integrated via elliptic functions.
- The sub-Riemannian geodesics are the projections of the integral curves on V.

SE(2) geodesics

- p_x and p_y are constant. Write

  $(p_x\,,\ p_y) = \rho \exp(i\beta)$. Then

$$\dot{p}_\theta = \frac{1}{2}\rho^2 \sin\left(2\left(\theta - \beta\right)\right)$$

and H yields the first integral :

$$\rho^2 \cos^2\left(\theta - \beta\right) + p_\theta^2 = c$$

and the ODE for θ (c , ρ and β are cst.) :

$$\dot{\theta}^2 = p_\theta^2 = c - \rho^2 \cos^2\left(\theta - \beta\right)$$

- For $\beta = 0$ (rotation invariance), the equations become $(p_x = \rho, p_y = 0)$:

$$\begin{cases} \dot{x} = \rho \cos^2(\theta) \\ \dot{y} = \rho \cos(\theta) \sin(\theta) = \frac{1}{2}\rho \sin(2\theta) \\ \dot{\theta} = p_\theta \\ \dot{p}_\theta = \frac{1}{2}\rho^2 \sin(2\theta) \end{cases}$$

- For $\rho = 1$, $\varphi = \pi/2 - \theta$, and $\mu = 2\varphi = \pi - 2\theta$, we get a <u>pendulum</u> equation

$$\ddot{\mu} = -\sin(\mu)$$

with first integral

$$\dot{\varphi}^2 + \sin^2(\varphi) = c$$

- We show the trajectories in the $(\varphi , \dot{\varphi})$ plane :

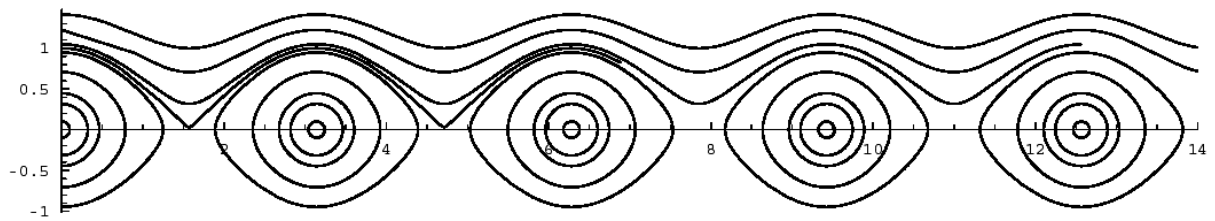

- As

$$dt = \pm \frac{1}{\sqrt{c}} \frac{d\varphi}{\sqrt{1 - \frac{1}{c}\sin^2(\varphi)}}$$

the system can be explicitely integrated via elliptic functions, $1/c$ being the module.

- F elliptic integral of the first kind of modulus k

$$F(\psi, k) = \int_0^{\psi} \frac{1}{\sqrt{1 - k\sin^2(\theta)}} d\theta$$

- E elliptic integral of the second kind

$$E(\psi, k) = \int_0^{\psi} \sqrt{1 - k\sin^2(\theta)} d\theta$$

- am Jacobi amplitude, inverse of F : $\psi = am(u, k)$ iff $u = F(\psi, k)$,
- Jacobi functions $\mathrm{sn}(u) = \sin(\psi)$, $\mathrm{cn}(u) = \cos(\psi)$, $\mathrm{dn}(u) = (1 - k\sin^2(\psi))^{1/2}$.

- We get for t

$$t = \int_0^t dt = \frac{1}{\sqrt{c}} \int_{\varphi(0)}^{\varphi(t)} \frac{d\varphi}{\sqrt{1 - \frac{1}{c}\sin^2(\varphi)}}$$

$$= \frac{1}{\sqrt{c}} \left(F\left(\varphi(t), \frac{1}{c}\right) - F\left(\varphi(0), \frac{1}{c}\right) \right)$$

- For $\varphi(0) = 0$ ($\theta(0) = \pi/2$), and $c > 1$ (modulus $1/c < 1$), the pendulum makes complete turns.

$$\varphi(t) = \mathrm{am}\left(t\sqrt{c}, \frac{1}{c}\right) + k\pi$$

$$x(t) = ct - \sqrt{c}E\left(\varphi(t), \frac{1}{c}\right)$$

$$y(t) = \sqrt{c}\left(\mathrm{dn}\left(t\sqrt{c}, \frac{1}{c}\right) - 1\right)$$

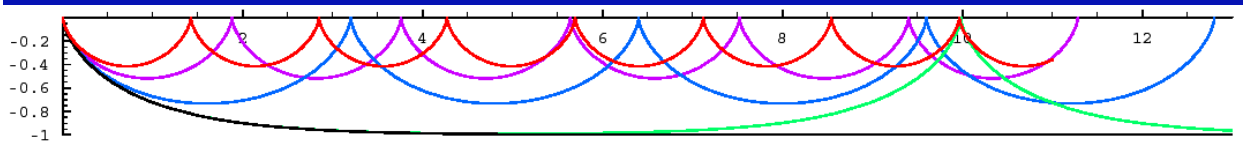

FIGURE 30. Différentes géodésiques sous-riemanniennes pour c décroissant de 2 à 1 : $c = 2$ (rouge), $c = 1.5$ (violet), $c = 1.1$ (bleu), $c = 1.001$ (vert), $c = 1$ (noir). (D'après les calculs d'A. Agrachev).

- For $c < 1$ (modulus $1/c > 1$), the pendulum oscillates between two extremal values $-\varphi_{ex}$, $+\varphi_{ex}$ with $\varphi_{ex} = \mathrm{Arcsin}\left(\sqrt{c}\right)$

$$\theta(t) = \mathrm{Arccos}\left(\sqrt{c}\,\mathrm{am}\left(t, c\right)\right)$$

$$x(t) = t - E\left(\mathrm{am}\left(t, c\right), c\right)$$

$$y(t) = \sqrt{c}\left(\mathrm{cn}\left(t, c\right) - 1\right)$$

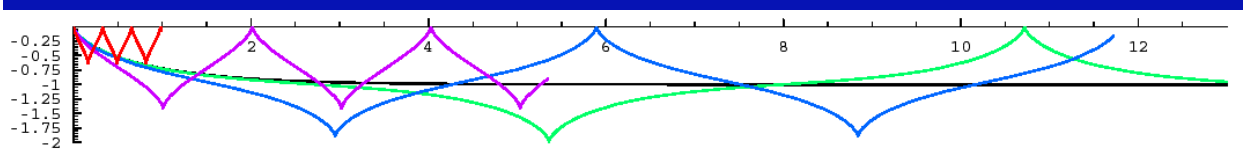

FIGURE 31. Différentes géodésiques sous-riemanniennes pour c croissant de 0.1 à 1 : $c = 0.1$ (rouge), $c = 0.5$ (violet), $c = 0.9$ (bleu), $c = 0.99$ (vert), $c = 1$ (noir). (D'après les calculs d'A. Agrachev).

Scale-space and symplectic structures

- The contact structure of V is defined as the kernel field of the 1-form ω .
- But this field is only defined up to a scale factor $s = e^{\sigma}$, ω and $s\omega$ having the same kernels.
- It is therefore natural to <u>enlarge</u> the 3 dimensional contact space $V = \mathbb{R}^2 \times \mathbb{S}^1$ to the 4 dimensional space $G = \mathbb{R}^2 \times \mathbb{S}^1 \times \mathbb{R}$ with coordinates (x, y, θ, σ).

- G is the affine group of the plane and its invariant basis is now

$$\begin{cases} X_1 = e^{\sigma}\left(\cos(\theta)\partial_x + \sin(\theta)\partial_y\right) \\ X_2 = \partial_\theta \\ X_3 = e^{\sigma}\left(-\sin(\theta)\partial_x + \cos(\theta)\partial_y\right) \\ X_4 = \partial_\sigma \end{cases}$$

the invariant 1-form being now

$$\omega = e^{-\sigma}\left(-\sin(\theta)dx + \cos(\theta)dy\right)$$

- $d\omega$ is the symplectic 2-form on G

$$\begin{aligned} d\omega &= \left(e^{-\sigma}\cos(\theta)dx + e^{-\sigma}\sin(\theta)dy\right)\wedge d\theta + \\ &\quad \left(-e^{-\sigma}\sin(\theta)dx + e^{-\sigma}\cos(\theta)dy\right)\wedge d\sigma. \end{aligned}$$

deduced via left translations from the canonical symplectic 2-form at 0

$$dx \wedge d\theta + dy \wedge d\sigma$$

- Indeed, the translated of dx and dy are

$$\begin{cases} \upsilon = e^{-\sigma}\left(\cos(\theta)dx + \sin(\theta)dy\right) \\ \omega = e^{-\sigma}\left(-\sin(\theta)dx + \cos(\theta)dy\right) \end{cases}$$

and $d\omega = \upsilon \wedge d\theta + \omega \wedge d\sigma$

- $d\omega$ can be writen using an antisymmetric matrix B

$$d\omega(X, X') = \langle BX, X' \rangle$$

$$B = e^{-\sigma}\begin{pmatrix} 0 & 0 & -\cos(\theta) & \sin(\theta) \\ 0 & 0 & -\sin(\theta) & -\cos(\theta) \\ \cos(\theta) & \sin(\theta) & 0 & 0 \\ -\sin(\theta) & \cos(\theta) & 0 & 0 \end{pmatrix}$$

- $-B^2 = BB^*$ is positive definite $-B^2 = e^{-2\sigma}I$ and we can therefore consider

$$P = \sqrt{-B^2} = e^{-\sigma} I$$

- Then, $J = BP^{-1} = e^{\sigma} B$ satisfies $J^2 = -I$

  and defines a complex structure

$$J = \begin{pmatrix} 0 & 0 & -\cos(\theta) & \sin(\theta) \\ 0 & 0 & -\sin(\theta) & -\cos(\theta) \\ \cos(\theta) & \sin(\theta) & 0 & 0 \\ -\sin(\theta) & \cos(\theta) & 0 & 0 \end{pmatrix}$$

- If we define a new scalar product by

$$(X|Y) = e^{-\sigma} \langle X|Y \rangle$$

  then $d\omega(X,Y) = (JX|Y)$

- The planes Span$\{ X_1, X_2 \}$, Span$\{ X_3, X_4 \}$ are complex lines (real planes), on which J acts as multiplication by i.

- The equation of the contact curves is

$$\begin{aligned} \gamma'(t) &= X_1(\gamma(t)) + k(t)X_2(\gamma(t)), \\ \gamma(0) &= (x_0, y_0, \theta_0, \sigma_0), \end{aligned}$$

- For $k = \mathrm{cst}$, solutions are

$$\begin{cases} x &= \frac{1}{k}\left(\sin(kt + \theta_0) - \sin(\theta_0) + kx_0\right), \\ y &= \frac{1}{k}\left(-\cos(kt + \theta_0) + \cos(\theta_0) + ky_0\right), \\ \theta &= kt + \theta_0, \\ \sigma &= \sigma_0. \end{cases}$$

- For the distribution $\{ X_3, X_4 \}$, the equation of the integral curves is

$$\begin{aligned} \gamma'(t) &= X_3(\gamma(t)) + k(t)X_4(\gamma(t)), \\ \gamma(0) &= (x_0, y_0, \theta_0, \sigma_0). \end{aligned}$$

- For $k = \mathrm{cst}$, solutions are

$$\begin{cases} x &= -\frac{\sin(\theta_0)}{k} e^{\sigma_0}\left(e^{kt} - 1\right) + x_0, \\ y &= \frac{\cos(\theta_0)}{k} e^{\sigma_0}\left(e^{kt} - 1\right) + y_0, \\ \theta &= \theta_0, \\ \sigma &= kt + \sigma_0. \end{cases}$$

- The projections on the (x, y) plane are :
  - circles of radius $1/k$ tangent to the x-axis
  - lines <u>independent</u> of k through (x_0, y_0) and orthogonal to the direction θ_0 in the fixed "vertical" plane Span$\{ X_3, X_4 \}$.

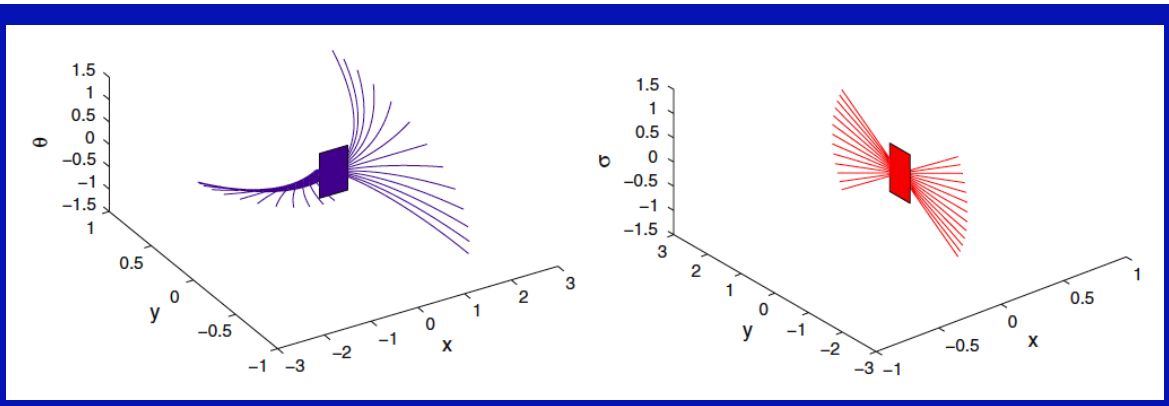

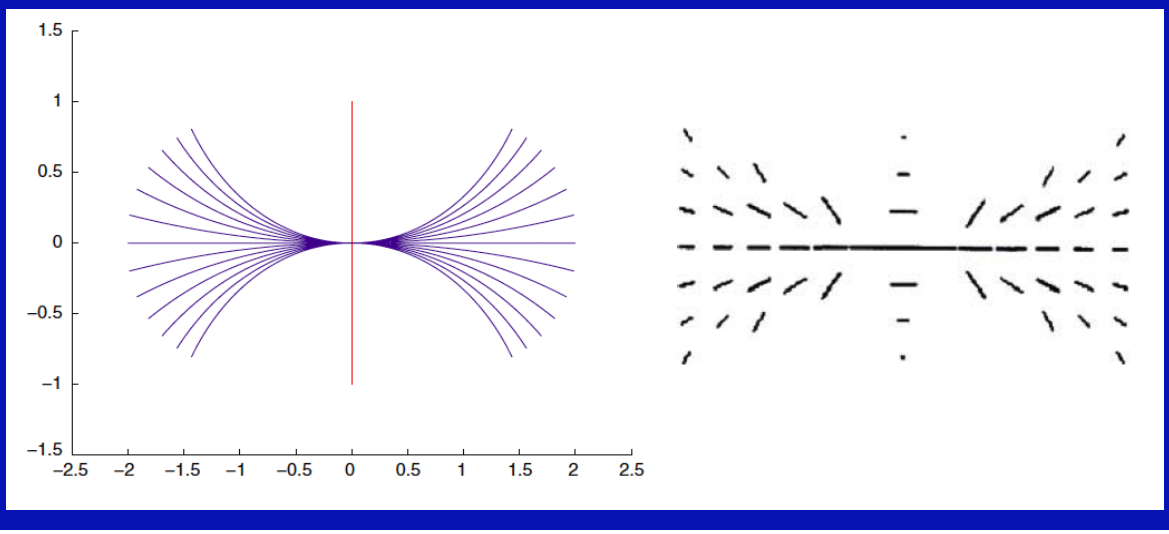

- Another (logarithmic) model for the scale-space (zoom and blow-up). See Citti, Sarti, Petitot, *J. of Phys. Paris*, 103, 1-2, 2009.
- We take

$$\omega = \sigma^{-1}\left(-\sin(\theta)dx + \cos(\theta)dy\right)$$

- Then

$$\begin{aligned} d\omega &= \sigma^{-1}\left(\cos(\theta)dx + \sin(\theta)dy\right) \wedge d\theta \\ &\quad + \sigma^{-2}\left(-\sin(\theta)dx + \cos(\theta)dy\right) \wedge d\sigma \\ &= \sigma^{-1}\omega_1 \wedge \omega_2 + \sigma^{-2}\omega_3 \wedge \omega_4 \end{aligned}$$

- The scaled tangent vectors are

$$X_1, X_2, \sigma X_3, \sigma X_4.$$

- For $\sigma = 0$ we get the contact subRiemannian geometry and for $\sigma = 1$ we get the Euclidean geometry.

$$\gamma'(t) = X_1(\gamma(t)) + k_2 X_2(\gamma(t)) + k_3 \sigma X_3(\gamma(t)) + k_4 \sigma X_4(\gamma(t))$$

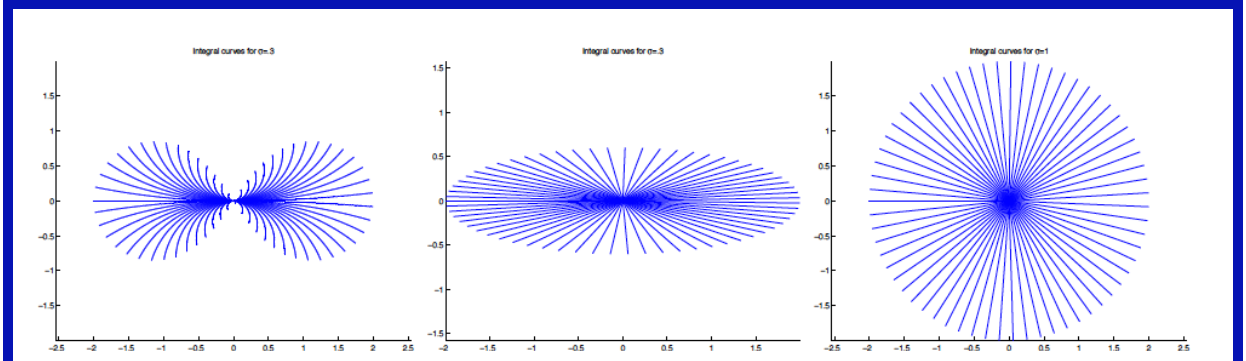

Minimal surfaces in V1

- It seems that illusory contours are in fact boundaries of illusory minimal surfaces in V1.
- The theory of surfaces *S* in a contact manifold endowed with a sub-Riemannian geometry is rather difficult.
- There are in general "characteristic" (generically isolated) points where S is tangent to the contact plane and where the normal vector relative to $\mathcal{K}$ is not defined.
- See Scott Pauls : « Minimal surfaces in the Heisenberg group ».

Coherent states and harmonic analysis on Lie groups

- The natural context of signal analysis in natural vision is therefore that of *coherent states*. We have
  - An Hilbert space $\mathcal{H} = L^2(\mathbb{R}^2)$
  - A (locally compact) Lie group G acting on $\mathcal{H}$ via an irreducible unitary representation π.
  - A well localized « mother » wavelet $\varphi_0 \in \mathcal{H}$

- Coherent state = G-orbit $\{\varphi_g\}_{g\in G}$ of φ_0
- Harmonic analysis of a signal f :

$$f(x) = \int_G T_f(g)\,\varphi_g(x)\,d\mu(g)$$

- The transform of f is :

$$T_f(g) = \langle f, \varphi_g \rangle \in L^2(G)$$

- The Gabor transform corresponds to the analysis :

$$G_f(a,\omega) = \int_{\mathbb{R}} f(x) e^{-i\omega(x-a)} g(x-a)^* \, dx \in L^2(\mathbb{R}^2)$$

with the synthesis :

$$f(x) = \frac{1}{2\pi \|g\|^2} \int_{\mathbb{R}} G_f(a,\omega)\, e^{i\omega(x-a)} g(x-a)\, da d\omega.$$

- The coherent states are :

$$g_{a,\omega}(x) = e^{i\omega(x-a)} g(x-a)$$

- For classical wavelets, the coherent states are

$$\varphi_{a,s}(x) = \frac{1}{\sqrt{s}}\varphi\left(\frac{x-a}{s}\right)$$

and must satisfy the admissibility condition

$$c_\varphi = \int_R \left|\widehat{\varphi}(\xi)\right|^2 \frac{d\xi}{\xi} < \infty$$

- The synthesis is given by the Calderon identity with $T_f(a,s) = \langle f, \varphi_{a,s}\rangle$

$$f(x) = \frac{1}{c_\varphi}\int_{\mathbb{R}_+^* \times \mathbb{R}} T_f(a,s)\,\varphi_{a,s}(x)\frac{ds}{s}\frac{da}{s}$$

- Coherent states enable to represent a signal $f \in \mathcal{H}$ by its transform

$$T_f(g) = \langle f, \varphi_g\rangle \in L^2(G)$$

- It is what is done by V1, the $\langle f, \varphi_g\rangle$ being the measure of f by the receptive profiles φ_g.

Harmonic analysis and symmetry axis

- We can apply this to the mother wavelet

$$\varphi_{(0,\sigma)}(x,y) = \frac{1}{e^{2\sigma}} e^{\frac{-(x^2+y^2)}{e^{2\sigma}}} e^{\frac{2iy}{e^{\sigma}}}$$

  and look at the associatated coherent state.

- Let C be a closed boundary in the retinal plane $\mathbb{R}^2$ and $a = (x, y)$ a point inside C.

- Citti-Sarti : If we look at the maximal responses of the receptive profiles centered at a, and if c is the nearest point of C relative to a, then

$$d\left((x,y),c\right) = \frac{1}{\sqrt{2}} e^{\bar{\sigma}}$$

  and $\bar{\theta}$ is the direction of C at c.

- We can therefore lift $\mathbb{R}^2$ to a surface Σ in G

$$\Sigma = \left\{(x, y, \bar{\theta}(x,y), \bar{\sigma}(x,y))\right\}$$

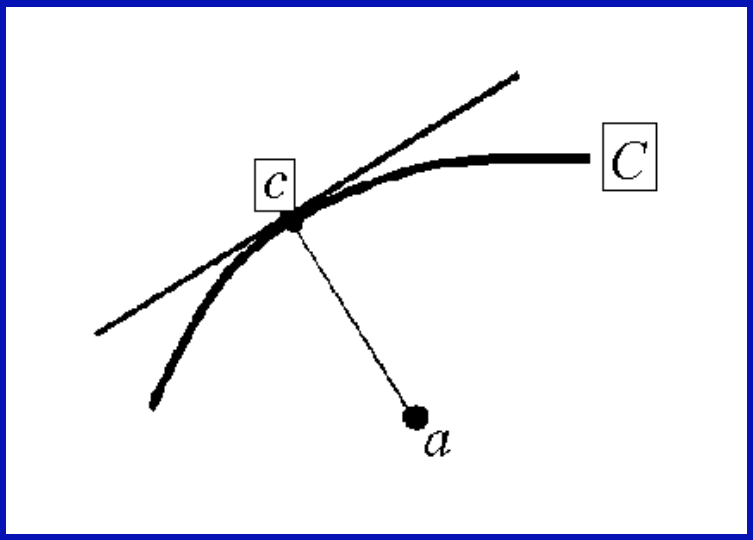

- The tangent vecteur over $a = (x, y)$

$$X_1 = e^{\bar{\sigma}} \left(\cos(\bar{\theta}) \partial_x + \sin(\bar{\theta}) \partial_y \right)$$

is parallel to C at c which is at <u>minimal</u> distance and therefore, as a derivative, satisfies

$$X_1 \left(\bar{\sigma} \right) = 0$$

- The tangent vector over $a = (x, y)$

$$X_3 = e^{\bar{\sigma}} \left(-\sin(\bar{\theta})\partial_x + \cos(\bar{\theta})\partial_y \right)$$

is orthogonal to C at c and $\bar{\theta}$ is constant along this direction. Therefore

$$X_3 \left(\bar{\theta} \right) = 0$$

- Now, the tangent plane to Σ: $T_{x,y,\bar{\theta},\bar{\sigma}}\Sigma$ is generated by the 2 vectors

$$\begin{cases} X_1 + X_1 \left(\bar{\theta} \right) X_2 + X_1 \left(\bar{\sigma} \right) X_4 \\ X_3 + X_3 \left(\bar{\theta} \right) X_2 + X_3 \left(\bar{\sigma} \right) X_4 \end{cases}$$

- But, since

$$X_1 \left(\bar{\sigma} \right) = X_3 \left(\bar{\theta} \right) = 0$$

it is in fact generated by

$$\begin{cases} X_1 + X_1 \left(\bar{\theta} \right) X_2 \\ X_3 + X_3 \left(\bar{\sigma} \right) X_4 \end{cases}$$

- As $d\omega = \upsilon \wedge d\theta + \omega \wedge d\sigma = \omega_1 \wedge \omega_2 + \omega_3 \wedge \omega_4$

we see that $d\omega$ <u>vanishes</u> on $T\Sigma$: Σ is therefore a *Lagrangian* submanifold of G.

- The transform of a closed contour C by this coherent state realizes the propagation of C via the *eikonal equation* of geometrical optics (Huyghens or "grassfire" model).
- The singular locus of this propagation is like the "symmetry axis" or "medial axis" whose role in vision has been strongly emphasized by many authors after Harry Blum : René Thom, David Marr, David Mumford, Steve Zucker, James Damon, Benjamin Kimia, etc.

- MA of a rectangle

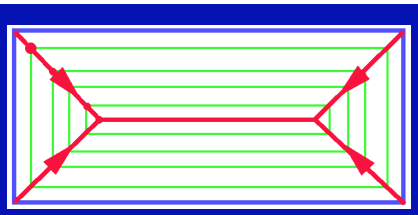

- MA of an ellipse computed by A. Sarti using the coherent state

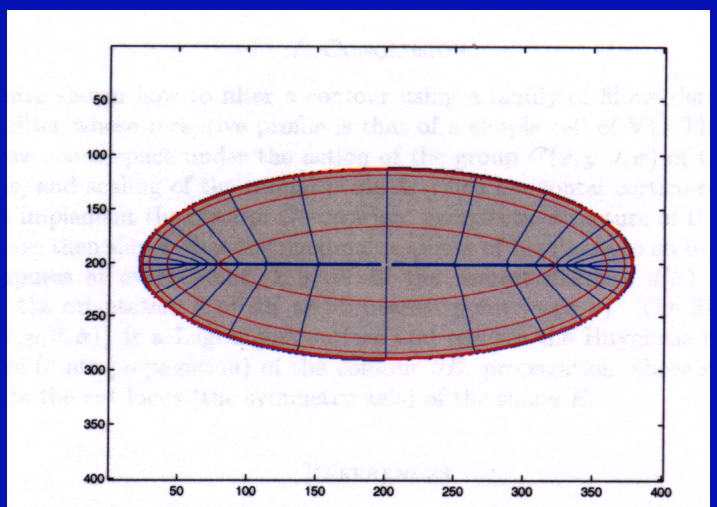

FIGURE 11. Level curves of $\bar{\theta}(x, y)$ (blue) and $\bar{\sigma}(x, y)$ (red).

Noncommutative harmonic analysis and SR geometry

- Using this geometrical analysis of the functional archictecture of V1, it is interesting to study the diffusion (heat kernel) and advection-diffusion (Fokker-Planck) processes on this subriemannian geometry of SE(2).

- For the Heisenberg group, R. Beals, B. Gaveau, P. Greiner, D-Ch Chang, constructed the heat kernel.
- The problem is rather difficult since there are singularities (cut points) in every neighborhood of each point (B. Gaveau, IHP, 26-10-2005).

The sub-Riemannian Heisenberg case

- Gaveau, Beals, Greiner, Chang.
- Coordinates (z, t) in $\mathbb{R}^3$. Heat equation :

$$\frac{\partial f(z,t,s)}{\partial s} = \Delta_{\mathcal{K}} f(z,t,s)$$

with the sub-Riemannian Laplacian.

- Heat kernel :

$$\begin{aligned} P(z,t,s) &= \frac{1}{(2\pi s)^2} \int_{\mathbb{R}} \frac{2\tau}{\sinh(2\tau)} e^{\left(\frac{i\tau t}{s} - \left(\frac{\|z\|^2}{2s}\right)\frac{2\tau}{\tanh(2\tau)}\right)} d\tau \\ &= \frac{1}{(2\pi s)^2} \int_{\mathbb{R}} V(\tau)\, e^{\left(-\frac{\Sigma(z,t,\tau)}{s}\right)} d\tau \end{aligned}$$

with $V(\tau) = \frac{2\tau}{\sinh(2\tau)}$ $\Sigma(z,t,\tau) = -i\tau t + \|z\|^2 \frac{\tau}{\tanh(2\tau)}$

to be compared with

$$P(\mathbf{x}, s) = \frac{1}{(2\sqrt{\pi s})^3} e^{-\frac{\|\overline{\mathbf{x}}\|^2}{4s}}$$

- As the action Σ is complex, P is an oscillatory integral if $t \neq 0$ (especially when $z = 0$).
- One must use techniques such as the stationary phase principle (semi-classical approximation).
- For $s \to 0$, the oscillatory integral

$$I(q,s) = \frac{1}{(2\pi s)^{p/2}} \int e^{i\frac{\varphi(q,\tau)}{s}} a(q,\tau,s)d\tau$$

concentrates on $\frac{\partial\varphi(q,\tau)}{\partial\tau} = 0$

- One can use the non-commutative Fourier transform defined on the dual of the group G.
- For the polarized Heisenberg group V (1-jet space), the dual V^* of V is the set of unitary irreducible representations (unirreps) of V in the Hilbert space of functions

$$\{u(s)\} = \mathrm{L}^2(\mathbb{R}, \mathbb{C}).$$

- We have seen that the unirreps of V are infinite dimensional ones (Stone - Von Neumann).

$$\pi_\lambda(x, y, p)\, u(s) = e^{i\lambda(y+xs)} u(s+p), \text{ with } \lambda \neq 0$$

- For $\lambda = 0$ they degenerate into trivial representations of dimension 1 : multiplication by

$$\pi_{\mu,\nu}(x, y, p) = e^{i(\mu x + \nu p)}$$

- Recently (2008), Andrei Agrachev, Ugo Boscain, Jean-Paul Gauthier and Francesco Rossi have found the heat kernel for $G = SE(2)$ and other unimodular groups.
- The hypo-elliptic Laplacian is the sum of squares of the bracket generating Lie subalgebra :

$$\Delta_{\mathcal{K}} = X_1^2 + X_2^2$$

- The subriemannian diffusion on G is highly <u>anisotropic</u> since it is restricted to an angular diffusion of θ and a spatial diffusion only along the X_1 direction.
- It is a diffusion constrained by the “good continuation” constraint.
- Example :

- Completion of an image (inpainting) : Jean-Paul Gauthier.
- Even if the image is highly corrupted the reconstruction is quite good.

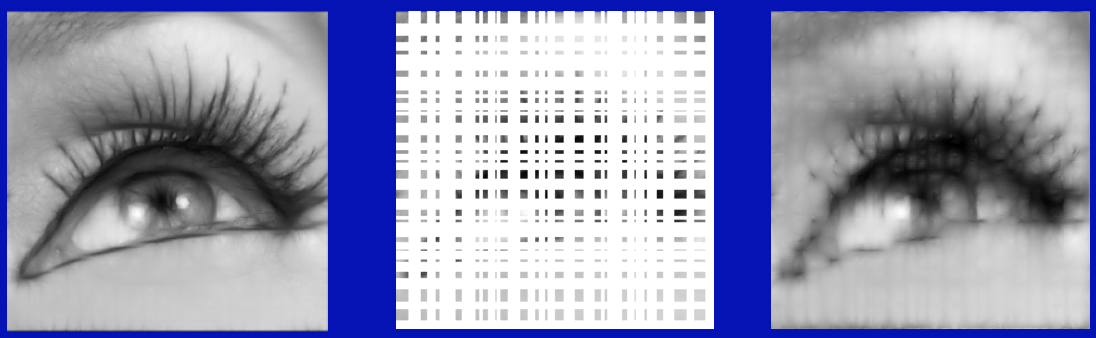

- The dual G^* of G is the set of unitary irreducible representations of G in the Hilbert space $\{\psi(\theta)\} = \mathcal{H} = L^2(S^1, \mathbb{C})$
- If the elements of G are

$$g = \begin{pmatrix} \cos(\alpha) & -\sin(\alpha) & x \\ \sin(\alpha) & \cos(\alpha) & y \\ 0 & 0 & 1 \end{pmatrix}$$

then the unirreps are parametrized by a positive real λ :

$$\begin{array}{rcl} \mathcal{X}^\lambda : G & \to & \mathcal{U}(\mathcal{H}) \\ g & \mapsto & \mathcal{X}^\lambda(g) : \mathcal{H} \to \mathcal{H} \\ & & \psi(\theta) \mapsto e^{i\lambda(x\sin(\theta)+y\cos(\theta))}\psi(\theta+\alpha) \end{array}$$

- This means that to every element g of G one associates an automorphism $\mathcal{X}^\lambda(g)$ of the Hilbert space $\mathcal{H}$.
- Such an automorphism associates to each function $\psi(\theta)$ in $\mathcal{H}$ another function in $\mathcal{H}$.

- There exists a measure on G^*, the Plancherel measure, given by $dP(\lambda) = \lambda d\lambda$, which enables to make integrations.
- To compute the Fourier transform of the sub-Riemannian Laplacian we have to look at the action of the differential of the unirreps on the left-invariant vector fields X.
- These X are given by the left translation of vectors of the Lie algebra $\mathfrak{g}$ of G.

- By definition,

$$d\mathcal{X}^\lambda : X \to d\mathcal{X}^\lambda(X) := \left.\frac{d}{dt}\right|_{t=0} \mathcal{X}^\lambda\left(e^{tX}\right)$$

and

$$\widehat{X_i}^\lambda = d\mathcal{X}^\lambda(X_i)$$

- It is easy to apply these formulas.

$$\psi(\theta) \mapsto e^{i\lambda(x\sin(\theta)+y\cos(\theta))}\psi(\theta+\alpha)$$

$$\begin{aligned}
X_1 &= (1,0,0) \\
e^{tX_1} &= (t,0,0) \\
\mathcal{X}^\lambda\left(e^{tX_1}\right)\psi(\theta) &= e^{i\lambda t\sin(\theta)}\psi(\theta) \\
\widehat{X_1}^\lambda\psi(\theta) &= d\mathcal{X}^\lambda(X_1)\psi(\theta) = \left.\frac{d}{dt}\right|_{t=0}\mathcal{X}^\lambda\left(e^{tX_1}\right)\psi(\theta) \\
&= \left.\frac{d}{dt}\right|_{t=0} e^{i\lambda t\sin(\theta)}\psi(\theta) = i\lambda\sin(\theta)\psi(\theta)
\end{aligned}$$

$$\psi(\theta) \mapsto e^{i\lambda(x\sin(\theta)+y\cos(\theta))}\psi(\theta+\alpha)$$

$$\begin{aligned}
X_2 &= (0,0,1) \\
e^{tX_2} &= (0,0,t) \\
\mathcal{X}^\lambda\left(e^{tX_2}\right)\psi(\theta) &= \psi(\theta+t) \\
\widehat{X_2}^\lambda\psi(\theta) &= d\mathcal{X}^\lambda(X_2)\psi(\theta) = \left.\frac{d}{dt}\right|_{t=0}\mathcal{X}^\lambda\left(e^{tX_2}\right)\psi(\theta) \\
&= \left.\frac{d}{dt}\right|_{t=0}\psi(\theta+t) = \frac{d\psi(\theta)}{d\theta}
\end{aligned}$$

- The GFT of the sub-Riemannian Laplacian is therefore the Hilbert sum (integral on λ with the Plancherel measure $dP(\lambda) = \lambda d\lambda$) of the $\widehat{\Delta_{\mathcal{K}}}^{\lambda}$

  with

$$\widehat{\Delta_{\mathcal{K}}}^{\lambda}\psi(\theta) = \left(\left(\widehat{X_1}^{\lambda}\right)^2 + \left(\widehat{X_2}^{\lambda}\right)^2\right)\psi(\theta) = \frac{d^2\psi(\theta)}{d\theta^2} - \lambda^2\sin^2(\theta)\,\psi(\theta)$$

  which is the *Mathieu equation*.

- The heat kernel is

$$P(g,t) = \int_{G^*} Tr\left(e^{t\widehat{\Delta_{\mathcal{K}}}^{\lambda}}\mathcal{X}^{\lambda}(g)\right)dP(\lambda)\,,\ t \geq 0$$

- For small angles we find the equation

$$\hat{\Delta}^{\lambda} : y''(s) - \lambda^2 s^2 y(s)$$

which gives the Mehler kernel.

If the $\widehat{\Delta_{\mathcal{K}}}^{\lambda}$ have <u>discrete</u> spectrum with a complete set of normalized eigenfunctions $\{\psi_n^{\lambda}\}$ with eigenvalues $\{\alpha_n^{\lambda}\}$ then

$$P(g,t) = \int_{G^*} \left(\sum_n e^{\alpha_n^{\lambda} t} \left\langle \psi_n^{\lambda}, \mathcal{X}^{\lambda}(g) \left(\psi_n^{\lambda}\right) \right\rangle \right) dP(\lambda), \; t \geq 0$$

- It is the case here. The 2π-periodic eigenfunctions satisfy :

$$\frac{d^2\psi(\theta)}{d\theta^2} - \lambda^2 \sin^2(\theta)\,\psi(\theta) = E\psi(\theta)$$

- As $\sin^2(\theta) = \frac{1}{2}(1 - \cos(2\theta))$ this means :

$$\frac{d^2\psi(\theta)}{d\theta^2} - \frac{\lambda^2}{2}\psi(\theta) - E\psi(\theta) + \frac{\lambda^2}{2}\cos(2\theta)\,\psi(\theta) = 0$$

$$\frac{d^2\psi(\theta)}{d\theta^2} + (a - 2q\cos(2\theta))\,\psi(\theta) = 0, \text{ with } a = -\frac{\lambda^2}{2} - E \text{ and } q = -\frac{\lambda^2}{4}$$

- The normalized 2π-periodic eigenfunctions of the Mathieu equation are known. They are even or odd : $\mathrm{ce}_n(\theta, q)$ and $\mathrm{se}_n(\theta, q)$.
- The associated $a_n(q)$ and $b_n(q)$ are called characteristic values.
- There can exist parametric resonance phenomena when

$$a = -\frac{\lambda^2}{2} - E = n^2$$

Coadjoint repres. of E(2)

- The unirreps correspond (Kirillov) to the orbits of the coadjoint representation.
- Let $g = (x, y, \alpha)$

  $\gamma = adx + bdy + cd\alpha \in \mathfrak{g}^*$
- The orbit is

$$Ad_g^*(\gamma) = a'dx + b'dy + c'd\alpha$$

$$\begin{cases} a' = a\cos(\alpha) - b\sin(\alpha) \\ b' = a\sin(\alpha) + b\cos(\alpha) \\ c' = ay - bx + c \end{cases}$$

- The point (a', b') moves along the circle C_{ab} centered at 0 and passing through (a, b).
- If $(a, b) \neq 0$, then the orbit is the full cylinder over C_{ab} parallel to the $d\alpha$-axis. These cylinders are parametrized by their radius.
- If $(a, b) = 0$, then all the points of the $d\alpha$-axis are degenerate orbits.

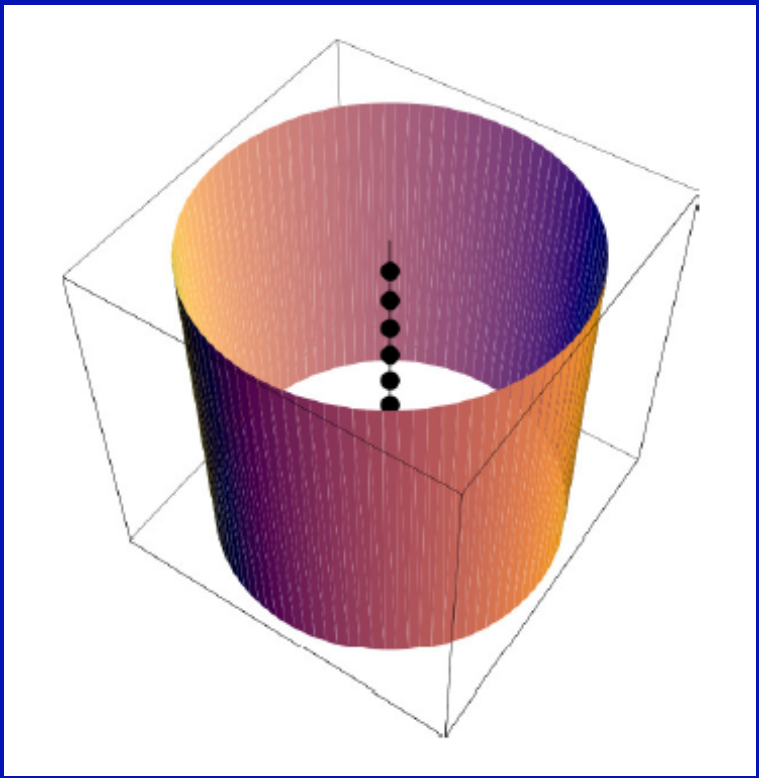

- For the limit $\lambda \to 0$, $\pi_\lambda(x, y, p)$ becomes the translation $\pi_0(u(s)) = u(s + p)$.
- It is highly reducible and in fact π_0 is the integral of $\pi_{\mu,0}$ over μ.

Confluence

- We can construct an interpolation between the E(2) model and the H(3) model.
- It corresponds to a confluence of singularities between the two associated equations.
- See e.g. Dominique Manchon.

$$X_1 = \cos(\theta)\,\partial_x + \sin(\theta)\,\partial_y$$
$$X_2 = \partial_\theta$$
$$X_3 = -\sin(\theta)\,\partial_x + \cos(\theta)\,\partial_y$$
$$[X_1, X_2] = -X_3$$
$$[X_2, X_3] = X_1$$
$$[X_1, X_3] = 0$$
$E(2)$ with $S^1 = \frac{\mathbb{R}}{2\pi\mathbb{Z}}$
$$X_1(\psi(\theta)) = i\lambda \sin(\theta)\,\psi(\theta)$$
$$X_2(\psi(\theta)) = \psi'(\theta)$$
$$\hat{\Delta}^\lambda : \psi''(\theta) - \lambda^2 \sin^2(\theta)\,\psi(\theta)$$
$$\psi''(\theta) + (\mu - \lambda^2)\sin^2(\theta)\,\psi(\theta) = 0$$
$$\sin^2(\theta) \to t$$
$$t(1-t)\,y''(t) + \tfrac{1}{2}(1-2t)\,y'(t) + \\ + \tfrac{1}{4}(\mu - \lambda^2 t)\,y(t) = 0$$
3 sing.: $0, 1$ regular, ∞ irregular

$$X_1^0 = \partial_x + p\partial_y$$
$$X_2^0 = \partial_p$$
$$X_3^0 = \partial_y$$
$$[X_1^0, X_2^0] = -X_3^0$$
$$[X_2^\alpha, X_3^\alpha] = 0$$
$$[X_1^\alpha, X_3^\alpha] = 0$$
$H(3)$ with $S_0^1 = \mathbb{R}$
$$X_1^0(y(s)) = i\lambda s y(s)$$
$$X_2^0(y(s)) = y'(s)$$
$$\hat{\Delta}^\lambda : y''(s) - \lambda^2 s^2 y(s)$$
$$y''(s) + (\mu - \lambda^2)\,s^2 y(s) = 0$$
$$s^2 \to t$$
$$t y''(t) + \tfrac{1}{2} y'(t) + \\ + \tfrac{1}{4}(\mu - \lambda^2 t)\,y(t) = 0$$
2 sing.: 0 regular, $\alpha^{-2} = \infty$ irregular
CONFLUENCE

$$X_1^\alpha = \cos(\theta)\,\partial_x + \tfrac{1}{\alpha}\sin(\alpha\theta)\,\partial_y$$
$$X_2^\alpha = \partial_\theta$$
$$X_3^\alpha = -\alpha\sin(\alpha\theta)\,\partial_x + \cos(\theta)\,\partial_y$$
$$[X_1^\alpha, X_2^\alpha] = -X_3^\alpha$$
$$[X_2^\alpha, X_3^\alpha] = \alpha^2 X_1^\alpha$$
$$[X_1^\alpha, X_3^\alpha] = 0$$
$E_\alpha(2)$ with $S_\alpha^1 = \frac{\mathbb{R}}{2\pi\alpha^{-1}\mathbb{Z}}$
$$X_1^\alpha(\psi(\theta)) = i\lambda\alpha^{-1}\sin(\alpha\theta)\,\psi(\theta)$$
$$X_2^\alpha(\psi(\theta)) = \psi'(\theta)$$
$$\hat{\Delta}^\lambda : \psi''(\theta) - \tfrac{\lambda^2}{\alpha^2}\sin^2(\alpha\theta)\,\psi(\theta)$$
$$\psi''(\theta) + \left(\mu - \tfrac{\lambda^2}{\alpha^2}\sin^2(\alpha\theta)\right)\psi(\theta) = 0$$
$$\frac{\sin^2(\alpha\theta)}{\alpha^2} \to t$$
$$t(1-\alpha^2 t)\,y''(t) + \tfrac{1}{2}(1-2\alpha^2 t)\,y'(t) + \\ + \tfrac{1}{4}(\mu - \lambda^2 t)\,y(t) = 0$$
3 sing.: $0, \alpha^{-2}$ regular, ∞ irregular

$X_1 = \cos(\theta)\,\partial_x + \sin(\theta)\,\partial_y$	$X_1^\alpha = \cos(\theta)\,\partial_x + \frac{1}{\alpha}\sin(\alpha\theta)\,\partial_y$	$X_1^0 = \partial_x + p\partial_y$
$X_2 = \partial_\theta$	$X_2^\alpha = \partial_\theta$	$X_2^0 = \partial_p$
$X_3 = -\sin(\theta)\,\partial_x + \cos(\theta)\,\partial_y$	$X_3^\alpha = -\alpha\sin(\alpha\theta)\,\partial_x + \cos(\theta)\,\partial_y$	$X_3^0 = \partial_y$
$[X_1, X_2] = -X_3$	$[X_1^\alpha, X_2^\alpha] = -X_3^\alpha$	$[X_1^0, X_2^0] = -X_3^0$
$[X_2, X_3] = X_1$	$[X_2^\alpha, X_3^\alpha] = \alpha^2 X_1^\alpha$	$[X_2^\alpha, X_3^\alpha] = 0$
$[X_1, X_3] = 0$	$[X_1^\alpha, X_3^\alpha] = 0$	$[X_1^\alpha, X_3^\alpha] = 0$
$E(2)$ with $S^1 = \frac{\mathbb{R}}{2\pi\mathbb{Z}}$	$E_\alpha(2)$ with $S_\alpha^1 = \frac{\mathbb{R}}{2\pi\alpha^{-1}\mathbb{Z}}$	$H(3)$ with $S_0^1 = \mathbb{R}$
$X_1(\psi(\theta)) = i\lambda\sin(\theta)\,\psi(\theta)$	$X_1^\alpha(\psi(\theta)) = i\lambda\alpha^{-1}\sin(\alpha\theta)\,\psi(\theta)$	$X_1^0(y(s)) = i\lambda s y(s)$
$X_2(\psi(\theta)) = \psi'(\theta)$	$X_2^\alpha(\psi(\theta)) = \psi'(\theta)$	$X_2^0(y(s)) = y'(s)$
$\hat{\Delta}^\lambda : \psi''(\theta) - \lambda^2\sin^2(\theta)\,\psi(\theta)$	$\hat{\Delta}^\lambda : \psi''(\theta) - \frac{\lambda^2}{\alpha^2}\sin^2(\alpha\theta)\,\psi(\theta)$	$\hat{\Delta}^\lambda : y''(s) - \lambda^2 s^2 y(s)$
$\psi''(\theta) + (\mu - \lambda^2)\sin^2(\theta)\,\psi(\theta) = 0$	$\psi''(\theta) + \left(\mu - \frac{\lambda^2}{\alpha^2}\sin^2(\alpha\theta)\right)\psi(\theta) = 0$	$y''(s) + (\mu - \lambda^2)\,s^2 y(s) = 0$
$\sin^2(\theta) \to t$	$\frac{\sin^2(\alpha\theta)}{\alpha^2} \to t$	$s^2 \to t$
$t(1-t)\,y''(t) + \frac{1}{2}(1-2t)\,y'(t) +$ $+\frac{1}{4}(\mu - \lambda^2 t)\,y(t) = 0$	$t(1-\alpha^2 t)\,y''(t) + \frac{1}{2}(1-2\alpha^2 t)\,y'(t) +$ $+\frac{1}{4}(\mu - \lambda^2 t)\,y(t) = 0$	$t y''(t) + \frac{1}{2}y'(t) +$ $+\frac{1}{4}(\mu - \lambda^2 t)\,y(t) = 0$
3 sing.: $0, 1$ regular, ∞ irregular	3 sing.: $0, \alpha^{-2}$ regular, ∞ irregular	2 sing.: 0 regular, $\alpha^{-2} = \infty$ irregular

Direction processes in G

- One can go further and express the anisotropy through an angular diffusion of θ and a spatial advection (a drift and no longer a diffusion) along the X_1 direction.
- Remco Duits, Markus van Almsick, Giovanna Citti and Alessandro Sarti recently developed this idea initially due to David Mumford (but Mumford worked in $\mathbb{R}^2$ and not in G).

- So, one considers advection-diffusion equations, and especially direction processes in G.
- This allows a stochastic approach to contour completion.

- Let $g_0 = (x_0, y_0, \theta_0)$ be an initial point in G.
- We look at equations (with $dt = ds$)

$$\begin{cases} \dot{x} = \cos(\theta) \\ \dot{y} = \sin(\theta) \\ \dot{\theta} \sim N(0, \sigma^2) \end{cases}$$

- $d\theta/ds$ is the curvature.
- Whithout noise, the trajectories are straight lines : coaxiality

$$\theta = \theta_0, x = x_0 + \cos(\theta_0)\, t, y = y_0 + \sin(\theta_0)\, t$$

- The evolution equation for the probability $P(g, t)$ is

$$\frac{\partial P}{\partial t}(g,t) = -\left(\cos(\theta)\frac{\partial P}{\partial x}(g,t) + \sin(\theta)\frac{\partial P}{\partial y}(g,t)\right) + \frac{\sigma^2}{2}\frac{\partial^2 P}{\partial \theta^2}(g,t)$$

$$\frac{\partial P}{\partial t} = -X_1(P) + \frac{\sigma^2}{2}(X_2)^2(P)$$

- If the travelling time decays as $\alpha e^{-\alpha t}$

and if $U(g) = P(g,0)$ is an initial condition, then

$$p(g) = p(a,\theta) = \int_0^\infty P(a,\theta \mid T = t)\, p(T = t)\, dt$$

satisfies the equation :

$$-X_1(p) + \frac{\sigma^2}{2}(X_2)^2(p) + \alpha p = \alpha U$$

- One can compute explicitely the Green function ($U = \delta_e$).
- To complete a contour, one considers two direction processes :
  - a forward process starting at $g_0 = (a_0, \theta_0)$,
  - a backward process starting at $g_1 = (a_1, \theta_1)$.

  and compute the probability of collision of these two random walks.
- Duits' image (fast approximation) :

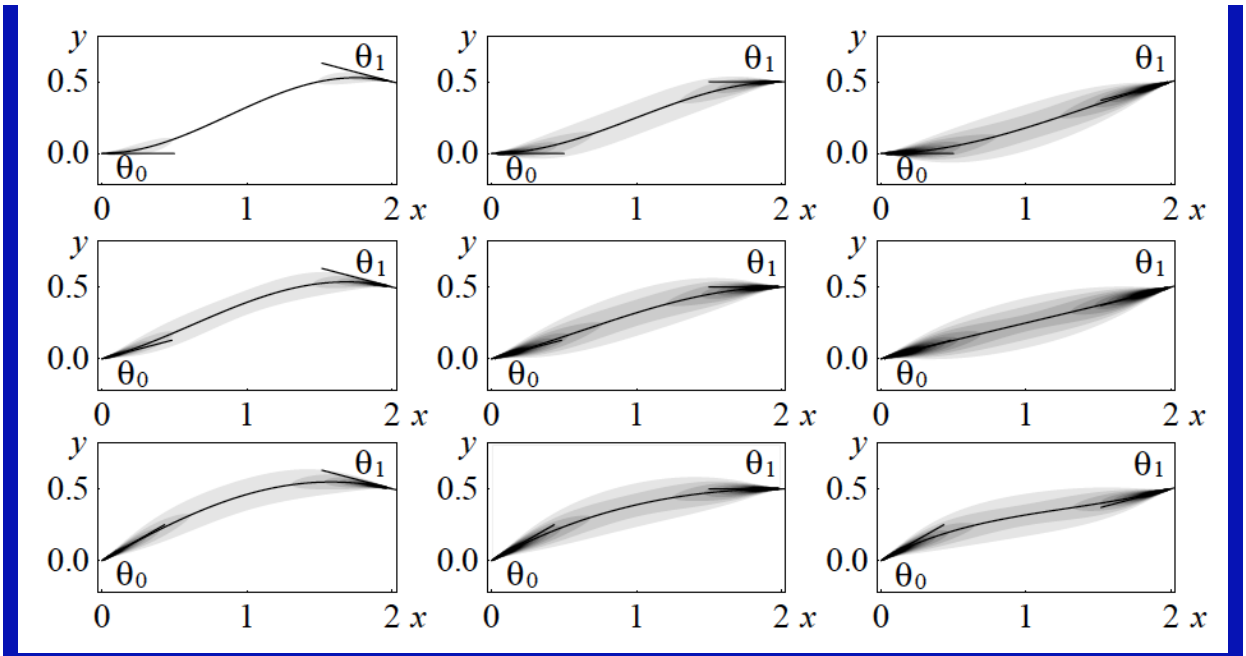

$a_0 = (0, 0)$, $a_1 = (2, 0.5)$, $\theta_0 = 0°, 15°, 30°$ (top to bottom), $\theta_1 = -15°, 0°, 15°$ (left to right), $\sigma = 1$, $\alpha = 2$. Marginal distributions (integral over θ of the product of the forw/backw solutions)

Application to spontaneous geometric visual patterns

- A beautiful application of these models of functional architecture concerns entoptic vision (hallucinations).
- Paul Bressloff, Jack Cowan, Martin Golubitsky :
- by encoding the functional architecture of V1 into the Hopfield equations of a neural net, one is able to deduce visual morphological patterns.

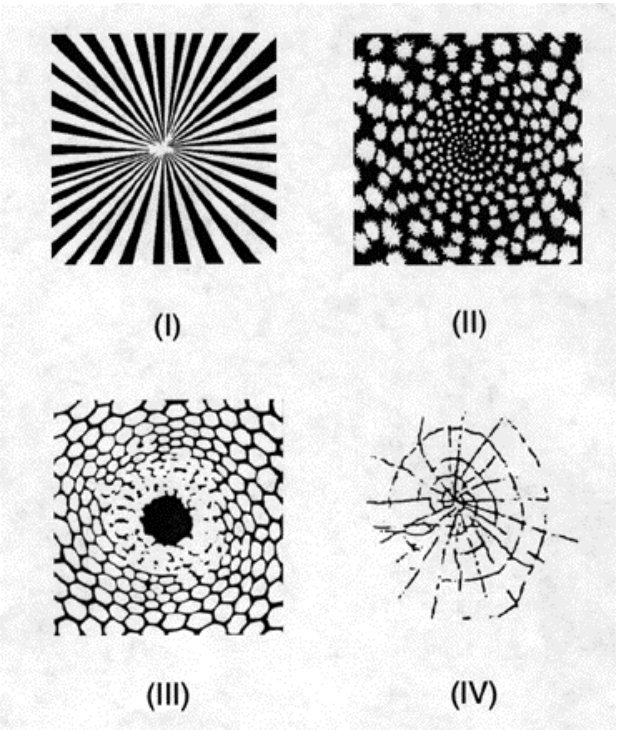

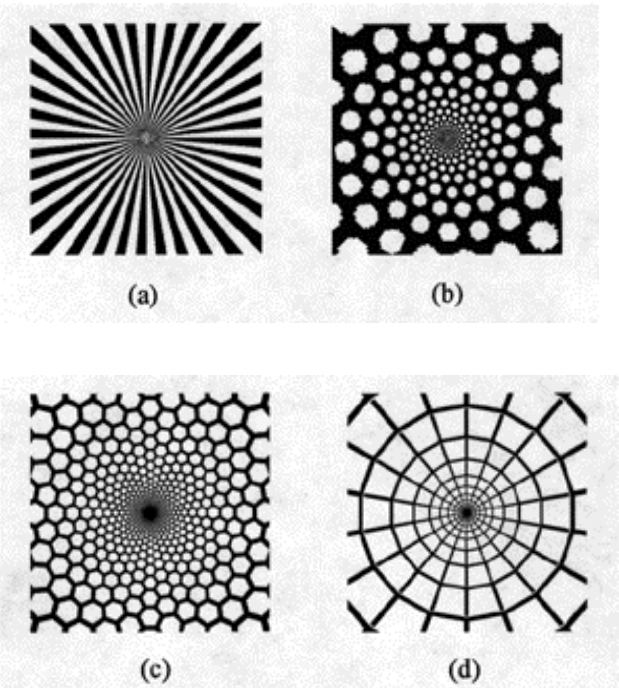

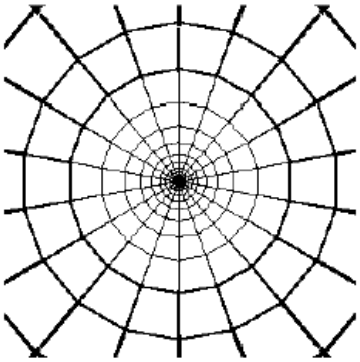

1. Even squares.

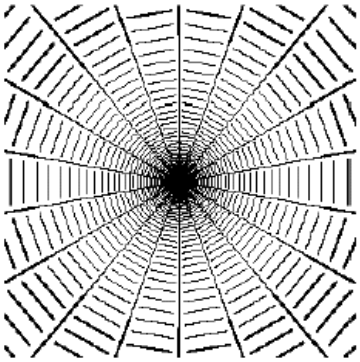

2. Even rolls.

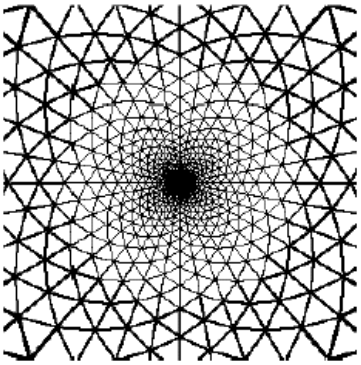

3. Even hexagons I.

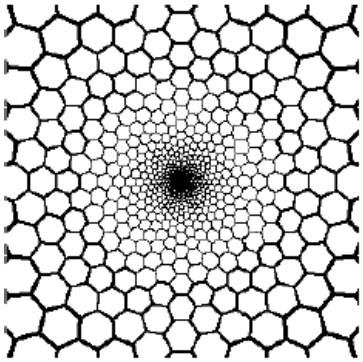

4. Even hexagons II.

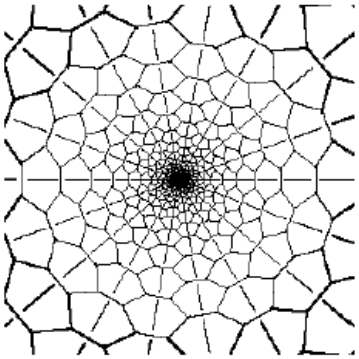

5. Even rhombs.

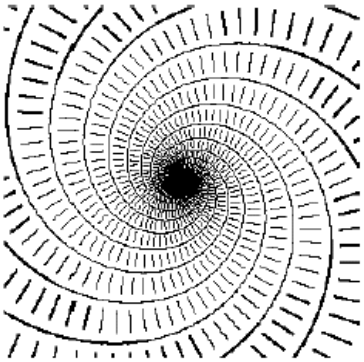

6. Even rhombic rolls.

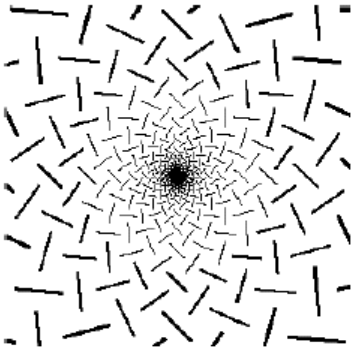

1. Odd squares.

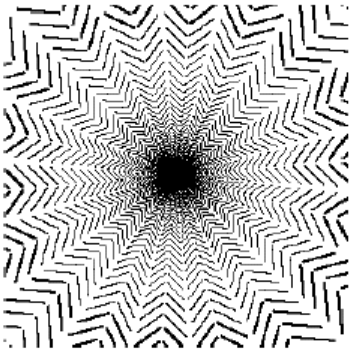

2. Odd rolls.

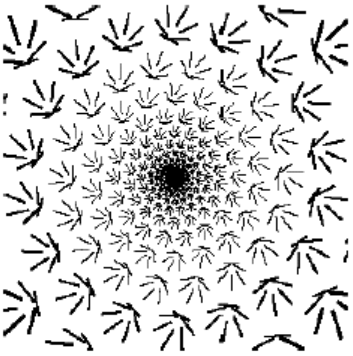

3. Odd hexagons I (triangl

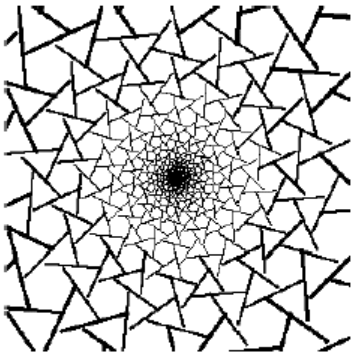

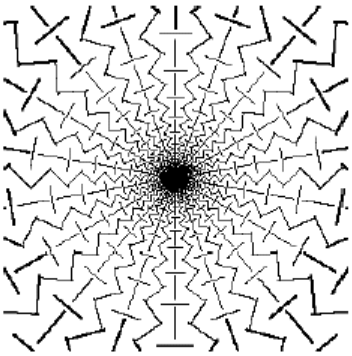

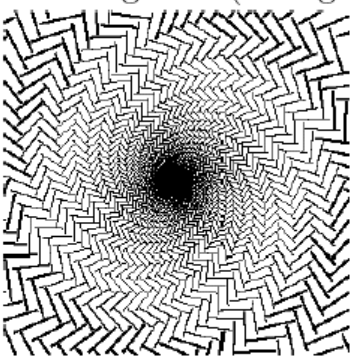

- Let $(\mathbf{x}, \theta)$ be local coordinates in the model V of V1.
- Let $a(\mathbf{x}, \theta, t)$ be the activity of V1. We look for the PDE governing the evolution of a.
- Using standard Hopfield equations for neural nets, we get :

$$\frac{\partial a(\mathbf{x},\theta,t)}{\partial t} = -\alpha a(\mathbf{x},\theta,t) + \frac{\mu}{\pi}\int_0^{\pi}\int_{\mathbb{R}} w\left\langle \mathbf{x},\theta|\mathbf{x}',\theta'\right\rangle \sigma\left(a(\mathbf{x}',\theta',t)\right) d\mathbf{x}' d\theta' + h(\mathbf{x},\theta,t)$$

where σ is a non linear gain function (with $\sigma(0) = 0$), h an external input and

$$w\left\langle \mathbf{x},\theta|\mathbf{x}',\theta'\right\rangle$$

is the weight of the connection between the neuron $v = (\mathbf{x}, \theta)$ and the neuron $v' = (\mathbf{x}', \theta')$, α a parameter of decay (α can be taken = 1) and μ a parameter of excitability of V1.

- The increasing of μ models an increasing of the excitability of V1 due to the action of substances on the nuclei which produce specific neurotransmitters (such as serotonin or noradrenalin).

Encoding the functional architecture into the synaptic weights

- Bressloff et al. encode only the strictly coaxial alignements. Here again, it is the simplest model.
- The local vertical connections inside a single hypercolumn yield a term:

$$w\left\langle \mathbf{x},\theta|\mathbf{x}',\theta'\right\rangle = w_{\mathrm{loc}}\left(\theta-\theta'\right)\delta\left(\mathbf{x}-\mathbf{x}'\right)$$

where δ is a Dirac function imposing

$$\mathbf{x} = \mathbf{x}'$$

- The lateral horizontal connections between different hypercolumns yield a term:

$$w\left\langle \mathbf{x},\theta|\mathbf{x}',\theta'\right\rangle = w_{\mathrm{lat}}\left(\mathbf{x}-\mathbf{x}',\theta\right)\delta\left(\theta-\theta'\right)$$

where the factor

$$\delta\left(\theta-\theta'\right)$$

imposes $\theta = \theta'$ and expresses the fact that the horizontal cortico-cortical connections connect parallel pairs.

- Moreover, the coaxiality $\theta = \theta' = \mathbf{x}\mathbf{x}'$

is expressed by the fact that

$$w_{\mathrm{lat}}\left(\mathbf{x}-\mathbf{x}',\theta\right) = w_{\mathrm{lat}}\left(s\right)\delta\left(\mathbf{x}-\mathbf{x}'-se_{\theta}\right) = \widehat{w}\left(r_{-\theta}\left(\mathbf{x}-\mathbf{x}'\right)\right)$$

where e_{θ} is the unit vector in the direction θ.

- As the weights w are $E(2)$-invariant, the PDE is itself $E(2)$-equivariant if $h = 0$.

Dynamically emerging morphologies and bifurcations

- We suppose that there exist no external input, that is $h = 0$. For $\mu = 0$, the state $a \equiv 0$ is trivially the state of the network and it is stable.
- $a \equiv 0$ is the "ground state". It can be very complex (endogeneous activity, spontaneous noise, etc.)

- Now, the analysis of the PDE shows that, as the parameter μ increases, this initial activation state $a \equiv 0$ can become unstable and bifurcate for critical values μ_c of μ.

- The new stable activation states present spatial patterns generated by an $\mathbf{E}(2)$ symmetry breaking.
- The bifurcations can be analyzed using classical methods:
  - Linearization of the PDE near the solution $a \equiv 0$ and the critical value μ_c.
  - Spectral analysis of the linearized equation.
  - Computation of its eigenvectors (eigenmodes).
  - Hypothesis of periodicity w.r.t. a lattice of R.
- Here are some examples of eigenmodes.

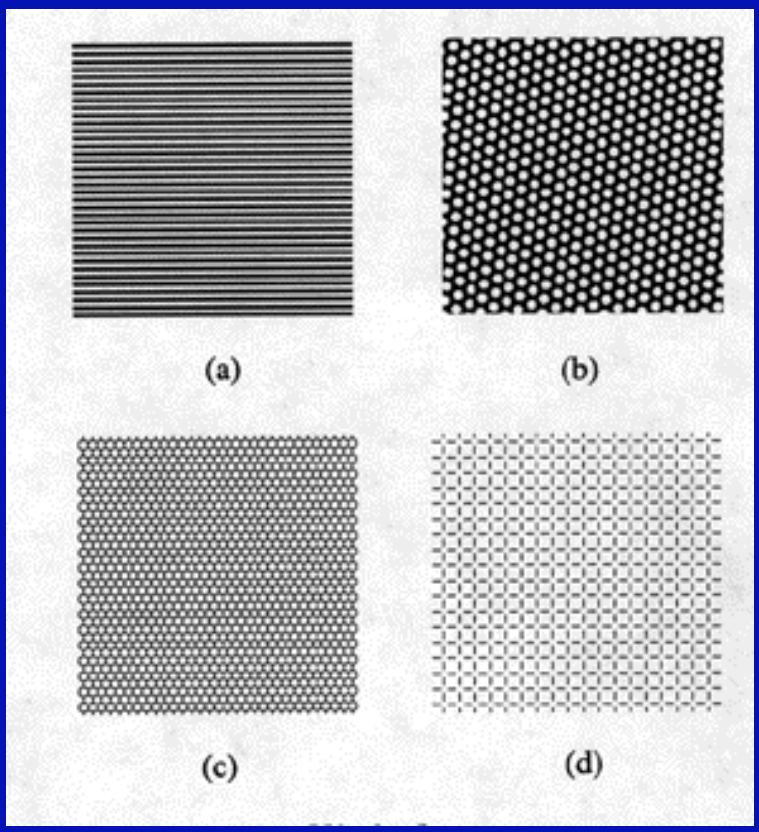

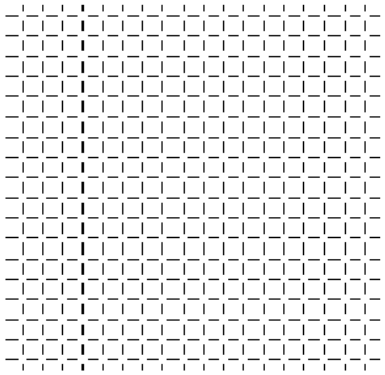

1. Even squares.

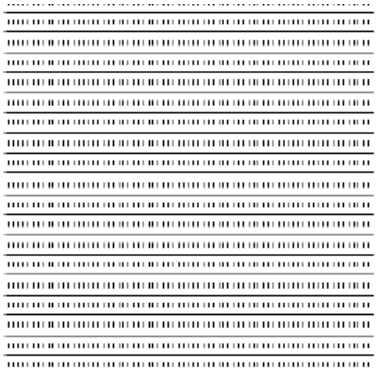

2. Even rolls.

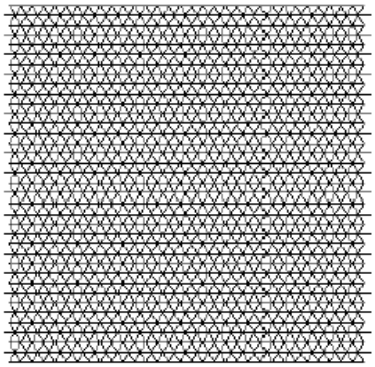

3. Even hexagons I.

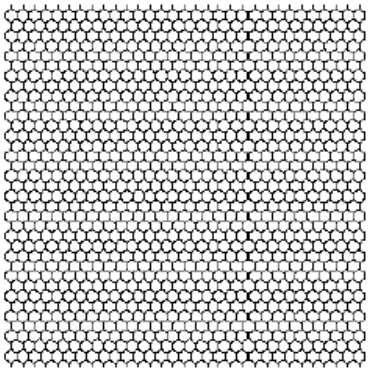

4. Even Hexagons II.

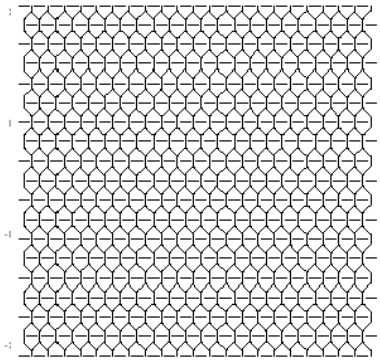

5. Even rhombs.

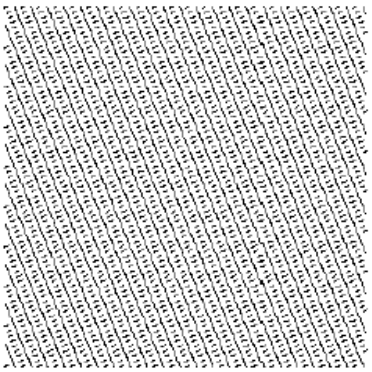

6. Even rhombic rolls.

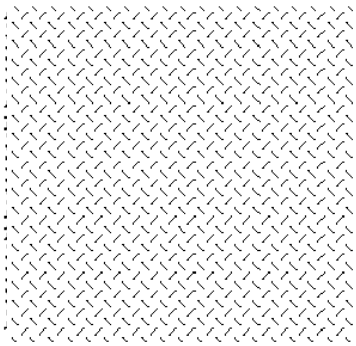

1. Odd squares.

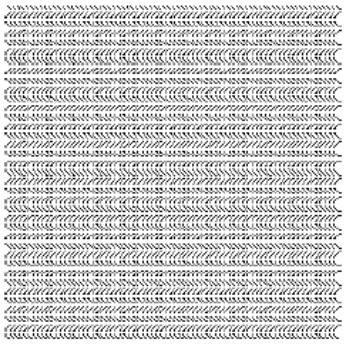

2. Odd rolls.

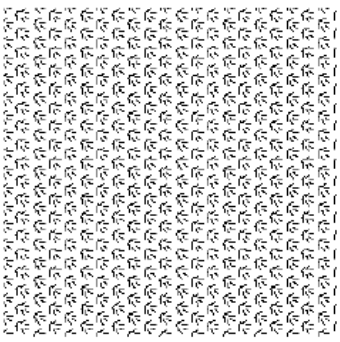

3. Odd hexagons I (triangles).

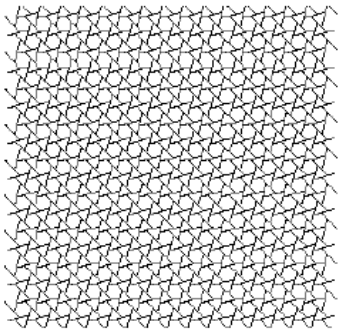

4. Odd hexagons II.

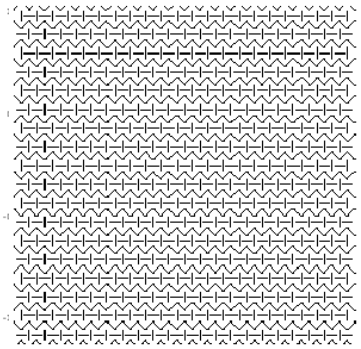

5. Odd rhombs.

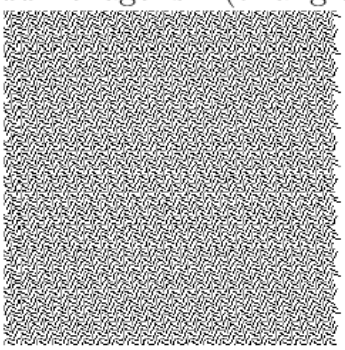

6. Odd rhombic rolls.

Patterns as virtual retinal images

- The last step is to reconstruct from eigenmodes in V1 corresponding virtual retinal images.
- For that, we must take into account the retinotopic conformal map mapping the retina R on V1.

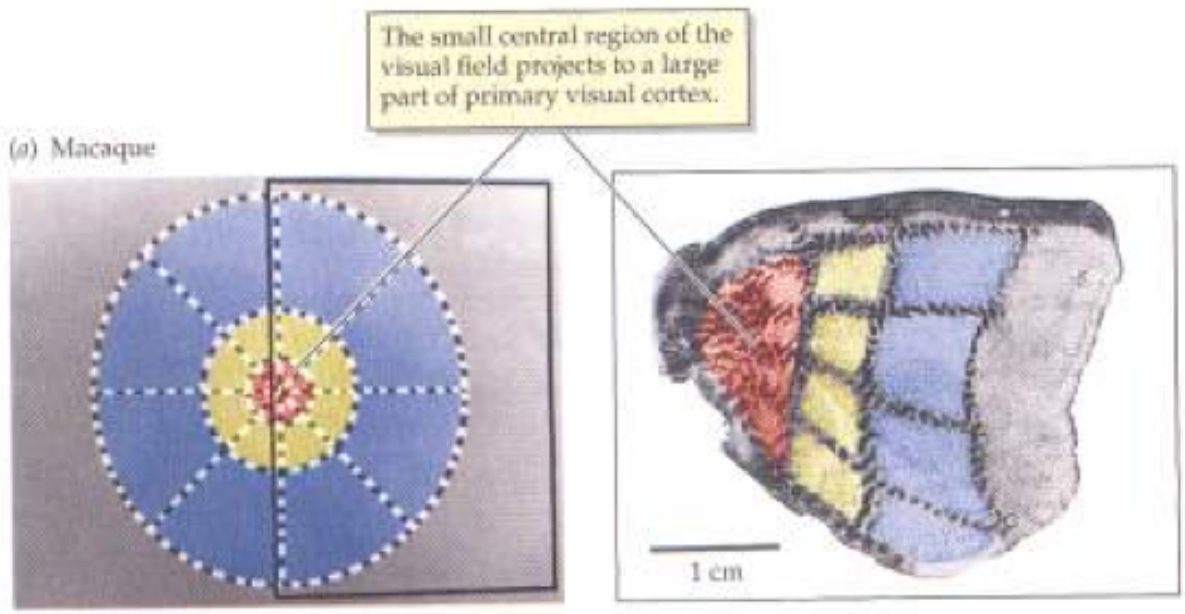

- A good model is a wedge-dipole model for V1, V2, and V3

$$\mathrm{Log}[(w(z)+a)/(w(z)+b)]$$

where $w(z)$ wedges the argument.

- Left (G) : V1-V2-V3 (Horton & Hoyt 1991).
- Right (H) : fit with a wedge-dipole model (Schwartz 2002).

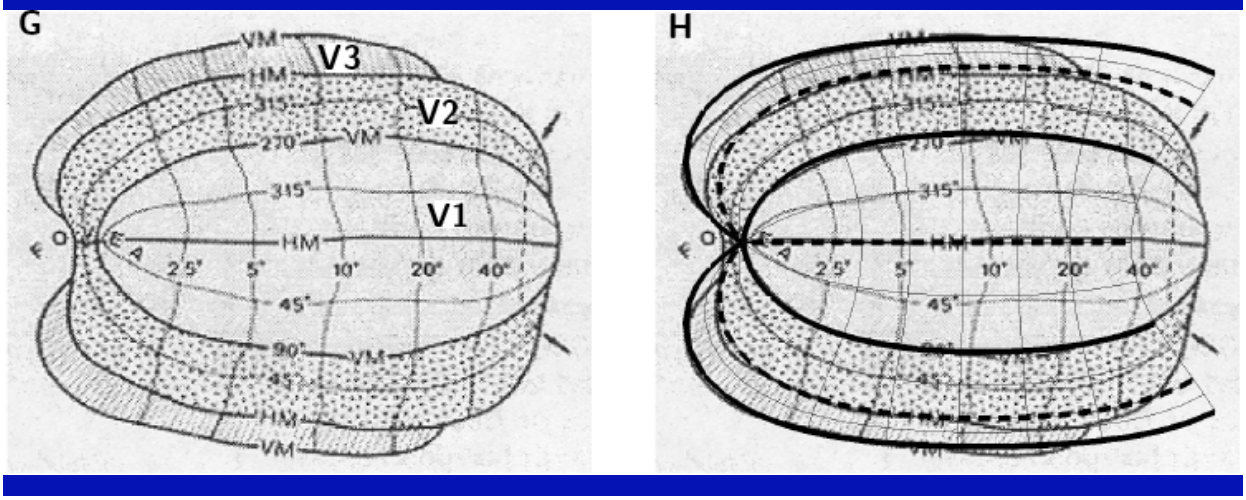

- Lines in V1 correspond qualitatively to spiral on the retina.

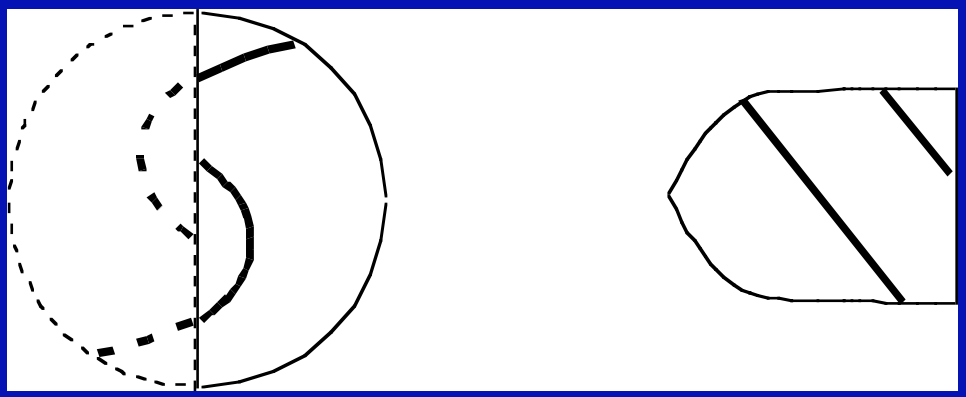

- If we apply the inverse of the conformal map to the eigenstates of the PDE (as if V1 activity was induced by a real stimulus) we get quite exact models of Klüver's planforms.

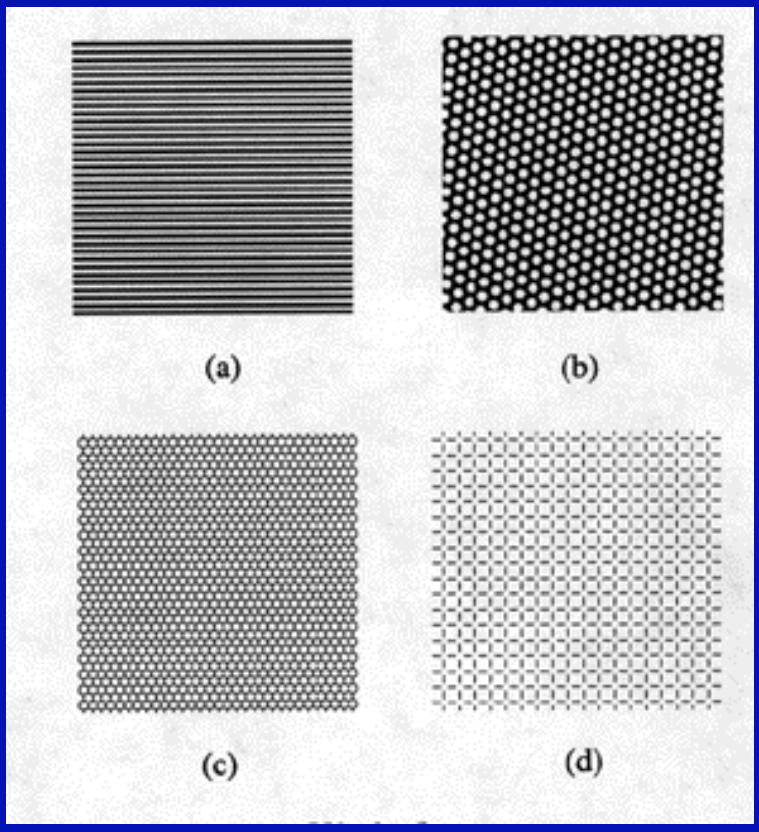
(a)
(b)
(c)
(d)

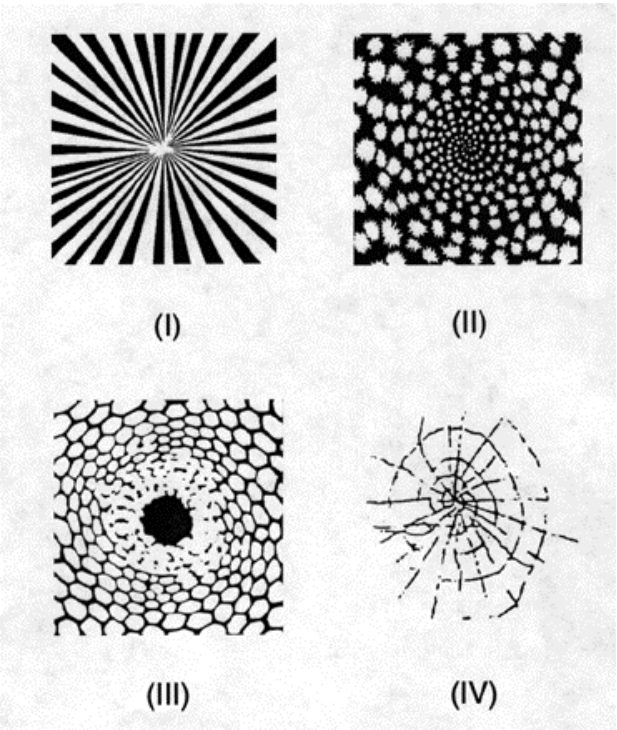
(I)
(II)
(III)
(IV)

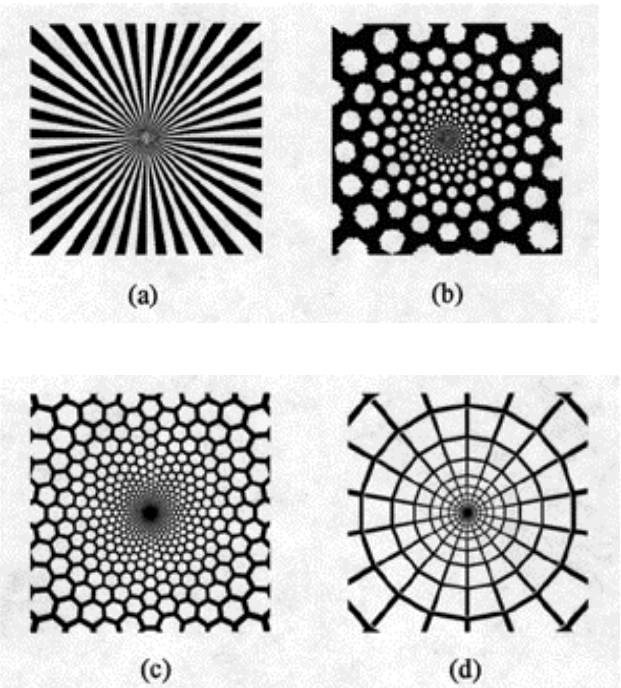
(a)
(b)
(c)
(d)

Faugeras-Chossat's model

- In a forthcoming paper, Olivier Faugeras and Pascal Chossat have generalized the model.
- Their main idea is that hypercolumns of V1 encode (at a given scale defined by the size of the receptive fields) not only local features such as orientation but the whole "structure tensor" $\mathcal{T}$ of the stimulus $I(x, y)$:

$$\mathcal{T} = \begin{pmatrix} I_x^2 & I_x I_y \\ I_x I_y & I_y^2 \end{pmatrix}$$

- "A hypercolumn in V1 can represent the structure tensor in the receptive field of its neuron as the average membrane potential values of some of its neuronal population."

- So, the activity is $a(\mathcal{T}, t)$ (t = time) for a hypercolum and $a(\mathbf{x}, \mathcal{T}, t)$ ($\mathbf{x}$ = position in the retina R or in the visual field) for the field of hypercolumns.
- The PDE becomes :

$$a_t(\mathbf{x}, \mathcal{T}, t) = -\alpha\, a(\mathbf{x}, \mathcal{T}, t) + \int_{\mathcal{H}\times R} w\,\langle \mathbf{x}, \mathcal{T}\,|\mathbf{x}', \mathcal{T}'\rangle\ \sigma\left(a(\mathbf{x}', \mathcal{T}', t)\right) d\mathbf{x}' d\mathcal{T}' + h\left(\mathbf{x}, \mathcal{T}, t\right)$$

with w = synaptic weights, $\mathcal{H}$ = space of the $\mathcal{T}$, σ = gain function, h = input (α can be taken = 1).

- Faugeras and Chossat consider only one hypercolum (no spatial variation **x**).
- The space $\mathcal{H}$ of 2 x 2 symmetric definite positive matrices $\mathcal{T}$ is the 3D hyperbolic quotient space

$$GL(2, \mathbb{R})/O(2)$$

foliated in 2D leaves by det$\mathcal{T}$.

- For $\det \mathcal{T} = 1$, the leaf is the quotient

$$\mathcal{H}_1 = SL(2,\mathbb{R})/SO(2)$$

which is isomorphic to the Poincaré disk .

- In the distance is

$$d(z,z') = \frac{1}{2}\log\left(\frac{|1-\bar{z}z'| + |z-z'|}{|1-\bar{z}z'| - |z-z'|}\right)$$

and the geodesics are diameters of or arcs of circles orthogonal to the boundary

$$\partial\mathbb{D} = \mathbb{S}^1$$

- The isomorphism $\mathcal{H}_1 =$ is

$$\text{If } \mathcal{T} = \begin{pmatrix} a & c \\ c & b \end{pmatrix}, \; a > 0, \; ab - c^2 = 1$$

$$\text{and then } b > 0, \; \text{Trace}(\mathcal{T}) = a + b \geq 2$$

$$z = \frac{a - b + 2ic}{2 + a + b}, \; z\overline{z} = \frac{a + b - 2}{a + b + 2}$$

$$\text{If } z = z_1 + iz_2 \in \mathbb{D}, \; a = \frac{1 + 2z_1 + z\overline{z}}{1 - z\overline{z}},$$

$$b = \frac{1 - 2z_1 + z\overline{z}}{1 - z\overline{z}}, \; c = \frac{2z_2}{1 - z\overline{z}}$$

- The group of (direct) isometries of is the group $\mathrm{SU}(1, 1)$ of 2 x 2 Hermitian matrices of det = 1 :

$$\gamma = \begin{pmatrix} \alpha & \beta \\ \overline{\beta} & \overline{\alpha} \end{pmatrix} \text{ with } \det \gamma = |\alpha|^2 - |\beta|^2 = 1$$

acting as

$$\gamma(z) = \frac{\alpha z + \beta}{\overline{\beta} z + \overline{\alpha}}$$

- There are 3 important subgroups :

$$K = O(2) = \text{ rotations } = \left\{ r_\varphi = \begin{pmatrix} e^{i\varphi/2} & 0 \\ 0 & e^{-i\varphi/2} \end{pmatrix} \right\}$$

(the orbits are concentric circles with center 0).

$$A = \text{ boosts } = \left\{ b_p = \begin{pmatrix} \cosh p & \sinh p \\ \sinh p & \cosh p \end{pmatrix}, \ p \in \mathbb{R} \right\}$$

(the orbits are "horizontal translations" from –1 ($p = -\infty$) to +1 ($p = +\infty$)).

$$N = \left\{ n_s = \begin{pmatrix} 1 + is & -is \\ is & 1 - is \end{pmatrix}, \ s \in \mathbb{R} \right\}$$

(the orbits are the horocycles, i.e. circles in tangent to S^1 at $+1$).

$n_0 = \mathrm{Id}$, $n_\infty = 1$.

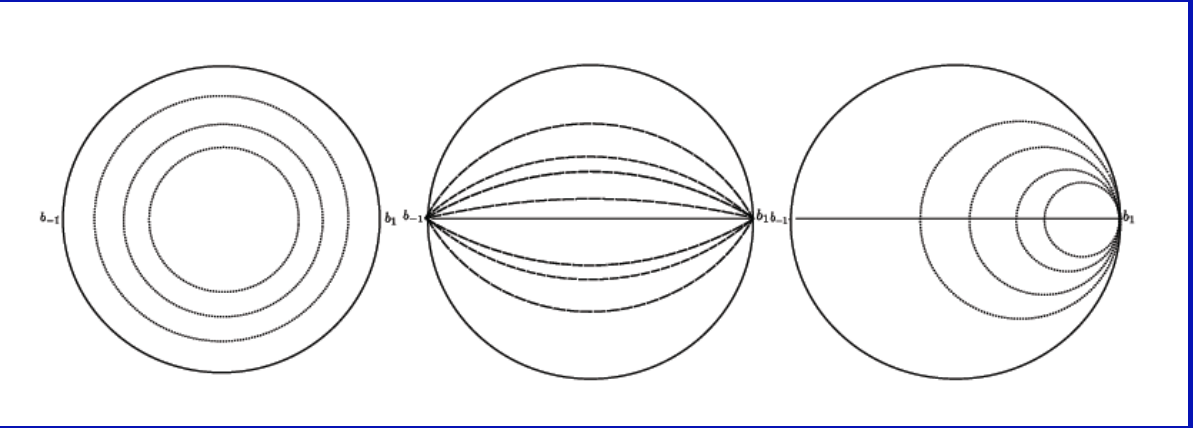

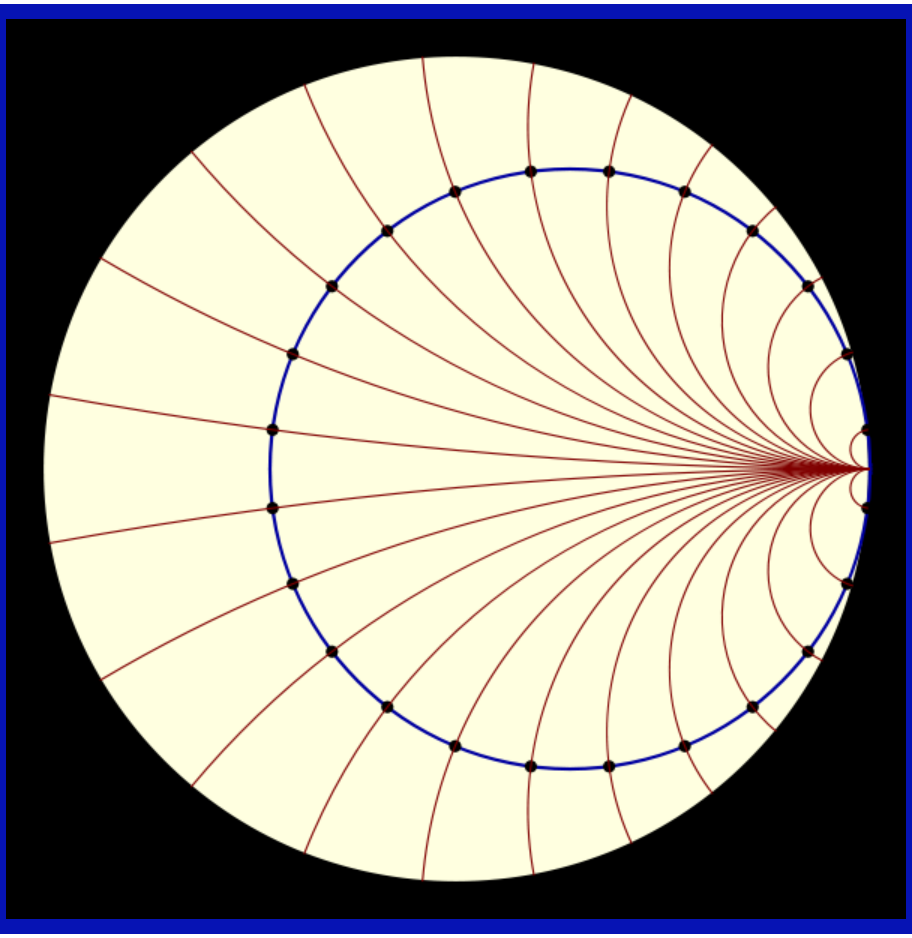

- The horocycle h passing through z intersects the real axis at $+1$ and ξ

$$\xi = \frac{2z\overline{z} - (z + \overline{z})}{-2 + (z + \overline{z})}$$

- Let $\delta(z) = \langle z,1 \rangle$ be the algebraic distance between ξ and 0 :

$$\delta(z) = \langle z, 1\rangle = -\frac{1}{2}\log\left(\frac{1+\xi}{1-\xi}\right) = -\frac{1}{2}\log\left(\frac{1-z\overline{z}}{(1-z)(1-\overline{z})}\right)$$

- The hyperbolic Laplacian is :

$$\Delta = 4\left(1-z\overline{z}\right)^2 \partial_z \partial_{\overline{z}} = \left(1-z\overline{z}\right)^2 \Delta_{\text{Euclid}}$$

- A particular class of eigenfunctions has been introduced by Helgason :

$$e_{\lambda,1}(z) = e^{(i\lambda+1)\delta(z)}, \ \lambda \in \mathbb{C}$$

- By construction, they are N-invariant, i.e. constant on horocycles, and their eigenvalues are

$$(i\lambda+1)^2 - 2(i\lambda+1) = -\left(\lambda^2+1\right)$$

- They constitute for the analog of the plane waves of the Euclidean case.
- Horocycles are like wave fronts and geodesics orthogonal to them are like rays.
- It is therefore natural to use horocyclic coordinates (s, p) defined by $z = n_s.b_p(0)$.

- Among the eigenfunctions $e_{\lambda,1}$ those for which $\lambda = \alpha + i$ (and therefore $i\lambda + 1 = i\alpha$) are particularly interesting.
- They write

$$e_{\alpha+i,1} = e^{i\alpha p}$$

and are periodic in p of period $2\pi / \alpha$.

- The bifurcation theory in is simple. The PDE is

$$a_t(z,t) = -a(z,t) + \int_{\mathbb{D}} w\,\langle z|z'\rangle\ \sigma\left(a(z',t)\right) dm(z')$$

with the measure

$$dm(z) = \frac{dz_1 dz_2}{\left(1-|z|^2\right)^2}$$

- If the state $a(z, t)$ is constant, we get

$$0 = -a + \int_{\mathbb{D}} w\,\langle 0|z'\rangle\ \sigma\left(a\right)\ dm(z') = -a + \sigma\left(a\right) W_0$$

with

$$W_0 = \int_{\mathbb{D}} w\,\langle 0|z'\rangle\ dm(z')$$

- We choose the gain function σ in such a way that $a = 0$ is the ground state. Let $\mu = \sigma'(0)$.

- The linearized equation near $a \equiv 0$ is

$$a_t(z,t) = -a(z,t) + \mu \int_{\mathbb{D}} w\,\langle z|z'\rangle\; a(z',t)\; dm(z')$$

- In horocyclic coordinates

$$dm(z') = e^{-2p'}\, dp'\, ds'$$

- Moreover, N-invariance implies

$$a\left(n_s.b_p(0),t\right) = a\left(b_p(0),t\right)$$

- One gets, for solutions of the form

$$a(z,t) = e^{\nu t} a(z) \text{ and } a\left(b_p(0)\right) = \widetilde{a}(p)$$,

the equation for the eigenvalues

$$\nu \widetilde{a} = -\widetilde{a} + \mu \widetilde{w} * \widetilde{a}, \text{ with } \widetilde{w}\left(\xi\right) = \int_{\mathbb{R}} w\,\langle b_\xi(0), n_x(0)\rangle$$

- For the special eigenvalues $\lambda = \alpha + i$, the eigenfunctions

$$e^{\nu t} e_{\alpha+i,1}(z) = e^{\nu t} e^{i\alpha p}$$

are N-invariant (constant along horocycles) and $2\pi/\alpha$ periodic in p.

- If we apply Fourier to the equation for eigenvalues, we get

$$\nu(\alpha) = -1 + \mu \widehat{w}(\alpha), \text{ with } \widehat{w} = \text{ Fourier transform of } \widetilde{w}$$

- There will be a bifurcation when the real part of ν vanishes, that is when :

$$-1 + \mu_c \operatorname{Re}(\widehat{w}(\alpha_c)) = 0$$

- Then ν is purely imaginary and the bifurcation is a Hopf bifurcation with period $T = 2\pi/\alpha$:

$$\nu = \pm i \mu_c \operatorname{Im}(\widehat{w}(\alpha_c)) = \pm i \omega_0$$